Effects and inducers of autoantibodies against *N*-methyl-D-aspartate (NMDA) receptors

Dissertation

for the award of the degree

"Doctor rerum naturalium" (Dr.rer.nat.)

of the Georg-August-Universität Göttingen

within the *Center for Systems Neuroscience (CSN)* doctoral program

of the Göttingen Graduate School for Neurosciences,

Biophysics and Molecular Biosciences (GGNB)

and of the Georg August University School of Science (GAUSS)

submitted by

Hong Pan

born in Zaozhuang, China

Göttingen, 2019

Doctoral thesis Committee:

Prof. Dr. Dr. Hannelore Ehrenreich (Supervisor, 1st referee)
Clinical Neuroscience
Max Planck Institute of Experimental Medicine

Prof. Dr. Jürgen Wienands (2nd referee)
University Medical Center Göttingen
Institute for Cellular and Molecular Immunology

Prof. Dr. Ralf Heinrich
Department of Cellular Neurobiology
Schwann-Schleiden Research Centre

Prof. Dr. Alexander Flügel
University Medical Center Göttingen
Institute for Neuroimmunology and Multiple Sclerosis Research

Members of the Examination Board

Prof. Dr. Klaus-Armin Nave
Department of Neurogenetics
Max Planck Institute of Experimental Medicine

Prof. Dr. Susann Boretius
Functional Imaging Laboratory
German Primate Center

Date of the thesis submission: November 22nd, 2019

Date of the oral examination: January 8th, 2020

Declaration

I hereby declare that the thesis 'Effects and inducers of autoantibodies against *N*-methyl-D-aspartate (NMDA) receptors' has been written independently and with no other sources and aids than quoted.

Hong Pan

Göttingen, November 22nd, 2019

Acknowledgements

How time flies! It's coming to the end now. It has been 4.5 year since I arrived in Germany, first time abroad, away from everyone/everything that I'm familiar with. Culture shock, language, new projects…everything is both exciting and strange, but I will never forget the time I spent in Göttingen.

Throughout my PhD life, first of all, I would like to thank my supervisor Prof. Dr. Dr. Hannelore Ehrenreich for giving me the opportunity to start my project here, and all the support and guidance you gave me. It was not always easy, but I grew a lot during these 4 years, with all the trainings, both scientific skills and soft skills.

I would like to thank Dr. Fred Lühder, for all the help and supervision you kindly offered me. I really had a good time and good training in your lab, I couldn't have made it without you.

I would also like to thank my thesis committee members: Prof. Dr. Ralf Heinrich, Prof. Dr. Jürgen Wienands, and Prof. Dr. Alexander Flügel. Thank you all for coming to my thesis committee meetings and all the constructive suggestion. It always helped me to improve. Thank Prof. Dr. Klaus-Armin Nave and Prof. Dr. Susann Boretius for taking your time to be on my examination board.

Moreover, I would like to thank all the collaborators over the years. The Bochum team: Prof. Michael Hollmann, Daniel and Christina, I enjoyed every time when we met, in Göttingen or Bochum. The Hannover team: Prof. Karin Weissenborn and Nadine, always nice to meet you.

My lovely colleagues and friends at clinical neuroscience (past and present), I'm so lucky to work with all of you. I appreciated all the help and support from you. I always believe, it's a unique experience every time meeting new people. With some people you met, you will never meet again in one's lifetime. So I try to keep the memories, and hope the best for all of you. It would be great to meet somewhere at some point again.

Wiebke, thanks for taking care of everything, I would have been so lost without you.

Anja, Nadine, Viktoria, thanks for always be there for me, during Christmas/late night/when I was stressed or depressed, it was my pleasure to work with you.
Debia, thanks for all the talks and nice trips, I'm so happy to have such an experience of travelling together and sharing one room.
Laura, you are always confident and secure, thanks for sharing all the conversations, and listening to me whenever I needed to talk.
Umer, thanks for your wise advices, sometimes it's helpful.
Jan, thanks for explaining all the statistics, and being a good psychologist.
Sahab, thanks for all the jokes you shared, it was a lot of fun when you were imitating.
Anna, thanks for the help at work, it was always nice to see you outside. I enjoyed the time with you.
Justus, thanks for helping me, it was nice working with you.
Agnes, thanks for the help, I'm happy to work with you.
Franzi, thanks for taking care of the animal paper work, and explaining things to me whenever I ask.
Imam, thanks for your help and the positive attitude every time I asked.
Esther, my dear postdoc, thanks for getting me started in my first 6 months here. Wish I could have more time with you.
Hana, thanks for answering my questions whenever I asked, and delicious food.
Anes, you are kindest girl I met, wish you all the best.
Remi, I really enjoyed every time we met, Eiswiese, Vapiano…
Thanks Carolina for teaching me swimming. I will practice more.
Thanks to my Chinese friends, Xiaoting, Linna, Chao, Bicheng, Mi, Qian…it was my pleasure to have you as friends.

Special thanks to Arne, thanks for being such a good listener, and being always patient with me. Besides, your family is so caring and supporting.
Last but not least, to my family, I cannot make it without your unconditional love and support. I hope I will be there for you too when you need me.

There is no never-ending feast, all good things will come to an end (translated from a Chinese proverb)! Hope the people I love and who love me all the best! And enjoy the sunshine whenever we can because sometimes it rains.

Table of Contents

Chapter 1
Introduction

Introduction

The immune system & autoantibodies

The immune system is defined as the biological system of protecting the host from infection and the damage they cause. It consists of two different mechanisms, the innate immune system and adaptive immune system. The innate immune system is the first line defense system by macrophages, natural killer cells, dendritic cells, granulocytes, and etc. The innate immune response is fast and non-specific, whereas the adaptive immune response is usually slow to develop and highly specific to the antigens. In addition, the adaptive immune system can also form memory resulting in fast response after subsequent presentation of the same antigens. The adaptive immune system is mainly composed of the B and T lymphocytes, which are derived from the bone marrow. B cells become mature in the bone marrow; however, the precursors of T cells migrate to the thymus where they develop as mature T cells. Upon activation, B cells can differentiate into the plasma cells which secrete antibodies against antigens. T cells can recognize the signal from antigen presenting cells, then differentiate either into helper T cells ($CD4^+$) that activate other cells of the immune system or cytotoxic T cells ($CD8^+$) that directly destroy the infected cells (Murphy, 2012).

Although the fundamental role of the immune system is to distinguish non-self from self-molecules, sometimes it produces antibodies that react to self-molecules which are defined as autoantibodies. In healthy individuals, the high affinity of self-reactive T and B lymphocytes in the thymus and bone marrow are eliminated (negative selection) or functionally inactivated (anergy) to maintain self-tolerance. The most common autoantibodies in healthy individuals are mainly low affinity IgM, and occasionally low titer of IgG (Elkon et al., 2008).

Normally, these autoantibodies do not cause serious harm to the host. Study has shown their beneficial effects, such as the autoantibodies against TNF-α have been reported to suppress rheumatoid arthritis (Wildbaum et al., 2003). The self-reactive lymphocytes are required for a functional immune system. However, the strong response to self-antigens can lead to autoimmune diseases that are characterized by tissue damage. For example, in rheumatoid arthritis, autoreactive T cells against antigens of joint synovium can result in joint inflammation and arthritis (Lee, D. M. et al., 2001). In systemic lupus

erythematosus (SLE), there are autoantibodies produced against DNA, chromatin proteins, and ubiquitous ribonucleoprotein antigens which lead to glomerulonephritis, vasculitis, and rash (Rahman et al., 2008). In multiple sclerosis, it was shown that autoreactive T cells against myelin antigens produce the sclerotic plaques in the brain with destruction of myelin sheaths (Correale et al., 2017). Type 1 diabetes is an autoimmune disease characterized by autoreactive T cells against pancreatic islet cell antigens, which can cause destruction of pancreatic islet β cells resulting in non-production of insulin (Li et al., 2017).

There are multiple tolerance mechanisms that can prevent autoimmunity, and these mechanisms are named as checkpoints. Each checkpoint prevents autoreactive responses, and together they can provide efficient protection against autoimmunity. The central tolerance mechanism eliminates those newly formed strongly autoreactive lymphocytes in the thymus and bone marrow (Hogquist et al., 2005; Nemazee, 2017). In the periphery, regulatory T cells (Tregs) suppress the T cell response through cytokine secretion and intercellular signals and self-reactive B and T cells can also be eliminated. The self-reactive lymphocytes remain in low affinity and can be ignored, but they can also be activated under certain circumstances (Cyster et al., 1994; Goodnow et al., 1989; Goodnow et al., 2005; Nemazee, 2006; Russell et al., 1991; Shlomchik, 2008).

The mechanisms of autoimmune disease have not been elucidated yet. An explanation is that it's a combination of genetic susceptibility, self-tolerance breakdown, and environmental triggers such as infections. In human, *AIRE* gene can cause APS-1 (autoimmune polyglandular syndrome 1). *CTLA4* gene is associated with Grave's disease, type 1 diabetes, and etc. (Rioux et al., 2005). The circulating lymphocytes normally have a low affinity for self-antigens, however, they are activated when their autoantigens are also the ligands for Toll-like receptors (TLRs). TLRs are an important protein family expressed on macrophages and other immune cells, which can recognize and bind to different antigens. For example, Toll-like receptor 9 (TCR9) binds to unmethylated CpG sequences in the DNA which is common in bacteria and apoptotic mammalian cells. Once the unmethylated CpG sequences are released as apoptotic fragments, they are recognized and bound by B cell receptors that are specific for chromatin components, the complex can be internalized into B cells. These sequences bind

to TLR9 (expressed in the cytoplasm of B cells) intracellularly, leading to a co-stimulatory signal, together with the signal from B cell receptor, activating the anti-chromatin B cells (Marshak-Rothstein, 2006). Besides, a theory of molecular mimicry proposed that when pathogens share similar structure with human proteins, it will result in the immune system targeting on self-proteins, which will also lead to autoimmune response (Plotz, 2003; Rose, 2001).

Autoimmunity in the brain

The brain is an immunologically privileged site. It is surrounded by the blood-brain barrier (BBB) that prevents the entry of microorganisms and lymphocytes, to protect the neuronal tissue from infection. At the same time, the BBB also blocks complete clearance of pathogens that entered the brain, or protects tumors in the brain (Joyce et al., 2015; Miller et al., 2016). The BBB is composed of brain microvascular endothelial cells, astrocytes and pericytes. The brain microvascular endothelial cells form tight junctions that prevent large molecules to enter. Astrocytes and pericytes help the microvascular endothelial cells to maintain the intact barrier property, which is shown in figure 2 (Kim, K. S., 2008).

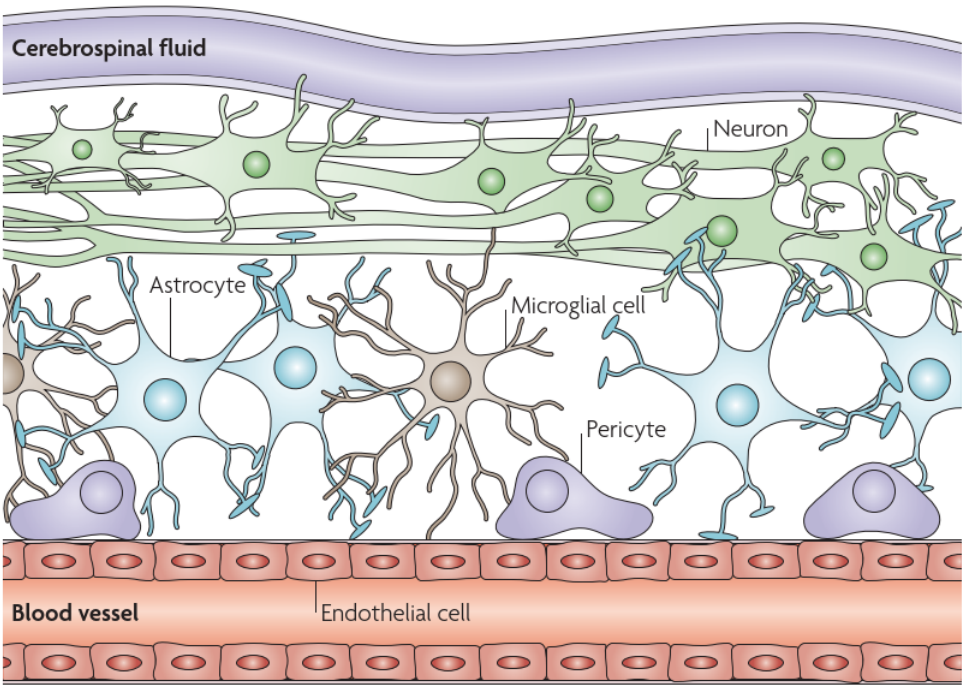

Figure 1 The structure of the blood-brain barrier. The brain microvascular endothelial cells form tight junctions that prevent large molecules to enter the brain. Astrocytes and pericytes help the microvascular endothelial cells to maintain the intact barrier property, modified from (Kim, K. S., 2008).

Autoimmune encephalitis refers to an inflammation in the brain, associated with antibodies against neuronal and synaptic proteins. Once the BBB breaks down, activated T cells enter the brain, which results in further progression of the brain inflammation. For example, in multiple sclerosis, brain inflammation leads to the permeability of the BBB, and activated T cells that are specific for central nervous system (CNS) antigen reencounter the antigen presented by microglia. Th17 and Th1 cells infiltrate into the brain and produce IL-17 and IFN-γ, which recruit and activate myeloid cells that exacerbate the inflammation, resulting in further recruitment of T cells, B cells and innate immune cells. Autoreactive B cells produce autoantibodies against myelin, ultimately leading to demyelination and an alteration of neuronal function (Steinman, 1996).

There are different ways for the antibodies and immune cells to cross the BBB: (I) Systemic cytokines break down the tight junctions in the brain-cerebrospinal fluid barrier, allowing the antibodies or immune cells to enter. (II) Olfactory ensheathing glia facilitate transport of IgGs or immune cells into the brain. (III) Inflammatory cytokines in the blood damage the tight junctions of BBB, allowing the entry of antibodies or immune cells. (IV) Fc receptor mediates transcytosis from the blood vessels, e.g. in systemic lupus erythematosus (Knowland et al., 2014; Platt et al., 2017; Zhao et al., 2015).

Anti-NMDA receptor encephalitis

Dalmau and colleagues described a new autoimmune disease termed as 'anti-NMDA receptor encephalitis' in 2007 (Dalmau et al., 2007). The authors reported that those patients had paraneoplastic encephalitis accompanied by the presence of anti-NMDA receptor antibodies in the serum/cerebrospinal fluid. They also described that this disease is associated with ovarian teratoma, and the patients were mostly young females. Furthermore, these patients developed psychiatric symptoms such as psychosis, seizures, memory deficits, and etc. The mechanism of anti-NMDA receptor encephalitis was interpreted as a decreased density of surface NMDA receptors due to binding of the autoantibodies against NMDA receptors in postsynaptic dendrites (Dalmau et al., 2008; Dalmau et al., 2018; Dalmau et al., 2011; Dalmau et al., 2007).

NMDA receptor & brain function

The NMDA receptors belong to the ionotropic glutamate receptor family. Glutamate is the most important neurotransmitter in normal brain function, especially in the excitatory neurons in the CNS. The glutamate is synthesized in the presynaptic terminals and packaged into synaptic vesicles, released into the synaptic cleft, and bound to the glutamatergic receptors of postsynaptic neurons (Halterman, 2005; Niciu et al., 2012). There are two types of glutamate receptors on the post synaptic neurons: the metabotropic glutamate receptors (mGluRs) and the ionotropic glutamate receptors (iGluRs). The mGluRs are G-protein-coupled receptors, with eight different subtypes (mGluR1-8), and these receptors modulate postsynaptic ion channels indirectly by coupling to different pharmacological agents (Crupi et al., 2019). There are three major iGluRs identified: NMDA receptors (NMDAR), AMPA receptors, and kainate receptors. The iGluRs are nonselective cation channels, allowing Na^+, and K^+ to pass, thus produce excitatory postsynaptic responses. As shown in Figure 2A, the NMDA receptor is a transmembrane protein. When the membrane is at resting potential, the NMDA receptor is blocked by Mg^{2+} ion in the channel pore (Figure 2B). Mg^{2+} is pushed out of the channel pore during depolarization of the postsynaptic neuronal membrane, which allows other cations (Ca^{2+} in addition to Na^+ and K^+) influx, resulting in the activation of the NMDA receptor (Figure 2C). The binding of glutamate and glycine is also required for the activation (Halterman, 2005).

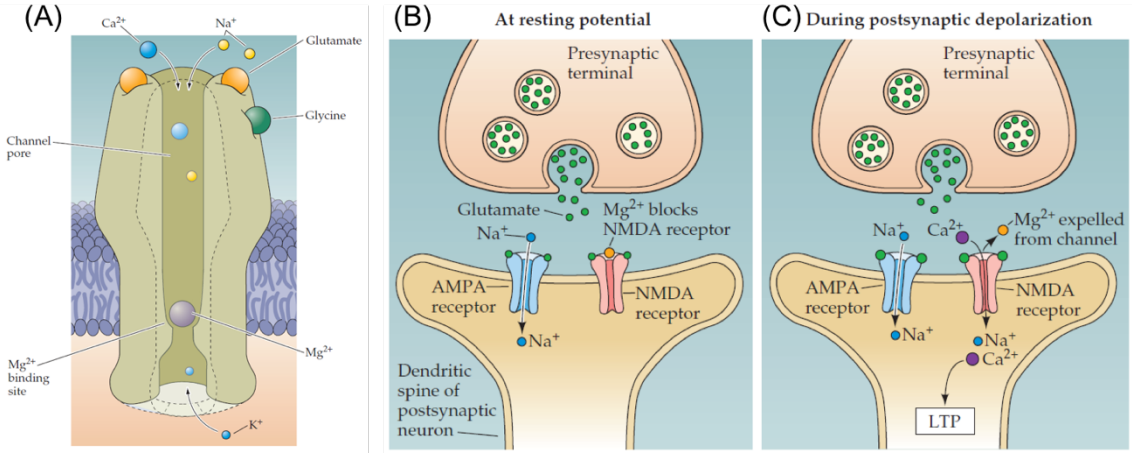

Figure 2 The mechanism of NMDA receptor activation. (A) The structure of NMDA receptor channel as transmembrane protein and its binding sites of Mg^{2+}, glutamate and glycine. Through the receptor pore, Ca^{2+}, Na^{+} and K^{+} can pass through. (B) Synapse at the resting potential; Mg^{2+} blocks NMDA receptor preventing cation flux through receptor. (C) The NMDA receptor at depolarization state: During depolarization, Mg^{2+} is removed from the channel pore, which allows other cations (Ca^{2+} in addition to Na^{+} and K^{+}) influx, resulting in the activation of the NMDA receptor (Halterman, 2005).

There are 7 subunits of NMDA receptor identified so far: GluN1 subunits, 4 GluN2 subunits (GluN2A-GluN2D), and 2 GluN3 subunits (GluN3A, GluN3B). All of these subunits are encoded by separate genes which translated into 900 to over 1480 amino acids (Paoletti et al., 2013). The NMDA receptor is a heterotetrametric complex, GluN1 subunit is the obligatory subunit in all functional NMDA receptors (Kew et al., 2005). It was shown that the subunits of NMDA receptor are expressed differentially in developing and adult brains, also among different brain regions (Akazawa et al., 1994; Henson et al., 2010; Monyer et al., 1994).

NMDA receptors are critical for the foundation of learning and memory through mechanism of long-term potentiation (LTP) (Lynch et al., 1983; Nicoll, 2017). Moreover, dysfunction of NMDA receptor is found in many brain disorders, such as in Alzheimer's disease, Parkinson's disease, depression, schizophrenia, anti-NMDAR encephalitis, and etc. (Paoletti et al., 2013).

NMDAR autoantibodies in human health and disease

Dalmau and his colleagues claimed that anti-NMDA receptor encephalitis was caused by the IgG class of the anti-NMDA receptor antibodies (Dalmau et al., 2008; Dalmau et al., 2007).

Meanwhile, this view has been challenged by the work form our group. We reported a similar seroprevalence of autoantibodies against NMDA receptor subunit GluN1 (NMDAR1-AB) in both healthy and disease human groups, and an increase upon aging. Moreover, all these antibodies are functional regardless of the immunoglobulin classes (IgA, IgG, and IgM), and they also do not differ regarding epitope binding to the NMDA receptors (Castillo-Gomez et al., 2017; Dahm et al., 2014; Ehrenreich, 2017, 2018; Hammer et al., 2014).

Investigation of NMDAR1-AB in non-human mammals (Project 1)

In 2015, the NMDAR1-AB were first described in non-human mammals, a polar bear named Knut, in Berlin Zoological Garden. After epileptic seizures in 2011, the pathological analyses in Kunt's brain showed signs of encephalitis, and NMDAR1-AB were found in his cerebrospinal fluid (Prüss et al., 2015). We believe that the NMDAR1-AB belong to the natural autoantibody repertoire, thus they might also be found in other non-human mammals. To prove it, we screened the NMDAR1-AB seroprevalence in mice, rats, dogs, cats and monkeys (baboons and rhesus macaques).

In addition, we immunized both *ApoE*$^{-/-}$ (with compromised BBB) and WT mice with a mixture of 4 peptides against GluN1 subunit of the NMDA receptor. After 4 weeks of immunization, we performed open field testing with MK801 (NMDA receptor antagonist) treatment and looked for inflammation markers in the brain after the termination of the experiment. All the results are presented and discussed in Chapter 2 (Project 1).

Investigation of potential NMDAR1-AB inducers (Project 2)

Shown in the cases of anti-NMDAR encephalitis, the presence of NMDAR1-AB seems to be associated with tumor, such as ovarian teratoma (Dalmau et al., 2008; Dalmau et al., 2011; Dalmau et al., 2007). Other studies have also suggested the association of NMDAR1-AB with patients who were infected with influenza A/B (Castillo-Gomez E, 2016; Hammer et al., 2014). Herpes simplex virus encephalitis was also reported as a trigger for NMDAR1-AB production (Prüss et al., 2012).

In our design, we investigated more potential inducers including brain injury, checkpoint inhibitor, and chronic life stress in mice/human, which is detailed described in Chapter 3 (Project 2).

Scope of the present work

As discussed in the introduction, it remains unclear what is the mechanism behind the anti-NMDA receptor encephalitis. What are the effects of carrying high level of NMDAR1-AB and what are the inducers of the NMDAR1-AB formation? Thus, my present thesis aimed to answer these questions.

In my 1st project, we aimed at (i) the seroprevalence and functionality of NMDAR1-AB in non-human mammals; (ii) the consequences of high circulating levels of endogenously produced NMDAR1-AB of the IgG class (by immunization) in mice with compromised BBB, by behavioral and morphological testing.

In my 2nd project, we aimed at (i) the course of spontaneously formed NMDAR1-AB in mouse and human upon long-term observation, with intact and compromised BBB; (ii) brain lesion (cryolesion mocel) as a potential inducer of NMDAR1-AB; (iii) immune checkpoint inhibitor: CTLA4-AB as a potential inducer; (iv) chronic stress as a potential inducer: our hypothesis derived from project 1.

Chapter 2
Project I

2. Project I:
Uncoupling the widespread occurrence of anti NMDAR1 autoantibodies from neuropsychiatric disease in a novel autoimmune model

Overview of project I

NMDAR1-AB (IgG class) has been reported to be associated with anti-NMDAR1 encephalitis by Dalmau and colleagues (Dalmau et al., 2008; Dalmau et al., 2011; Dalmau et al., 2007). However, previous work from our group showed a considerable seroprevalence in health as well as in disease groups, and the seroprevalence increases with age (Castillo-Gomez et al., 2017; Dahm et al., 2014; Hammer et al., 2014). The NMDAR1-AB in different groups also exhibited similar functionality and epitopes binding to the NMDA receptor (Castillo-Gomez et al., 2017; Hammer et al., 2014).

Next, there are still several questions that we would like to address:

(I) Whether the properties of NMDAR1-AB are unique in human or not? To answer this question, we screened the existence of NMDAR1-AB in the blood samples of dogs, cats, mice, rats, and monkeys (baboons and rhesus macaques). We found NMDAR1-AB in all the species tested. Furthermore, an age-dependent increase of NMDAR1-AB in all the species except for monkeys (baboons and rhesus macaques), which already had a high seroprevalence at an early age. Therefore, we hypothesized that chronic life stress might be associated with the NMDAR1-AB production. Since the monkeys were not domesticated animals but were the 1st or 2nd generation in captivity. Driven by this hypothesis, we wondered if there is a pre-disposition for high seroprevalence of NMDAR1-AB in humans if they were also under chronic life stress. We screened the NMDAR1-AB in the blood samples from the 1st and 2nd generation of human migrants in our GRAS (Göttingen Research Association for Schizophrenia) database (Begemann et al., 2010; Hammer et al., 2014; Ribbe et al., 2010; Stepniak et al., 2015). GRAS is a unique database established in our group, with the design of associating the genetic information with neuropsychiatric phenotypes. Indeed, we observed a high seroprevalence of NMDAR1-AB in the

young migrants, especially IgA class. This served as an indirect indicator that chronic life stress could be one of the inducers of the NMDAR1-AB.

(II) What are the effects of carrying high titer of NMDAR1-AB in mice?
In order to study the effect of NMDAR1-AB produced endogenously in mice, we immunized both WT and *ApoE*$^{-/-}$ (*Apolipoprotein E* deficient) mice with GluN1 antigen cocktail which contains 4 different peptides from the extracellular structure of NMDA receptor. Since apolipoprotein E (ApoE) mediates lipoprotein uptake, the *ApoE*$^{-/-}$ mice have a high cholesterol level, which is believed to increase the BBB permeability. The level of the BBB breakdown has shown to be increased upon aging or after injury in mice (Hafezi-Moghadam et al., 2007; Methia N et al., 2001). Another study reported that the BBB breakdown is likely due to the activation of cyclophilin A (CypA) which led to vascular defects in the *ApoE*$^{-/-}$ mice (Bell et al., 2012).

The titer of NMDAR1-AB was confirmed by ELISA, and it showed a similar kinetics as ovalbumin (OVA). In the open field test, we observed a higher level of locomotion after MK801 (dizocilpine) treatment in *ApoE*$^{-/-}$ mice carrying NMDAR1-AB compared to the WT mice carrying NMDAR1-AB. MK801 is a noncompetitive antagonist of the NMDA receptor, binding to the core of the NMDA receptor channel. Studies have shown that administration of MK801 in rodents induce locomotor hyperactivity, it was used in modelling psychosis-like behavior in rodents (Hammer et al., 2014; Lee, G. et al., 2019; Vishnoi et al., 2015; Zuo et al., 2006). Next, we wondered if encephalitis was developed due to a high titer of NMDAR1-AB IgG classes produced in mice. However, no signs of inflammation was detected in mouse brains, clearly suggesting that the mice carrying functional NMDAR1-AB do not necessarily develop anti-NMDA receptor encephalitis. Therefore, we hypothesized that pre-existing encephalitis plus circulating NMDAR1-AB will lead to Dalmau's anti-NMDAR1 encephalitis. This project is currently running in our group by immunizing a mouse model followed by induction of brain inflammation.

Original publication

Pan H*, Oliveira B*, Saher G*, Dere E, Tapken D, Mitjans M, Seidel J, Wesolowski J, Wakhloo D, Klein-Schmidt C, Ronnenberg A, Schwabe K, Trippe R, Mätz-Rensing K, Berghoff S, Al-Krinawe Y, Martens H, Begemann M, Stöcker W, Kaup FJ, Mischke R, Boretius S, Nave KA, Krauss JK, Hollmann M, Lühder F, Ehrenreich H. Uncoupling the widespread occurrence of anti-NMDAR1 autoantibodies from neuropsychiatric disease in a novel autoimmune model. Mol Psychiatry. 2019 Oct; 24(10):1489-1501. doi: 10.1038/s41380-017-0011-3. Epub 2018 Feb 9.

* Shared first authorship.

Personal contribution: I was responsible for the conduction of most of the experiments and data analyses of this study under the supervison of HE and FL, including cross-validation of NMDAR1-AB detection method (Figure 1a); NMDAR1-AB determination in mice, rats, dogs, cats, baboons, rhesus macaques (Figure 1b), and human migrants (Figure 1c migrants); mouse immunization study: all the blood collection, ELISA (Figure 2c), behavior tests (Figure 2d), immunohistochemistry staining and quantification for CD3 (Figure 2e CD3). In additon, I also contributed to the figure design and paper wirting.

Molecular Psychiatry (2019) 24:1489–1501
https://doi.org/10.1038/s41380-017-0011-3

ARTICLE

Uncoupling the widespread occurrence of anti-NMDAR1 autoantibodies from neuropsychiatric disease in a novel autoimmune model

Hong Pan[1] · Bárbara Oliveira[1] · Gesine Saher[2] · Ekrem Dere[1] · Daniel Tapken[3] · Marina Mitjans[1] · Jan Seidel[1] · Janina Wesolowski[1] · Debia Wakhloo[1] · Christina Klein-Schmidt[3] · Anja Ronnenberg[1] · Kerstin Schwabe[4] · Ralf Trippe[3] · Kerstin Mätz-Rensing[5] · Stefan Berghoff[2] · Yazeed Al-Krinawe[4] · Henrik Martens[6] · Martin Begemann[1] · Winfried Stöcker[7] · Franz-Josef Kaup[5] · Reinhard Mischke[8] · Susann Boretius[9] · Klaus-Armin Nave[2,10] · Joachim K. Krauss[4] · Michael Hollmann[3] · Fred Lühder[11] · Hannelore Ehrenreich[1,10]

Received: 29 August 2017 / Revised: 20 October 2017 / Accepted: 30 October 2017 / Published online: 9 February 2018

Abstract

Autoantibodies of the IgG class against N-methyl-D-aspartate-receptor subunit-NR1 (NMDAR1-AB) were considered pathognomonic for anti-NMDAR encephalitis. This view has been challenged by the age-dependent seroprevalence (up to >20%) of functional NMDAR1-AB of all immunoglobulin classes found in >5000 individuals, healthy or affected by different diseases. These findings question a merely encephalitogenic role of NMDAR1-AB. Here, we show that NMDAR1-AB belong to the normal autoimmune repertoire of dogs, cats, rats, mice, baboons, and rhesus macaques, and are functional in the NMDAR1 internalization assay based on human IPSC-derived cortical neurons. The age dependence of seroprevalence is lost in nonhuman primates in captivity and in human migrants, raising the intriguing possibility that chronic life stress may be related to NMDAR1-AB formation, predominantly of the IgA class. Active immunization of $ApoE^{-/-}$ and $ApoE^{+/+}$ mice against four peptides of the extracellular NMDAR1 domain or ovalbumin (control) leads to high circulating levels of specific AB. After 4 weeks, the endogenously formed NMDAR1-AB (IgG) induce psychosis-like symptoms upon MK-801 challenge in $ApoE^{-/-}$ mice, characterized by an open blood–brain barrier, but not in their $ApoE^{+/+}$ littermates, which are indistinguishable from ovalbumin controls. Importantly, NMDAR1-AB do not induce any sign of inflammation in the brain. Immunohistochemical staining for microglial activation markers and T lymphocytes in the hippocampus yields comparable results in $ApoE^{-/-}$ and $ApoE^{+/+}$ mice, irrespective of immunization against NMDAR1 or ovalbumin. These data suggest that NMDAR1-AB of the IgG class shape behavioral phenotypes upon access to the brain but do not cause brain inflammation on their own.

Introduction

Autoantibodies (AB) of the immunoglobulin G (IgG) class against the N-methyl-D-aspartate-receptor subunit-NR1 (NMDAR1) were originally interpreted as pathognomonic for a condition called "anti-NMDAR encephalitis", characterized by high serum and cerebrospinal fluid (CSF) titers of these AB, as well as a variably favorable response to immunosuppressive therapy. The reported syndrome, reflecting typical NMDAR1 antagonistic actions, consisted of psychosis, epileptic seizures, dyskinesia, cognitive decline, reduced consciousness, and autonomic dysregulation [1–4]. However, work on >5000 individuals, healthy or affected by different diseases, consistently revealed overall comparable age-dependent seroprevalence of functional NMDAR1-AB of all Ig classes, nurturing serious doubts regarding a purely pathological role of NMDAR1-AB of any Ig class [5–10].

NMDAR1-AB apparently belong to a pre-existing autoimmune repertoire [11–17], where Ig isotypes are determined by extracellular vs. intracellular antigen location [6]. This may explain the rarity of the IgG class among AB directed against extracellular epitopes, e.g., NMDAR1,

Hong Pan, Bárbara Oliveira, and Gesine Saher contributed equally to this work.

✉ Hannelore Ehrenreich
ehrenreich@em.mpg.de

Extended author information available on the last page of the article

MOG, and CASPR2. In contrast, AB that recognize intracellular antigens, e.g., amphiphysin, ARHGAP26, or GAD65, show predominance of IgG [6]. Despite this apparent "physiological autoimmunity", no report exists that systematically screened mammals other than humans for the presence of NMDAR1-AB. In recent work, we found that all naturally occurring NMDAR1-AB are functional and thus have pathogenic potential irrespective of epitope and Ig class [10]. Pathophysiological significance may emerge in conditions of compromised blood–brain barrier (BBB), for instance, upon injury, infection, inflammation, or genetic predisposition (*APOE4* haplotype), which then allows substantial access of circulating NMDAR1-AB to the brain where they act as NMDAR antagonists [5, 9, 18–20]. Alternatively, AB-specific plasma cells may reside or settle in the brain and produce large amounts of AB intrathecally [14, 21]. The question whether abundant endogenously produced NMDAR1-AB of the IgG class can—upon access to the brain—induce inflammation and thus "anti-NMDAR1 encephalitis" has never been experimentally addressed.

The present paper has therefore been designed to (i) systematically screen mammals other than humans for seroprevalence of functional NMDAR1-AB and (ii) study mice with open BBB behavioral and morphological consequences of high circulating levels of endogenous NMDAR1-AB of the IgG class formed in response to immunization.

Materials and methods

Ethical approvals

Ethics committees of Georg-August University, Göttingen, and collaborating centers approved the Göttingen Research Association for Schizophrenia (GRAS) data collection and other studies "extended GRAS" acquiring human data, serum samples, and IPSC [5, 6, 8, 9, 22, 23]. Hannover Medical School Ethics Committee approved the neurosurgical specimen collection. Studies comply with Helsinki Declaration. Patients gave written informed consent. Mouse studies were approved by Animal Ethics (LAVES, Oldenburg) following German Animal Protection Law.

Notes: All experiments were performed by researchers unaware of group assignment. The new nomenclature GluN1 for NMDAR1 is mostly disregarded here for consistency with the respective literature.

Human samples

GRAS and "extended GRAS"

The GRAS [22, 23] subsample used here consists of deep-phenotyped patients ($N = 970$; age 39.29 ± 0.40 years; 66.3% men), diagnosed with schizophrenia or schizoaffective disorder according to DSM-IV-TR [24]. Subjects of "extended GRAS" ($N = 4933$; age 43.29 ± 0.24 years; 56.9% men) comprise healthy individuals and patients with different neuropsychiatric diagnoses, including schizophrenia, affective disorders, multiple sclerosis, Parkinson, ALS, stroke, and personality disorders (detailed description in [5, 6, 8, 9]). For this study, subjects are dichotomously classified as nonmigrants or migrants comprising first (patient migrated) and second generation (parents migrated). Identified migrants ($N = 301/N = 4933$) are from Europe (49.8%), Asia (36.9%), Africa (9%), North America (2%), South America (0.7%), or mixed (1.6%).

Neurosurgical patients

A total of $N = 72$ paired samples of serum and ventricular CSF were available from patients ($N = 45$ women; age 55.9 ± 2.2 years; $N = 27$ men; age 60.2 ± 2.7 years) undergoing neurosurgery for various reasons: meningiomas, metastases, and other brain tumors ($N = 25$); intracerebral/subarachnoid hemorrhages ($N = 20$); hydrocephalus ($N = 12$); arterial aneurysms ($N = 7$); trigeminal neuralgia ($N = 4$); and others ($N = 4$). Most pairs were taken simultaneously at the time point of surgery, i.e., <5 min ($N = 64$) or <30 min ($N = 8$) apart.

Other mammals

Dogs and cats

Serum samples from dogs and cats of different breeds were prospectively collected during routine (health check/vaccination) or diagnostic (spectrum of different disorders) workup of outpatients in the Small Animal Clinic, University of Veterinary Medicine, Hannover.

Monkeys

Serum samples from healthy baboons and rhesus macaques were obtained through routine checkups at the Leibniz Institute for Primate Research, Göttingen.

Rodents

Serum samples from healthy rats and mice were obtained at the Max Planck Institute of Experimental Medicine and the Institute for Multiple Sclerosis Research, Göttingen.

Serological analyses

NMDAR1-AB determination by clinical standard procedures

Human serum and ventricular CSF were tested for NMDAR1-AB positivity using commercially available kits,

based on HEK293T cells transfected with NMDAR1 and secondary AB against human IgG, IgM, or IgA (Euroimmun, Lübeck, Germany) [2, 25]. Mouse serum was analyzed using the same assay with secondary AB against mouse IgG, IgM, or IgA (M31001, A-31570, A-21042; Thermo Fisher, Rockford, USA).

NMDAR1-AB IgM screening in monkey samples

HEK293T cells (50,000) cultured at 37 °C/8% CO_2 in DMEM (high glucose, Life Technologies, Carlsbad, USA) were seeded on a 35 -mm dish, grown for 3 days, and transfected with 3 µg of myc-His-tagged GluN1-1b cloned into pcDNA4/TO/myc-His A (Invitrogen, Carlsbad, USA) using Metafectene-Pro (Biontex, Munich, Germany) [10]. One day post transfection, cells were split onto five poly-D-lysine-coated coverslips in a 35 -mm dish and 1 day later, they were fixed with 5% paraformaldehyde (PFA) for 20 min, washed 5× (PBS), permeabilized with 0.1% Triton X-100 for 5 min, again washed 5× (PBS), and blocked with 5% normal goat serum (NGS; Sigma-Aldrich, Munich, Germany) for 1 h. After five PBS washes, cells were incubated with serum and monoclonal mouse anti-myc IgG (clone 9E10, Hollmann-Lab, Bochum) for 1 h, washed with 10× (PBS), incubated for 1 h with fluorescein-labeled goat anti-monkey IgM (072-11-031; KPL, Gaithersburg, USA) and AlexaFluor®594-labeled goat anti-mouse IgG (A11005; Thermo Fisher) secondary AB, and PBS washed 5×. Cells were mounted in Fluoromount-G (Southern Biotech, Birmingham, USA) and analyzed via TCS-SP2-AOBS confocal microscope (63× oil immersion objective; Leica-Microsystems, Wetzlar, Germany). The results were independently assessed by three investigators.

Protein-A assay

Human serum (for cross-validating clinical standard procedure and protein-A method), as well as dog, cat, rat, and monkey serum were labeled with protein-A from *Staphylococcus aureus*, binding the Fc portion of immunoglobulins of different species [26]. Plasma (50 µl) and 25 µg of FITC-conjugated protein-A (Sigma-Aldrich) were incubated for 2 h in the dark at room temperature (RT). The mixture was then diluted to 250 µl (PBS) and unbound FITC–Protein-A was removed using 100- kDa Amicon filter units (Sartorius, Göttingen, Germany), reconcentrating to ~50 µl [27]. NMDAR1-AB seropositivity was determined using Euroimmun assay combined with commercial monoclonal mouse NMDAR1-AB (114011; M68, SYSY, Göttingen, Germany). Samples showing distinct double labeling were rated "positive" (>98% consensus of three investigators).

Endocytosis assay

Functional studies were conducted with sera following ammonium-sulfate precipitation of immunoglobulins [28] and dialysis (Slide-A-Lyzer® Mini Dialysis Units, 10,000 MWCO Plus Float, Thermo Fisher). To assess AB functionality, human IPSC-derived neurons were exposed to dialyzed serum [10]. For each species, arbitrarily selected seronegative ($N = 1$) and seropositive samples ($N = 2$–3) were analyzed. Briefly, cells were precooled on ice and washed prior to incubation in cold HBSS with 1:50 diluted dialyzed sera, control NMDAR1-AB (M68-SYSY), or HBSS alone (negative control) for 30 min/4 °C. After washing to remove unbound AB, neurons were returned to their media and incubated for 20 min at 37 °C (three coverslips/sample, endocytosis) or 4 °C (one coverslip/sample, endocytosis control). The remaining surface NMDAR1 was exposed to mouse anti-human NMDAR1-AB (N-terminal; ab134308; Abcam, Cambridge, UK, 1:100), followed by labeling with secondary donkey anti-mouse IgG (A10036; Life Technologies, AlexaFluor®546, 1:100). Neurons were fixed with ice-cold 4% PFA and double stained with chicken anti-NeuN-AB (266006; SYSY, 1:500) and secondary donkey anti-chicken AB (703-546-155; Life Technologies, AlexaFluor®488, 1:250). Nuclei were visualized using DAPI (Sigma-Aldrich, 0.01 µg/ml). After PBS wash, coverslips were mounted on SuperFrost®-Plus slides with Mowiol mounting media (Sigma-Aldrich). Confocal laser-scanning microscopy was used to quantify NMDAR1 density at the membrane (63× glycerol objective; TCS-SP5 Leica-Microsystems, Mannheim, Germany). From each coverslip, Z series of optical sections (0.5 µm apart) covering the three-dimensional extension of neurons were acquired (sequential scanning mode, identical acquisition parameters). FIJI-ImageJ software [29] was used to randomly select $NeuN^+$ cells and determine soma profile. Fluorescence intensity/cell surface area (AlexaFluor546) was automatically measured as readout of NMDAR1 surface expression. After background subtraction, the mean intensity for each coverslip was determined and fluorescence intensity ratio (37/4 °C) was calculated.

BBB-integrity testing

BBB integrity of 12-month-old $ApoE^{-/-}$ ($N = 5$) and $ApoE^{+/+}$ ($N = 5$) mice was determined using two different fluorescent tracers, Evans blue (50 mg/g body weight) [30] and sodium fluorescein (200 mg/g body weight). A detailed description of this method will be published elsewhere [31]. Briefly, for tracer quantification in the brain at 4 h after intravenous injection in the tail vein, animals were PBS perfused to remove the circulating tracer. Brains were dissected, immediately frozen on dry ice, weighed, and stored

at −80 °C. Tissue was lyophilized at −56 °C for 24 h under vacuum of 0.2 mBar (Christ LMC-1-BETA-1-16, Osterode, Germany). For tracer extraction, hemispheres were incubated with shaking in 10 ml formamide/mg brain at 57 °C for 24 h. Integrated density of tracer fluorescence was determined in triplicates on a fluorescent microscope (Observer Z2, Zeiss, Germany), equipped with AxioCamMRc3, 1×Camera-Adapter, and ZEN2012 blue-edition software, recorded at 10× magnification (Plan-Apochromat 10×/0.45M27). Tracer concentration was calculated using a standard curve and normalized to controls (set to 1).

Mouse immunization

Mice (12-month-old C57BL/6 littermates: $ApoE^{-/-}N = 20$ and $ApoE^{+/+}N = 23$; genders balanced) were immunized with a mixture of GluN1 extracellular peptides and/or chicken ovalbumin (Sigma-Aldrich), and emulsified in equal volume of complete Freund's Adjuvant (*Mycobacterium tuberculosis* H37RA plus incomplete Freund's Adjuvant; Becton-Dickinson, Sparks, USA) at a final concentration of 1 mg/ml [32]. At the tail base, 50 µg of GluN1 peptides and/or 20 µg of ovalbumin were injected subcutaneously (each side one).

Enzyme-linked immunosorbent assay (ELISA)

Orbital sinus blood of immunized mice was stored as EDTA plasma at −80 °C. ELISA plates (96 well) were coated with 0.5 µg of GluN1 peptide mixture or 0.2 µg of chicken ovalbumin in 50 µl PBS/well overnight at 4 °C and blocked with 5% BSA/PBS (Carl Roth, Karlsruhe, Germany). Mouse plasma (1:1000 or 1:50,000 5% BSA/PBS 50 µl/well) was added for 2 h at RT. The signal was amplified with horseradish peroxidase-linked anti-IgG (Sigma-Aldrich), and 3,3′,5,5′-Tetramethylbenzidine as colorimetric substrate (BD Biosciences, San Jose, USA). Absorbance at 450 nm was measured by microplate reader (Tecan-Trading AG, Männedorf, Switzerland).

Basic behavioral screening

The behavioral test battery was performed as described previously [33–36]. Starting at age 5 months, experimentally naïve $ApoE^{-/-}$ and $ApoE^{+/+}$ littermates underwent (during light phase) tests of anxiety, activity and exploratory behavior (elevated plus-maze, open field, hole-board), motor (rotarod, grip strength) and sensory function (visual cliff, olfaction, hearing, hot plate), sensorimotor gating (prepulse inhibition), pheromone-based social preference, and cognitive performance (IntelliCage place/reversal learning). Males and females were tested separately.

Baseline and post MK-801 locomotion in the open field

The open-field apparatus consisted of a gray circular Perspex-arena (120 cm diameter; wall height 25 cm). Indirect white light illumination ensured constant light intensity of 120 lux in the center. Locomotion was measured using automated tracking software (Viewer2-Biobserve, Bonn, Germany). $ApoE^{-/-}$ and $ApoE^{+/+}$ littermates received four baseline measurements preimmunization and post immunization (15 min each), the last followed by intraperitoneal MK-801 (Dizocilpine-[5S,10R]-(+)-5-methyl-10,11-dihydro-5H-dibenzo[a,d]cyclohepten-5,10-imine hydrogen maleate; 0.3 µg/10 µl PBS/g Sigma-Aldrich). MK-801 is a noncompetitive NMDAR antagonist, acting as a use-dependent ion-channel blocker, and known to induce psychosis-like hyperactivity in the open field (loss of inhibition) [37]. Directly post injection, locomotor activity in open field was analyzed (4 min intervals), with the first 4 min defined as reference locomotion to express changes over 120 min as % reference.

Immunohistochemistry

Mice were anesthetized with Avertin (2,2,2-Tribromoethanol, Sigma-Aldrich), and transcardially perfused with 4% PFA/Ringer solution (Braun-Melsungen, Germany). Brains were removed, postfixed in 4% PFA overnight at 4 °C, and incubated in 30% sucrose/PBS for 2 days at 4 °C. Brains were cryosectioned coronally into 30 µm slices and stored in 25% ethylene glycol and 25% glycerol/PBS at −20 °C. Frozen sections (three/mouse; rostral hippocampus), mounted on SuperFrost®-Plus slides (Thermo Fisher, Waltham, USA), were used for cell quantification. For CD3 staining, sections were microwaved 3× for 4 min in citrate buffer (1 mM, pH 6) and blocked with 5% normal horse serum (NHS), and 0.5% Triton X-100/PBS for 1 h at RT. Incubation with rat anti-mouse CD3 (MCA1477; BioRad, Hercules, USA; 1:100) diluted in 5% NHS, and 0.5% Triton X-100/PBS was performed for two nights/4 °C, followed by incubation with goat anti-rat AlexaFluor®647 (A-21247; Thermo Fisher, Schwerte, Germany; 1:1000) diluted in 5% NHS, and 0.5% Triton X-100/PBS for 2 h at RT. For Iba1, GFAP, CD68, and MHC-II staining, sections were blocked with 5% NGS and/or 5% NHS in 0.5% Triton X-100/PBS for 1 h at RT. Incubation with rabbit anti-mouse Iba1 (019-19741; Wako-Chemicals GmbH, Neuss, Germany; 1:1000), or mouse anti-mouse GFAP (NCL-GFAP-GA5; Novocastra-Leica, Newcastle upon Tyne, UK; 1:500), diluted in 3% NGS or 3% NHS, and 0.5% Triton X-100/PBS, was performed overnight, and incubation with rat anti-mouse CD68 (MCA1957GA; BioRad GmbH, München, Germany, 1:400) and rat

anti-mouse MHC-II (14-5321; eBioscience, San Diego, USA, 1:100) diluted in 3% NGS and 3% NHS, and 0.5% Triton X-100/PBS, was performed over two nights, all at 4 °C. Incubation with secondary antibodies was performed with goat anti-rabbit AlexaFluor®555 (A-21428; Thermo Fisher; 1:500) diluted in 3% NGS, 0.5% Triton X-100/PBS, or donkey anti-rabbit AlexaFluor®488 (A-21206; Thermo Fisher, 1:500) or donkey anti-mouse AlexaFluor488 (A21202; Thermo Fisher, 1:500) or goat anti-rat AlexaFluor®647 (A-21247; Thermo Fisher, 1:500), diluted in 3% NGS or 3% NHS, and 0.5% Triton X-100/PBS for 1.5 h at RT. Nuclei were counterstained with DAPI (Sigma-Aldrich, 0.01 µg/ml) and sections were mounted using Aqua-Poly/Mount (Polysciences, Warrington, USA). Tile scans of hippocampus were acquired using Leica-DMI6000 epifluorescence microscope (20× objective; Leica) and $Iba1^+$ and $CD3^+$ cells were counted using cell counter plug-in of FIJI-ImageJ software [29]. $GFAP^+$ cells in the hippocampus were quantified densitometrically upon uniform thresholding (expressed as % respective area).

Statistical analyses

Statistical analyses were performed using SPSSv.17 (IBM-Deutschland-GmbH, Munich, Germany) or Prism4 (GraphPad Software, San Diego, California, USA). Group differences in categorical and continuous variables were assessed using χ^2, Mann–Whitney U, or Student's *t*-tests depending on data distribution/variance homogeneity. ANOVA was employed as indicated in display item legends. All *p*-values are two tailed; significance is set to $p < 0.05$; data are presented as mean ± S.E.M.

Results

Cross-validation of NMDAR1-AB detection methods

To determine NMDAR1-AB seropositivity in mammals other than humans, we had to validate the protein-A detection method [27]. For that, $N = 72$ paired human serum and ventricular CSF samples, prospectively collected from random neurosurgical patients, were analyzed by the usual cell-based assay, employing specific secondary AB for all Ig classes. A total of $N = 5$ sera turned out NMDAR1-AB positive (titers ≤ 1:100; 3× IgM; 2× IgA; 0× IgG). Ventricular CSF samples were all negative. For cross-validation of NMDAR1-AB of the IgG class, we used serum of a seropositive stroke patient [8]. Application of protein-A method combined with double labeling for NMDAR1-AB M68 confirmed positive and negative results (Fig. 1a).

High seroprevalence of NMDAR1-AB across mammalian species

We next analyzed by protein-A method serum samples of dogs, cats, rats, baboons, and rhesus macaques. Strikingly, all mammalian species, independent of their respective life expectancy, show high NMDAR1-AB seropositivity (Fig. 1b). Mouse samples were analyzed using specific AB against murine IgA, IgM, and IgG. As known for humans [6], NMDAR1-AB of the IgG class were the rarest. For another cross-validation, all monkey samples ($N = 100$) were analyzed in blinded fashion by an independent lab (Bochum; using specific anti-monkey IgM). IgM-positive results coincided with the protein-A positivity by >97% (76 of 78). The fraction of protein-A positive but IgM-negative monkey samples (total 22%) likely presents NMDAR1-AB of IgA class and IgG class where specific AB were not available.

Age-dependent NMDAR1-AB seroprevalence except for nonhuman primates and human migrants

All species revealed age dependence of NMDAR1-AB seroprevalence (χ^2 test; dogs: $\chi^2(1) = 11.5$, $p = 0.01$; cats: $\chi^2(1) = 4.8$, $p = 0.03$; rats: $\chi^2(1) = 9.5$, $p = 0.002$; and mice: Fisher's exact test $p = 0.032$) as for humans [5, 8] with the exception of baboons ($\chi^2(1) = 1.0$, $p = 0.3$), where already >50% of young animals were seropositive. This surprising result made us investigate another monkey species, rhesus macaques, showing again high seroprevalence in old and young animals ($\chi^2(1) = 0.2$, $p = 0.6$) (Fig. 1b). We wondered what the difference between humans, dogs, cats, mice, and rats, on one hand, and monkeys, on the other hand, could be, leading to loss of the usual age pattern regarding seroprevalence. Postulating that captivity/non-domestication of young monkeys might induce chronic life stress due to maladaptation to the environment, we investigated in a hypothesis-driven way whether young human migrants would display a similar increase in NMDAR1-AB seropositivity. Of the GRAS data collection, detailed information on migration was available in a subsample of $N = 970$ individuals. While nonmigrants show the typical age association of NMDAR1-AB seroprevalence ($\chi^2(1) = 10.7$, $p = 0.001$), migrants do not ($\chi^2(1) = 0.6$, $p = 0.4$) (Fig. 1c). Seroprevalence in young migrants is significantly higher as compared to young nonmigrants ($\chi^2(1) = 5.381$, $p = 0.020$). In both monkey species and migrants, the IgM fraction still follows the expected age trend, while IgA seems to account for the early increase in NMDAR1-AB seroprevalence (Fig. 1c). Presentation of NMDAR1-AB by Ig class in the extended GRAS sample ($N = 4933$), with $N = 4632$ of likely nonmigrants (available information less detailed) and $N = 301$ known migrants, illustrates the

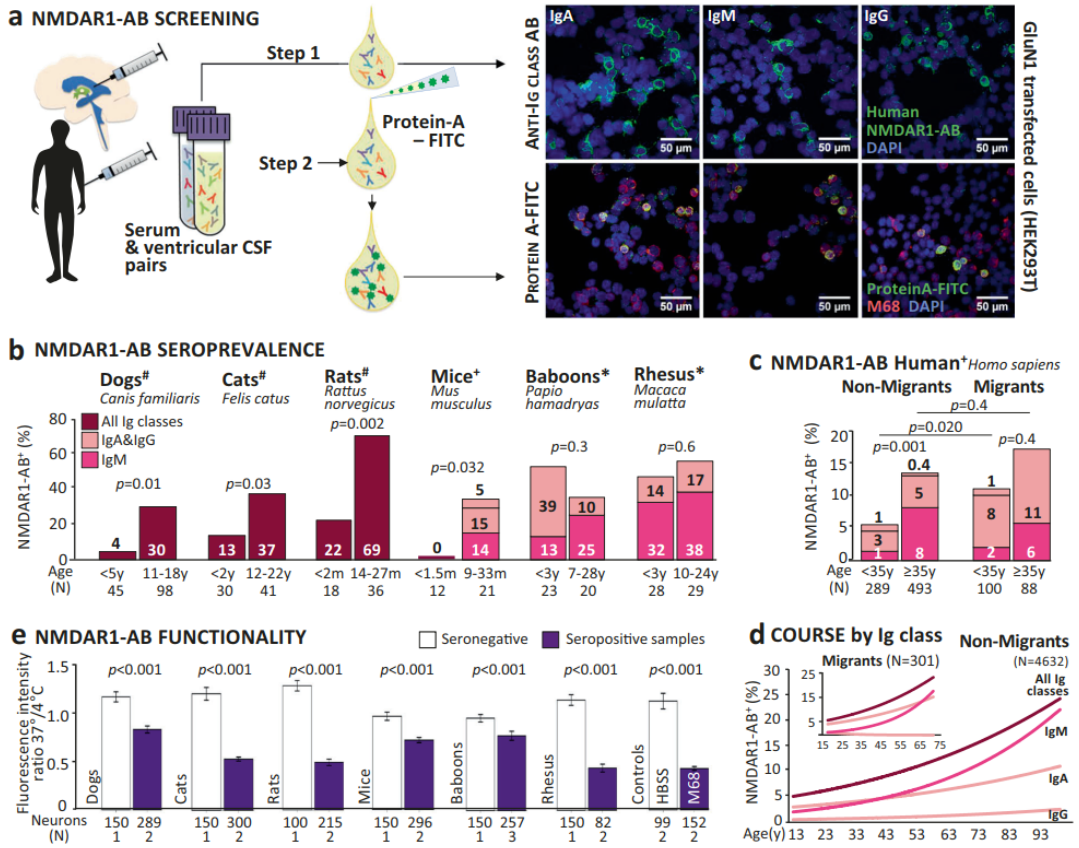

Fig. 1 NMDAR1-AB seropositivity and functionality across mammalian species. **a** Cross-validation of assays: paired serum and intraventricular CSF samples from neurosurgical patients were tested using a HEK293T cell-based clinical standard assay for NMDAR1-AB seropositivity (Euroimmun biochip). For step 1, fluorescently labeled IgA-specific, IgM-specific, and IgG-specific secondary AB were used; for method cross-validation (step 2), NMDAR1-AB seropositive and seronegative samples of each Ig class from step 1 were labeled with protein-A–FITC conjugate and tested for colocalization (yellow) of protein-A–FITC^{+} (green) and M68^{+} (monoclonal mouse NMDAR1-AB followed by Alexa555 donkey anti-mouse IgG red). Representative pictures of both methods using the same seropositive samples (IgA, IgM, and IgG) are displayed on the right: upper row step 1/lower row step 2. **b** NMDAR-AB seropositivity (%) of young and old mammals for all Ig classes combined ($^{\#}$protein-A–FITC/Euroimmun) or for individual classes ($^{+}$Euroimmun; *protein-A–FITC/Euroimmun and cross-validation with Euroimmun/monkey IgM) presented in the bars; color codes used for consistency and kept also in **c** and **d**; age given in months (m) or years (y); χ^2 or Fisher's exact test. **c** NMDAR-AB seropositivity of subjects with migration (first and second generation) vs. nonmigration history (GRAS data collection); all Ig classes presented; age split at 35 years; χ^2 test. **d** NMDAR1-AB course by Ig classes in serum over age groups in migrants vs. nonmigrants of the extended GRAS data collection. Note the different course particularly for IgA. **e**Functionality testing of NMDAR1-AB in human IPSC-derived cortical neurons: degree of internalization expressed as a ratio of fluorescence intensity measured at 37 and 4 °C; number of neurons and sera (N) given; Mann–Whitney U test

abnormal course of IgA vs. IgM/IgG seroprevalence over age in migrants (Fig. 1d).

Functionality of NMDAR1-AB from different mammalian species

To assess whether NMDAR1-AB of the tested species are functional, our endocytosis assay using IPSC-derived human cortical neurons [10] was employed. All positive sera provoked NMDAR1 internalization, verifying functionality (Mann–Whitney U; all $p < 0.001$) (Fig. 1e).

BBB dysfunction but normal behavior of *ApoE*$^{-/-}$ mice

We next induced endogenous NMDAR1-AB formation in a mouse model of BBB dysfunction, *ApoE*$^{-/-}$ mice vs. WT littermates, *ApoE*$^{+/+}$. Before that, we confirmed in 12-

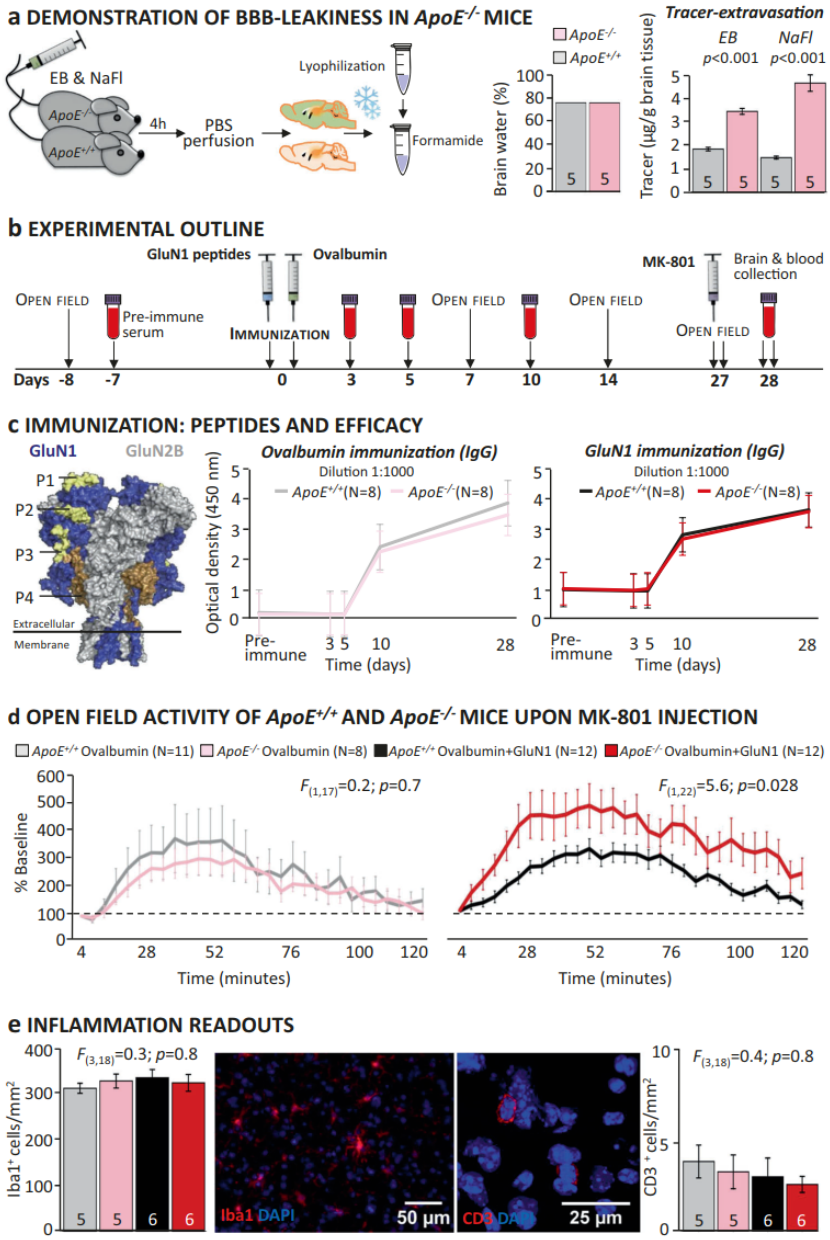

Fig. 2 Behavioral and morphological effects of endogenous NMDAR1-AB of the IgG class in a mouse model with open BBB. **a** Demonstration of BBB leakiness in *ApoE*$^{-/-}$ mice using an intravenously injected mixture of Evans blue (EB) and sodium fluorescein (NaFl): After brain cryopreservation/lyophilization, tracers were extracted with formamide and quantified; Student's *t*-test; **b** Experimental outline; **c** Immunization: Left: GluN1 peptides (P1–P4) located in the extracellular part of the receptor were used for immunization (compare Fig. 3); middle and right: Time course of anti-ovalbumin and anti-GluN1-AB (IgG) upon immunization in *ApoE*$^{-/-}$ and *ApoE*$^{+/+}$ mice; optical density at dilution 1:1000 shown; titers after day 10 reach up to 1:50,000; **d** Effect of MK-801 injection on activity in the open field; results presented as % change from baseline (first 4 min post MK-801 set to 100%); no difference in MK-801-induced hyperactivity between genotypes after ovalbumin immunization (one-way repeated measures ANOVA: treatment × group interaction: $F_{(1,17)} = 0.2$; $p = 0.7$); increase in hyperactivity (during rise, plateau, decline, and after-effect phases) upon MK-801 in *ApoE*$^{-/-}$ but not *ApoE*$^{+/+}$ mice immunized against GluN1 (one-way repeated measures ANOVA: treatment × group interaction: $F_{(1,22)} = 5.6$; $p = 0.028$). **e** Quantification of Iba1^{+} and CD3^{+} cells in the hippocampus to assess inflammation in the brain; one-way ANOVA; representative pictures of Iba1 (left) and CD3 (right) stainings in the middle

Table 1 Basic behavioral screening of male and female $ApoE^{+/+}$ and $ApoE^{-/-}$ mice

Behavioral paradigms	Males				Females			
	Age (month)	$ApoE^{+/+}$ (*N*)	$ApoE^{-/-}$ (*N*)	*p*-value	Age (month)	$ApoE^{+/+}$ (*N*)	$ApoE^{-/-}$ (*N*)	*p*-value
Anxiety and activity								
Elevated plus-maze (time open [%])	5	12.6±3.2 (10)	19.5±4.0 (10)	p=**0.14** U=30.0	5	17.5±2.9 (13)	14.8±1.3 (11)	p=**0.98** U=71.0
Exploratory behavior								
Hole-board (holes visited [#])	5	15.2±2.3 (10)	11.9±1.9 (10)	p=**0.30** $t(18)$=1.07	5	15.5±1.8 (13)	15.6±2.9 (13)	p=**0.96** $t(22)$=0.96
Open-field								
Locomotion [m]	5	31.8±1.7 (10)	32.7±1.5 (10)	p=**0.70** $t(18)$=0.39	5	42.7±1.3 (13)	43.7±3.2 (13)	p=**0.76** $t(22)$=0.31
Motor learning and coordination								
Rotarod day 1 (latency to fall [s])	6	89.3±11.6 (10)	130.0±15.3 (10)	p=**0.06** $t(18)$=2.01	5	130.9±14.0 (13)	133.3±16.0 (11)	p=**0.91** $t(22)$=0.11
Rotarod day 2 (latency to fall [s])	6	140.3±9.4 (10)	145.6±17.8 (10)	p=**0.81** $t(18)$=0.25	5	179.0±16.8 (13)	160.5±19.9 (11)	p=**0.5** $t(22)$=0.69
Muscle strength								
Grip-strength [au]	6	110.2±5.4 (10)	122.0±5.0 (10)	p=**0.15** $t(18)$=1.52	6	108.8±3.0 (13)	115.1±4.4 (11)	p=**0.26** $t(22)$=1.16
Heat/pain perception								
Hot-plate (latency to lick [s])	5	12.8±0.4 (10)	11.9±0.7 (10)	p=**0.22** $t(18)$=1.26	5	13.7±0.5 (12)	12.4±0.5 (10)	p=**0.15** $t(20)$=1.5
Vision								
Visual-cliff (time on "air" side [%])	5	26.5±7.2 (10)	22.0±5.6 (10)	p=**0.85** U=47.0	5	21.7±5.1 (13)	29.0±3.9 (11)	p=**0.13** U=45.0
Olfaction								
Buried food-test (latency to find cookie [s])	5	59.4±9.2 (10)	50.6±8.5 (9)	p=**0.52** $t(17)$=0.66	5	47.8±12.9 (12)	50.7±10.7 (11)	p=**0.87** $t(21)$=0.16
Hearing								
Acoustic startle at 65dB [AU]	6	0.5±0.04 (10)	0.5±0.04 (10)	p=**0.53** $F(1,18)$=0.42	8	0.4±0.1 (13)	0.5±0.04 (11)	p=**0.19** $F(1,22)$=1.82
Acoustic startle at 120dB [AU]		4.5±1.0 (10)	4.8±1.0 (10)			3.3±0.5 (13)	4.2±0.6 (11)	
Sensorimotor gating								
Mean pre-pulse inhibition [%]	6	44.8±6.7 (10)	40.6±7.4 (10)	p=**0.69** $F(1,18)$=0.16	8	57.7±4.1 (13)	50.4±6.3 (11)	p=**0.35** $F(1,22)$=0.91
Pheromone-based social preference								
Time spent in pheromone box [s]					15	1213±50.8 (12)	1115±83.7 (12)	p=**0.33** $t(22)$=1.0
Time spent in control box [s]						780.5±75.4 (12)	751.1±83.5 (12)	p=**0.84** $t(22)$=0.21
Cognitive performance in IntelliCage								
Place-learning [% target corner visits][a]					15	34.2±1.3 (12)	34.2±1.8 (13)	p=**0.76** U=72.0
Reversal-learning [% target corner visits][a]						34.2±1.3 (12)	34.2±1.8 (13)	p=**0.17** U=52.0

[a]as previously described in *Netrakanti* et al. *2015*

Note: All data in the table are mean ± S.E.M.

month-old mice (age of immunization) BBB leakiness using two fluorescent tracers. While brain water content was similar in both genotypes, pointing against inflammation, $ApoE^{-/-}$ mice showed increased tracer extravasation, confirming BBB dysfunction (Student's *t*-test: EB: $t(8) = -10.66$, $p < 0.001$; NaFl: $t(8) = -8.97$, $p < 0.001$) (Fig. 2a). We wondered whether this compromised BBB would by itself lead to behavioral abnormalities in $ApoE^{-/-}$ mice. A comprehensive behavioral battery, including tests for anxiety, activity, exploratory behavior,

motor and sensory function, sensorimotor gating, pheromone-based social preference, and cognitive performance did not reveal any differences between genotypes (Table 1).

Immunization of *ApoE*$^{-/-}$ and *ApoE*$^{+/+}$ mice against NMDAR1-peptides

To explore whether endogenously formed NMDAR1-AB would lead to measurable behavioral and morphological effects, we immunized 12-month-old *ApoE*$^{-/-}$ and *ApoE*$^{+/+}$ littermates against four peptides of the extracellular NMDAR1/GluN1-domain (including NTD-G7; N368/G369) and ovalbumin or against ovalbumin alone as immunization control (Fig. 2b–c). GluN1 shows >99% sequence homology among all here-tested mammalian species, with immunizing peptides being 100% homologous (Fig. 3). Immunization led to high circulating levels of specific IgG (titers up to 1:50,000). Efficacy of immunization and time course of IgG appearance as determined by ELISA were comparable for NMDAR1-peptides and ovalbumin across genotypes, making a simple boosting effect of NMDAR1-peptides on pre-existing NMDAR1-specific B cell clones rather improbable (Fig. 2c).

Psychosis-related behavior of *ApoE*$^{-/-}$ mice upon MK-801 challenge

Open-field tests measuring baseline preimmunization and postimmunization locomotion did not reveal any differences between genotypes and/or immunization groups (Fig. 2b; not shown). After 4 weeks, the endogenously formed NMDAR1-AB of the IgG class induced strong hyperactivity (psychosis-like symptoms [37]) upon MK-801 challenge in *ApoE*$^{-/-}$ mice only. In contrast, *ApoE*$^{+/+}$ mice behaved comparably to ovalbumin-only immunized mice of both genotypes (Fig. 2d; all $p > 0.5$). Thus, an open BBB together with sufficiently high titers of AB (to reach a threshold loss of NMDAR1 surface expression) is a prerequisite for the observed behavioral perturbation upon MK-801.

No inflammation in hippocampus of immunized *ApoE*$^{-/-}$ and *ApoE*$^{+/+}$ mice

Immunohistochemistry did not show any evidence of inflammation in either genotype and/or immunization group. Numbers of Iba1^{+} and CD3^{+} cells as markers of microglia and T cells, respectively, were comparable for total hippocampus (one-way ANOVA: Iba1: $F(3,18) = 0.3$; $p = 0.8$; CD3: $F(3,18) = 0.4$; $p = 0.8$) (Fig. 2e) and for all hippocampal subfields separately (all p-values > 0.2; not shown). Also, staining for microglial activity markers, CD68 and MHCII, was essentially negative and identical across groups. Moreover, staining for GFAP did not reveal any appreciable density increase in the hippocampus, and thus no sign of astrogliosis (data not shown).

Discussion

The present work demonstrates high seroprevalence of functional NMDAR1-AB of all Ig classes across mammals, indicating that these AB are part of a pre-existing autoimmune repertoire [11–17]. As in humans, NMDAR1-AB of the IgG class are the least frequent [6, 20]. The age related up to >50% NMDAR1-AB seropositivity is independent of the respective species' life expectancy, indicating that the aging process itself rather than years of exposure to a certain environment triggers NMDAR1-AB formation. However, our knowledge on predisposing factors and inducing mechanisms is limited. Specific autoimmune-reactive B cells may get repeatedly boosted by, e.g., infections, neoplasms, or the microbiome, and less efficiently suppressed over a lifespan likely owing to a gradual loss of immune tolerance upon aging [14].

Unexpectedly, we find the age-dependence lost in nonhuman primates and in human migrants that all display an early-life rise in NMDAR1-AB seropositivity, mainly of IgA. The intriguing possibility that chronic life stress, known to be present in human migrants [38] and animals in captivity [39], acts as a trigger of early NMDAR1-AB formation is worth pursuing experimentally in the future. A large proportion of migrants in our human samples are suffering from neuropsychiatric illness. This may additionally support our chronic stress hypothesis since migration is recognized as an environmental stressor predisposing to mental disease [40]. Further studies should screen wildlife monkeys and species in zoos for NMDAR1-AB. Experimental confirmation of our findings provided, NMDAR1-AB (IgA) may even serve as stress markers. In fact, earlier reports show that total serum-Ig of all classes, most prominently IgA, respond to psychological stress [41]. NMDAR1-AB might thus belong to a set of stress-boosted AB. Interestingly, we also find accumulated seroprevalence of 23 other brain-directed AB [6] in young migrants vs. nonmigrants increased (data not shown), suggesting a global inducer role of chronic stress in humoral autoimmunity.

Earlier work has shown that AB against brain antigens in general are common among mammals [42], but no study has so far systematically screened nonhuman mammals for NMDAR1-AB. As an exception, a recent report described "anti-NMDAR1 encephalitis" in the young polar bear Knut [27]. Based on the present findings, Knut may have belonged to those nondomesticated species in captivity—

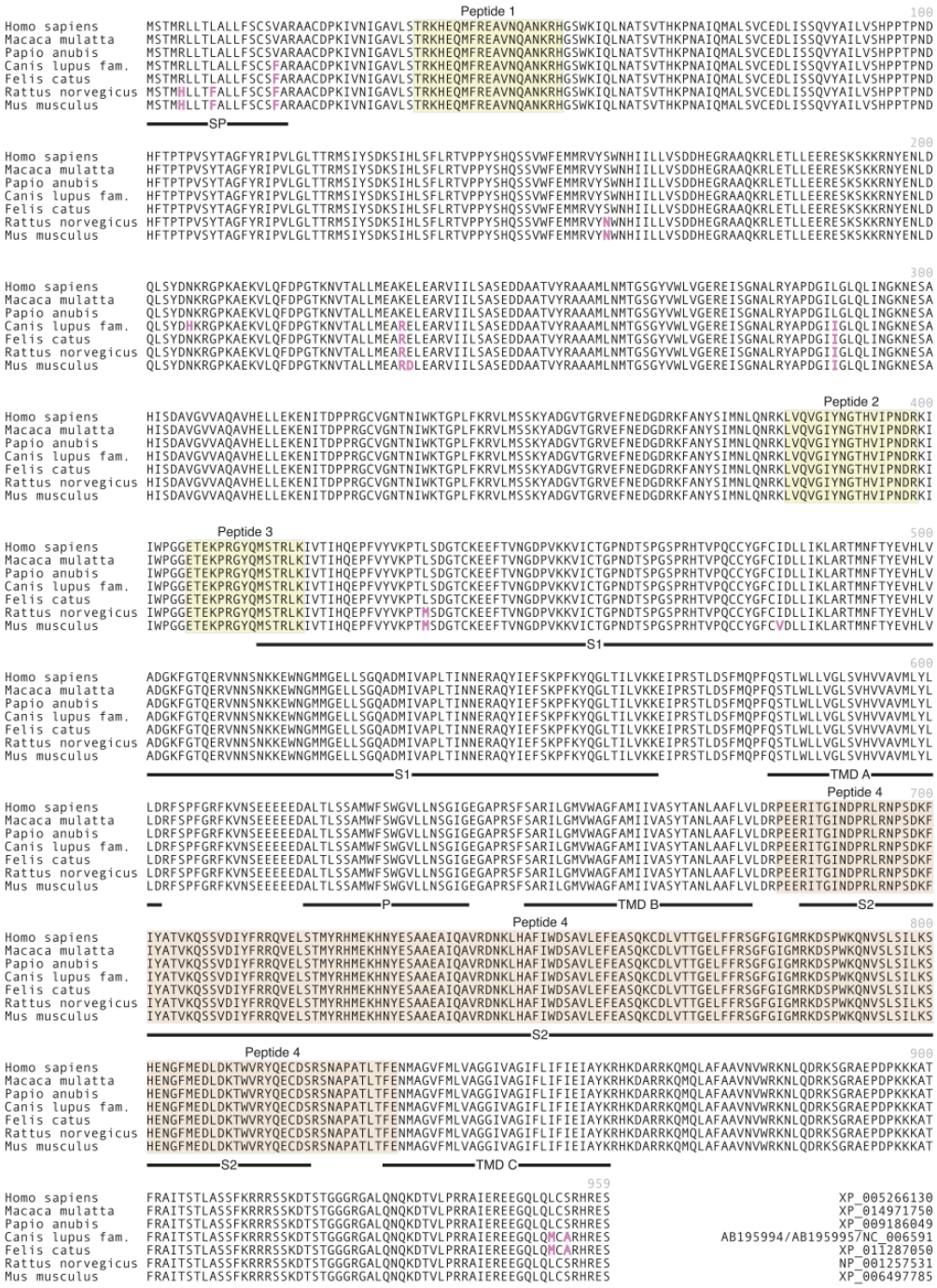

Fig. 3 Alignment of GluN1-1b receptor amino acid sequence across all mammalian species tested. Regions containing the four peptide sequences (peptides 1–4: P1: AA35–53, P2: AA361–376, P3: AA385–399, and P4: AA660–811) used in the immunization experiment are highlighted in yellow and light brown (compare three-dimensional presentation in Fig. 2c) and nonhomologous amino acids in pink. *SP* signal peptide, S1, S2 segments of the ligand-binding domain, *TMD A* transmembrane domain A, *TMD B* transmembrane domain B, *TMD C* transmembrane domain C

comparable to monkey species investigated here—that are affected by chronic early-life stress, inducing NMDAR1-AB seropositivity. Pre-existing NMDAR1-AB of this bear may have ultimately shaped the clinical picture of an encephalitis of unexplained origin (likely infectious according to the zoo's pathology reports) where an epileptic seizure led to drowning [27].

This interpretation is supported by our novel autoimmune model, namely, mice immunized against NMDAR1-peptides. Even high titers of endogenously formed NMDAR1-AB (IgG; up to 1:50,000) that induce psychosis-like behavior upon MK-801 challenge in $ApoE^{-/-}$ mice, with here-confirmed open BBB, do not lead to any appreciable signs of encephalitis. This dissociation of behavioral/symptomatic consequences and inflammation in the brain is of major importance for clinicians [14]. For instance, earlier studies reported an influence of NMDAR1-AB infusions into the hippocampus on learning and memory in mice [43], and others found increased NMDAR1-AB seroprevalence in patients with mild cognitive impairment and Alzheimer's disease [44, 45]. However, while all naturally occurring NMDAR1-AB that have pathogenic potential irrespective of epitope and Ig class [10], and upon entry to the brain (or via intrathecal production) can shape brain functions in the sense of NMDAR antagonism, only a fraction of individuals happens to have underlying encephalitis of various etiologies, which is then called anti-NMDAR encephalitis. The highly variable neuropathology and response to immunosuppression of this condition [2, 3, 46] may point to a broad range of possible encephalitogenic mechanisms (from infection to oncology or genetics) which need to be diagnosed and specifically treated [14].

Even though it is unclear how NMDAR1-AB are generated by chronic stress, it should be considered that NMDAR1 are not only expressed in the brain but also by peripheral organs and tissues, including adrenal glands and gut [47] which may be involved in triggering NMDAR1-AB formation but may also be functionally modulated by them. Since NMDAR antagonists are increasingly recognized as antidepressant, anxiolytic, and anti-inflammatory agents [48–52], we speculate that stress-induced NMDAR1-AB could serve as endogenous stress protectants. Remarkably, also in stroke, NMDAR1-AB can be protective [8].

In conclusion, the widespread occurrence of NMDAR1-AB across mammals, as well as the failure of even high titers of endogenously formed NMDAR1-AB of the IgG class to induce any signs of brain inflammation should lead to rethinking current concepts that link NMDAR1-AB to neuropsychiatric disease including encephalitis.

Acknowledgements This work was supported by the Max Planck Society, the Max Planck Förderstiftung, the DFG (CNMPB), EXTRABRAIN EU-FP7, and the Niedersachsen-Research Network on Neuroinfectiology (N-RENNT). The authors thank all subjects for participating in the study, and the many colleagues who have contributed over the past decade to the extended GRAS data collection.

Author contributions Concept, design, and supervision of the study: HE; Data acquisition/analysis/interpretation: HP, BO, ED, DT, MM, JS, JW, DW, CKS, AR, KS, RT, KMR, StB, YAK, HM, MB, WS, GS, FJK, RM, SB, KAN, JKK, MH, FL, and HE; Drafting manuscript: HE, with the help of BO and HP; Drafting display items: HE and BO, with the help of HP, MM, DT, and JS. All authors read and approved the final version of the manuscript.

Compliance with ethical standards

Conflict of interest WS is a member of the board and holds stocks in Euroimmun AG. HM is a full-time employee of Synaptic Systems GmbH. The remaining authors declare that they have no conflict of interest.

References

1. Dalmau J, Tuzun E, Wu HY, Masjuan J, Rossi JE, Voloschin A, et al. Paraneoplastic anti-N-methyl-D-aspartate receptor encephalitis associated with ovarian teratoma. Ann Neurol. 2007;61:25–36.
2. Dalmau J, Gleichman AJ, Hughes EG, Rossi JE, Peng X, Lai M, et al. Anti-NMDA-receptor encephalitis: case series and analysis of the effects of antibodies. Lancet Neurol. 2008;7:1091–8.
3. Dalmau J, Lancaster E, Martinez-Hernandez E, Rosenfeld MR, Balice-Gordon R. Clinical experience and laboratory investigations in patients with anti-NMDAR encephalitis. Lancet Neurol. 2011;10:63–74.
4. Titulaer MJ, McCracken L, Gabilondo I, Armangue T, Glaser C, Iizuka T, et al. Treatment and prognostic factors for long-term outcome in patients with anti-NMDA receptor encephalitis: an observational cohort study. Lancet Neurol. 2013;12:157–65.
5. Hammer C, Stepniak B, Schneider A, Papiol S, Tantra M, Begemann M, et al. Neuropsychiatric disease relevance of circulating anti-NMDA receptor autoantibodies depends on blood-brain barrier integrity. Mol Psychiatry. 2014;19:1143–9.
6. Dahm L, Ott C, Steiner J, Stepniak B, Teegen B, Saschenbrecker S, et al. Seroprevalence of autoantibodies against brain antigens in health and disease. Ann Neurol. 2014;76:82–94.

7. Steiner J, Teegen B, Schiltz K, Bernstein HG, Stoecker W, Bogerts B. Prevalence of N-methyl-D-aspartate receptor autoantibodies in the peripheral blood: healthy control samples revisited. JAMA Psychiatry. 2014;71:838–9.
8. Zerche M, Weissenborn K, Ott C, Dere E, Asif AR, Worthmann H, et al. Preexisting serum autoantibodies against the NMDAR subunit NR1 modulate evolution of lesion size in acute ischemic stroke. Stroke. 2015;46:1180–6.
9. Castillo-Gomez E, Kastner A, Steiner J, Schneider A, Hettling B, Poggi G, et al. The brain as immunoprecipitator of serum autoantibodies against N-Methyl-D-aspartate receptor subunit NR1. Ann Neurol. 2016;79:144–51.
10. Castillo-Gomez E, Oliveira B, Tapken D, Bertrand S, Klein-Schmidt C, Pan H et al. All naturally occurring autoantibodies against the NMDA receptor subunit NR1 have pathogenic potential irrespective of epitope and immunoglobulin class. Mol Psychiatry. 2016;22:1776–178.
11. Abramson J, Husebye ES. Autoimmune regulator and self-tolerance—molecular and clinical aspects. Immunol Rev. 2016; 271:127–40.
12. Cohen I, Young D. Autoimmunity, microbial immunity and the immunological homunculus. Immunol Today. 1991;12:105–10.
13. Coutinho A, Kazatchkine MD, Avrameas S. Natural autoantibodies. Curr Opin Immunol. 1995;7:812–8.
14. Ehrenreich H. Autoantibodies against the N-methyl-d-aspartate receptor subunit NR1: untangling apparent inconsistencies for clinical practice. Front Immunol. 2017;8:181.
15. Lobo PI. Role of natural autoantibodies and natural IgM anti-leucocyte autoantibodies in health and disease. Front Immunol. 2016;7:198.
16. Mader S, Brimberg L, Diamond B. The role of brain-reactive autoantibodies in brain pathology and cognitive impairment. Front Immunol. 2017;8:1101.
17. Nguyen TT, Baumgarth N. Natural IgM and the development of b cell-mediated autoimmune diseases. Crit Rev Immunol. 2016; 36:163–77.
18. Coutinho E, Harrison P, Vincent A. Do neuronal autoantibodies cause psychosis? A neuroimmunological perspective. Biol Psychiatry. 2014;75:269–75.
19. Diamond B, Huerta P, Mina-Osorio P, Kowal C, Volpe B. Losing your nerves? Maybe it's the antibodies. Nat Rev Immunol. 2009;9:449–56.
20. Hammer C, Zerche M, Schneider A, Begemann M, Nave KA, Ehrenreich H. Apolipoprotein E4 carrier status plus circulating anti-NMDAR1 autoantibodies: association with schizoaffective disorder. Mol Psychiatry. 2014;19:1054–6.
21. Kreye J, Wenke NK, Chayka M, Leubner J, Murugan R, Maier N, et al. Human cerebrospinal fluid monoclonal N-methyl-D-aspartate receptor autoantibodies are sufficient for encephalitis pathogenesis. Brain. 2016;139:2641–52.
22. Begemann MGS, Papiol S, Malzahn D, Krampe H, Ribbe K, et al. Modification of cognitive performance in schizophrenia by complexin 2 gene polymorphisms. Arch Gen Psychiatry. 2010;67: 879–88.
23. Ribbe. K, Friedrichs H, Begemann M, Grube S, Papiol S, Kästner. A, et al. The cross-sectional GRAS sample: a comprehensive phenotypical data collection of schizophrenic patients. BMC Psychiatry. 2010;10:0–20.
24. American Psychiatric Association. (2000) Diagnostic and statistical manual of mental disorders. 4th edn American Psychiatric Press, Washington, DC. .
25. Wandinger KP, Saschenbrecker S, Stoecker W, Dalmau J. Anti-NMDA-receptor encephalitis: a severe, multistage, treafa disorder presenting with psychosis. J Neuroimmunol. 2011;231:86–91.
26. Boyle MDP, Reis KJ. Bacterial Fc receptors. Nat Biotechnol. 1987;5:697–703.
27. Pruss H, Leubner J, Wenke NK, Czirjak GA, Szentiks CA, Greenwood AD. Anti-NMDA receptor encephalitis in the polar bear (Ursus maritimus) Knut. Sci Rep. 2015;5:1–7.
28. Toyka KBD, Pestronk A, Kao I. Myasthenia gravis: passive transfer from man to mouse. Science. 1975;190:397–9.
29. Schindelin J, Arganda-Carreras I, Frise E, Kaynig V, Longair M, Pietzsch T, et al. Fiji: an open-source platform for biological-image analysis. Nat Methods. 2012;9:676–82.
30. Berghoff SA, Gerndt N, Winchenbach J, Stumpf SK, Hosang L, Odoardi F, et al. Dietary cholesterol promotes repair of demyelinated lesions in the adult brain. Nat Commun. 2017;8:1–15.
31. Berghoff SA, Düking T, Spieth L, Winchenbach J, Stumpf SK, Gerndt N, et al. Blood-brain barrier hyperpermeability precedes demyelination in the cuprizone model. Acta Neuropathol Commun. 2017;5:94.
32. Wust S, van den Brandt J, Tischner D, Kleiman A, Tuckermann JP, Gold R, et al. Peripheral T cells are the therapeutic targets of glucocorticoids in experimental autoimmune encephalomyelitis. J Immunol. 2008;180:8434–43.
33. Dere E, Dahm L, Lu D, Hammerschmidt K, Ju A, Tantra M, et al. Heterozygous ambra1 deficiency in mice: a genetic trait with autism-like behavior restricted to the female gender. Front Behav Neurosci. 2014;8:181.
34. Dere E, Winkler D, Ritter C, Ronnenberg A, Poggi G, Patzig J, et al. Gpm6b deficiency impairs sensorimotor gating and modulates the behavioral response to a 5-HT2A/C receptor agonist. Behav Brain Res. 2015;277:254–63.
35. Netrakanti PR, Cooper BH, Dere E, Poggi G, Winkler D, Brose N, et al. Fast cerebellar reflex circuitry requires synaptic vesicle priming by munc13-3. Cerebellum. 2015;14:264–83.
36. Winkler D, Daher F, Wustefeld L, Hammerschmidt K, Poggi G, Seelbach A et al. Hypersocial behavior and biological redundancy in mice with reduced expression of PSD95 or PSD93. Behav Brain Res. 2017. https://doi.org/10.1016/j.bbr.2017.02.011 (e-pub ahead of print).
37. Radyushkin K, El-Kordi A, Boretius S, Castaneda S, Ronnenberg A, Reim K, et al. Complexin2 null mutation requires a 'second hit' for induction of phenotypic changes relevant to schizophrenia. Genes Brain Behav. 2010;9:592–602.
38. Akdeniz C, Tost H, Streit F, Haddad L, Wust S, Schafer A, et al. Neuroimaging evidence for a role of neural social stress processing in ethnic minority-associated environmental risk. JAMA Psychiatry. 2014;71:672–80.
39. Jacobson SL, Ross SR, Bloomsmith MA. Characterizing abnormal behavior in a large population of zoo-housed chimpanzees: prevalence and potential influencing factors. PeerJ. 2016;4: e2225.
40. Stepniak B, Papiol S, Hammer C, Ramin A, Everts S, Hennig L, et al. Accumulated environmental risk determining age at schizophrenia onset: a deep phenotyping-based study. Lancet Psychiatry. 2014;1:444–53.
41. Maes M, Hendriks D, Gastel AV, Demedts P, Wauters A, Neels H, et al. Effects of psychological stress on serum immunoglobulin, complement and acute phase protein concentrations in normal volunteers. Psychoneuroendocrinology. 1997;2: 397–409.
42. Nagele EP, Han M, Acharya NK, DeMarshall C, Kosciuk MC, Nagele RG. Natural IgG autoantibodies are abundant and ubiquitous in human sera, and their number is influenced by age, gender, and disease. PLoS ONE. 2013;8:4.
43. Planaguma J, Leypoldt F, Mannara F, Gutierrez-Cuesta J, Martin-Garcia E, Aguilar E, et al. Human N-methyl D-aspartate receptor antibodies alter memory and behaviour in mice. Brain. 2015;138:94–109.
44. Busse S, Brix B, Kunschmann R, Bogerts B, Stoecker W, Busse M. N-methyl-d-aspartate glutamate receptor (NMDA-R)

antibodies in mild cognitive impairment and dementias. Neurosci Res. 2014;85:58–64.
45. Doss S, Wandinger KP, Hyman BT, Panzer JA, Synofzik M, Dickerson B, et al. High prevalence of NMDA receptor IgA/IgM antibodies in different dementia types. Ann Clin Transl Neurol. 2014;1:822–32.
46. Tuzun E, Zhou L, Baehring JM, Bannykh S, Rosenfeld MR, Dalmau J. Evidence for antibody-mediated pathogenesis in anti-NMDAR encephalitis associated with ovarian teratoma. Acta Neuropathol. 2009;118:737–43.
47. Du J, Li XH, Li YJ. Glutamate in peripheral organs: biology and pharmacology. Eur J Pharmacol. 2016;784:42–8.
48. Gerhard DM, Wohleb ES, Duman RS. Emerging treatment mechanisms for depression: focus on glutamate and synaptic plasticity. Drug Discov Today. 2016;21:454–64.
49. Abdallah CG, Adams TG, Kelmendi B, Esterlis I, Sanacora G, Krystal JH. Ketamine's mechanism of action: a path to rapid-acting antidepressants. Depress Anxiety. 2016;33:689–97.
50. Alexander JK, DeVries AC, Kigerl KA, Dahlman JM, Popovich PG. Stress exacerbates neuropathic pain via glucocorticoid and NMDA receptor activation. Brain Behav Immun. 2009;23:851–60.
51. Rubio-Casillas A, Fernandez-Guasti A. The dose makes the poison: from glutamate-mediated neurogenesis to neuronal atrophy and depression. Rev Neurosci. 2016;27:599–622.
52. Nair A, Hunzeker J, Bonneau RH. Modulation of microglia and CD8(+) T cell activation during the development of stress-induced herpes simplex virus type-1 encephalitis. Brain Behav Immun. 2007;21:791–806.

Affiliations

Hong Pan[1] · Bárbara Oliveira[1] · Gesine Saher[2] · Ekrem Dere[1] · Daniel Tapken[3] · Marina Mitjans[1] · Jan Seidel[1] · Janina Wesolowski[1] · Debia Wakhloo[1] · Christina Klein-Schmidt[3] · Anja Ronnenberg[1] · Kerstin Schwabe[4] · Ralf Trippe[3] · Kerstin Mätz-Rensing[5] · Stefan Berghoff[2] · Yazeed Al-Krinawe[4] · Henrik Martens[6] · Martin Begemann[1] · Winfried Stöcker[7] · Franz-Josef Kaup[5] · Reinhard Mischke[8] · Susann Boretius[9] · Klaus-Armin Nave[2,10] · Joachim K. Krauss[4] · Michael Hollmann[3] · Fred Lühder[11] · Hannelore Ehrenreich[1,10]

1 Clinical Neuroscience, Max Planck Institute of Experimental Medicine, Göttingen, Germany

2 Department of Neurogenetics, Max Planck Institute of Experimental Medicine, Göttingen, Germany

3 Department of Biochemistry I—Receptor Biochemistry, Ruhr University, Bochum, Germany

4 Department of Neurosurgery, Hannover Medical School, Hannover, Germany

5 Department of Pathology, Leibniz Institute for Primate Research, Göttingen, Germany

6 Synaptic Systems GmbH, Göttingen, Germany

7 Institute for Experimental Immunology, affiliated to Euroimmun, Lübeck, Germany

8 Small Animal Clinic, University of Veterinary Medicine, Hannover, Germany

9 Functional Imaging Laboratory, Leibniz Institute for Primate Research, Göttingen, Germany

10 DFG Research Center for Nanoscale Microscopy and Molecular Physiology of the Brain (CNMPB), Göttingen, Germany

11 Department of Neuroimmunology, Institute for Multiple Sclerosis Research and Hertie Foundation, University Medicine Göttingen, Göttingen, Germany

Chapter 3
Project II

3. Project II:
Multiple inducers and novel roles of autoantibodies against the obligatory NMDAR subunit NR1: *A translational study from chronic life stress to brain injury*

Overview of project II

After we investigated the effects of NMDAR1-AB in both WT and *ApoE*$^{-/-}$ mice with compromised BBB (Pan et al., 2019), the next question which intrigued us was: what are the inducers of the NMDAR1-AB formation?

In this project, we employed multiple approaches, e.g. brain lesion, checkpoint inhibitor treatment, and chronic life stress, to answer our questions.

(I) The course of the NMDAR1-AB in mice and humans. We observed both in WT and *ApoE*$^{-/-}$ mice, that the NMDAR1-AB can stay positive, or stay negative, or being transiently positive (loss or gain of Ig classes) over a period of 3-6 months. Similar observations were made in human patients, from 24h till 1-3 years after ischemic stroke.

(II) Brain lesion (cryolesion in mice) as a potential inducer. We used a standardized brain lesion model: cryolesion (Sirén et al., 2006) in 4 weeks old male C57BL/6J mice, and detect the NMDAR1-AB seroprevalence 4 months after the surgery/sham. We found increased level of IgG and IgM classes of NMDAR1-AB in the cryolesion group compared to the sham group, also a slight increase of AB diversity in the cryolesion group.

(III) *CTLA4* genetic predisposition in human & CTLA4-AB treatment in mice. In human, *CTLA4* (*Cytotoxic T-Lymphocyte Associated antigen 4*) gene, is associated with autoimmune diseases, and there were studies which reported that the patients treated with checkpoint inhibitor: CTLA4-AB (also named as ipilimumab) often developed autoimmune diseases (Bartels et al., 2019; de Moel et al., 2019; Ikegami et al., 2006; June et al., 2017; Plenge et al., 2005). We found in our GRAS database, that two SNPs: rs3087243 (A/G) and

rs11571316 (A/G) of the human *CTLA4* gene were associated with NMDAR1-AB IgA+IgG seropositivity. However, in our mouse study with CTLA4-AB treatment for 4 weeks, we did not find an increase of NMDAR1-AB in the CTLA4-AB treated group compared to the control IgG treated group 5 weeks after the last treatment. These negative results triggered our next hypothesis: there might be immune challenges required in addition to CTLA4-AB treatment.

(IV) Chronic stress mouse model. According to our previous report that there is a high seroprevalence of NMDAR1-AB (especially the IgA class) in young migrants and monkeys (baboons and rhesus macaques), and we hypothesized that chronic life stress might contribute to the NMDAR1-AB production in those young individuals (Pan et al., 2019). To prove it, we designed a chronic life stress model in mice by housing the mice in rat environment, while the control mice stayed in the standard mouse environment. Here, we observed higher NMDAR1-AB seroprevalence, especially IgA carriers, in WT mice housed in rat environment compared to mouse environment. Besides, mice (NMDAR1-AB negative) housed in rat environment also showed a depressive phenotype in tail suspension test. *ApoE*$^{-/-}$ mice (compromised BBB) who carried the NMDAR1-AB showed anti-depressant behavior compared to WT NMDAR1-AB carriers by tail suspension test. Moreover, human *ApoE4*+NMDAR1-AB carriers have lower depressive and anxious rating as compared to the controls who were *ApoE4*- and/or NMDAR1-AB negative.

Original publication

Pan H, Steixner-Kumar A. A, Seelbach A, Deutsch N, Ronnenberg A, Tapken D, von Ahsen N, Mitjans M, Worthmann H, Trippe R, Klein-Schmidt C, Schopf N, Rentzsch K, Begemann M, Wienands J, Stöcker W, Weissenborn K, Hollmann M, Nave KA, Lühder F and Ehrenreich H. Multiple inducers and novel roles of autoantibodies against the obligatory NMDAR subunit NR1: A translational study from chronic life stress to brain injury. Mol Psychiatry (2020). https://doi.org/10.1038/s41380-020-0672-1.

Personal contribution: I was responsible for the conduction of most of the experiments, and data analyses under the supervison of HE and FL: blood collection from all mice; NMDAR1-AB determination in old WT and *ApoE*$^{-/-}$ mice (Figure 1a,b,c,d), human stroke patients (Figure 1e,f), human migrants (Figure 3f), CTLA4-AB/control IgG treated mice (Figure 2h), chronic stress mice (Figure 3c,d,e); data organization and analysis of cryolesion mice seropositivity (Figure 2b,c); CTLA4-AB confirmation by flow cytometry (Figure 2f, under the guidance of FL) and spleen cytospin (Figure 2g); cFos experiment and quantification (Figure 3a); illustration images generation (Figure 2g, Figure 3a right panel); flow cytometry of blood, lung and small intestine of the chronic stress young cohort (data not shown); behavioral tests in the chonic stress young cohort (Figure 3g). After all the data analyses, I prepared the figures under the guidance of HE, and contributed to the paper writing.

Molecular Psychiatry
https://doi.org/10.1038/s41380-020-0672-1

ARTICLE

Multiple inducers and novel roles of autoantibodies against the obligatory NMDAR subunit NR1: a translational study from chronic life stress to brain injury

Hong Pan[1] · Agnes A. Steixner-Kumar[1] · Anna Seelbach[1] · Nadine Deutsch[2] · Anja Ronnenberg[1] · Daniel Tapken[3] · Nico von Ahsen[4] · Marina Mitjans[1] · Hans Worthmann[2] · Ralf Trippe[3] · Christina Klein-Schmidt[3] · Nadine Schopf[1] · Kristin Rentzsch[5] · Martin Begemann[1,6] · Jürgen Wienands[7] · Winfried Stöcker[5] · Karin Weissenborn[2] · Michael Hollmann[3] · Klaus-Armin Nave[8] · Fred Lühder[9] · Hannelore Ehrenreich[1]

Received: 5 November 2019 / Revised: 13 January 2020 / Accepted: 23 January 2020

Abstract

Circulating autoantibodies (AB) of different immunoglobulin classes (IgM, IgA, and IgG), directed against the obligatory N-methyl-D-aspartate-receptor subunit NR1 (NMDAR1-AB), belong to the mammalian autoimmune repertoire, and appear with age-dependently high seroprevalence across health and disease. Upon access to the brain, they can exert NMDAR-antagonistic/ketamine-like actions. Still unanswered key questions, addressed here, are conditions of NMDAR1-AB formation/boosting, intraindividual persistence/course in serum over time, and (patho)physiological significance of NMDAR1-AB in modulating neuropsychiatric phenotypes. We demonstrate in a translational fashion from mouse to human that (1) serum NMDAR1-AB fluctuate upon long-term observation, independent of blood–brain barrier (BBB) perturbation; (2) a standardized small brain lesion in juvenile mice leads to increased NMDAR1-AB seroprevalence (IgM + IgG), together with enhanced Ig-class diversity; (3) *CTLA4* (immune-checkpoint) genotypes, previously found associated with autoimmune disease, predispose to serum NMDAR1-AB in humans; (4) finally, pursuing our prior findings of an early increase in NMDAR1-AB seroprevalence in human migrants, which implicated chronic life stress as inducer, we independently replicate these results with prospectively recruited refugee minors. Most importantly, we here provide the first experimental evidence in mice of chronic life stress promoting serum NMDAR1-AB (IgA). Strikingly, stress-induced depressive-like behavior in mice and depression/anxiety in humans are reduced in NMDAR1-AB carriers with compromised BBB where NMDAR1-AB can readily reach the brain. To conclude, NMDAR1-AB may have a role as endogenous NMDAR antagonists, formed or boosted under various circumstances, ranging from genetic predisposition to, e.g., tumors, infection, brain injury, and stress, altogether increasing over lifetime, and exerting a spectrum of possible effects, also including beneficial functions.

✉ Hannelore Ehrenreich
ehrenreich@em.mpg.de

1 Clinical Neuroscience, Max Planck Institute of Experimental Medicine, Göttingen, Germany

2 Department of Neurology, Hannover Medical School, Hannover, Germany

3 Department of Biochemistry I–Receptor Biochemistry, Ruhr University, Bochum, Germany

4 Institute of Clinical Chemistry, University Medical Center Göttingen, Göttingen, Germany

5 Institute for Experimental Immunology, Euroimmun, Lübeck, Germany

6 Department of Psychiatry & Psychotherapy, University Medical Center Göttingen, Göttingen, Germany

7 Institute for Cellular and Molecular Immunology, Georg August University, Göttingen, Germany

8 Neurogenetics, Max Planck Institute of Experimental Medicine, Göttingen, Germany

9 Institute for Neuroimmunology and Multiple Sclerosis Research, University Medical Center Göttingen, Göttingen, Germany

Published online: 24 February 2020

SPRINGER NATURE

Introduction

N-methyl-D-aspartate receptors (NMDAR) are abundantly expressed in mammalian brain. Acting as glutamate-gated cation channels, they form heteromers of NR1, NR2, and NR3 subunits, with NR1 as the mandatory partner (NMDAR1, *new nomenclature GluN1 disregarded here for consistency with most of the respective autoantibody literature*). NMDAR are crucial for regulating neuronal/synapse function, but are also expressed by, e.g., astrocytes, oligodendrocytes, as well as different cell types in the periphery, where their role is less understood [1–6].

NMDAR1 autoantibodies (NMDAR1-AB) of the immunoglobulin G (IgG) class in serum and CSF have originally been described as pathognomonic for "anti-NMDAR encephalitis", characterized by psychosis, cognitive decline, dyskinesia, epileptic seizures, loss of consciousness, and autonomic instability [7–10]. As a pathophysiological mechanism, NMDAR1-AB-induced receptor internalization had been proposed [11]. Shortly thereafter, NMDAR1-AB of other Ig-classes (IgM and IgA) were also deemed relevant for neuropsychiatric phenotypes [12–17]. In vitro assays revealed similar effects of NMDAR1-AB, independent of Ig-class, on receptor internalization in human IPSC-derived and primary mouse neurons, as well as on glutamate-evoked currents in *Xenopus laevis* oocytes [17–19]. In vivo studies confirmed comparable influence of serum NMDAR1-AB of all Ig-classes on brain functions, with blood–brain barrier (BBB) permeability deciding on their pathophysiological significance [16–21].

Entirely unexpected was the demonstration of age-dependent >20% NMDAR1-AB seroprevalence in humans, including IgM, IgA, and IgG, with comparable titers and epitopes in health and disease [16–18, 21–23]. Thus, other mammals, namely, dogs, cats, rats, and mice, were screened and found age-dependently highly seropositive for functional NMDAR1-AB [20]. This age dependence was lost in baboons and rhesus macaques, i.e., non-human primates in captivity, and in human migrants, raising the intriguing possibility that NMDAR1-AB formation (predominantly of the IgA class) is related to early chronic life stress [20]. Apart from these newer observations, the occurrence of NMDAR1-AB has previously been associated with oncological conditions (teratoma) [7], influenza A/B seropositivity [17, 21], and herpes encephalitis [13]. A possible genetic predisposition was explored by a genome-wide association study, uncovering the genetic marker, rs524991, related to NMDAR biology [17].

Together, these findings indicate that naturally occurring, functional NMDAR1-AB belong to the normal autoimmune repertoire of mammals, and may have physiological roles as well as pathogenic potential, irrespective of the epitope and Ig-class [18, 20]. In the present translational work from mouse to human, we address for the first time the spontaneous intraindividual course of NMDAR1-AB in serum over time, describe novel conditions of NMDAR1-AB formation/boosting, e.g., experimental chronic life stress, and demonstrate thus far unrecognized properties of NMDAR1-AB in modulating neuropsychiatric phenotypes, i.e., ketamine-like antidepressant effects.

Materials and methods

Ethical approvals

Ethics Committees of Georg August University, Göttingen, and collaborating centers approved the Göttingen Research Association for Schizophrenia (extended GRAS) data collection [16, 17, 21, 22, 24, 25], Ethics Committee of Hannover Medical School permitted inclusion of stroke patients, all in agreement with Helsinki Declaration. Participants gave written informed consent. Mouse experiments were approved by the local animal care/use committee (LAVES). Experiments were performed by investigators unaware of group assignment/treatments (fully blinded).

Human studies

Stroke patient follow-up

Paired blood samples of ischemic stroke patients (within 24 h after stroke and at 1–3 years follow-up; $N = 114$, 60.5% men, age at stroke 73.4 ± 11.0 [48–95] years) were collected prospectively at Hannover Medical School.

CTLA4 genotypes and NMDAR1-AB seropositivity

Genetic information and serology were available for 2934 subjects (63% men, age 42.9 ± 16.3 [17–95] years) of extended GRAS ($N = 1082$ schizophrenia/schizoaffective disorder, $N = 1256$ healthy, $N = 260$ Parkinson, $N = 248$ other neuropsychiatric diseases, and $N = 88$ stroke) after random exclusion of one individual/pair of second-degree relatives (PIHAT > 0.185, $N = 83$) to avoid spurious associations due to relatedness. Genotyping was performed using our semicustom Axiom-myDesign genotyping-array (Affymetrix, Santa Clara, CA, USA) described before [17, 26]. Two *CTLA4* (±5 kb flanking regions) variants, rs11571316 (MAF = 0.42) and rs3087243 (MAF = 0.46), were selected due to the highest MAF, providing maximal statistical power. Both variants were in Hardy–Weinberg equilibrium ($p > 0.05$) and strong linkage disequilibrium ($R^2 = 0.94$).

NMDAR1-AB seropositivity in migrants and age-matched controls

Prospectively recruited healthy migrants ($N = 46$; 21.9 ± 4.4 [17–33] years), at the time of immigration to Germany aged 18.7 ± 4.6 years, and $N = 821$ age-matched non-migrant controls of extended GRAS were analyzed.

Psychopathology in *APOE4*-positive NMDAR1-AB carriers

GRAS individuals ($N = 1046$) with schizophrenia/schizoaffective disorder according to *Diagnostic and Statistical Manual of Mental Disorders (DSM-IV-TR)* and information on NMDAR1-AB serostatus, *APOE4*-carrier status [19], and *Brief Symptom Inventory* [27] items depression or anxiety were included.

Serological analyses

NMDAR1-AB determination

An established commercial assay, based on NMDAR1-transfected HEK293 cells (Euroimmun, Lübeck, Germany), was used to detect NMDAR1-AB in serum/plasma with the respective secondary antibodies against human (Euroimmun, Lübeck, Germany) [8, 28] or mouse IgA, IgG, or IgM (62-6700, custom-labeled with Alexa-Fluor488; A-21202; A-21042; ThermoFisher Scientific, Waltham, USA). For cryolesion experiment, an analogous noncommercial assay (HEK293T cells, mycoplasma free, Hollmann-Lab, Bochum) was used [18, 20]. The results were evaluated by three independent investigators (Figs. 1–3).

Mouse studies

Right parietal cortical cryolesion model

This model was described in detail earlier [29]. In brief, 4-week-old WT C57BL/6J male mice received a standardized cryolesion using a liquid nitrogen-cooled copper cone with 1-mm-diameter tip, placed stereotactically for 60 s on the right parietal skull after scalp incision. Sham surgery was performed with the uncooled cone.

CTLA4-AB purification

CTLA4-AB was purified from hamster UC10-4F10-11 hybridoma (HB-304, ATCC, Manassas, USA). Cells were expanded in RPMI-1640 medium, and, upon appropriate density, cultured in PFHM-II (both ThermoFisher) for 2 weeks. Protein purification of CTLA4-AB from cell culture supernatant was conducted using 1 ml HiTrap-Protein-G High-Performance Columns (GE Healthcare, Chicago, USA). Eluted fractions were desalted using PD-10 desalting columns (GE Healthcare). CTLA4-AB was eluted in PBS and quantified using Nanodrop (Peqlab, Radnor, USA).

CTLA4-AB confirmation by flow cytometry

Purified CTLA4-AB was labeled with SeTau647-di-NHS (SETA-BioMedical, Urbana, USA). Labeled antibodies were separated from unconjugated dye via PD-10 desalting columns (GE Healthcare), eluted (PBS), and concentrated using Pierce Protein-Concentrators (10K, ThermoFisher). Single-cell suspension was prepared from lymph nodes (C57BL/6 mouse) and resuspended after centrifugation in FACS buffer (2% BSA, PBS). Cells were stained with following antibodies for 30 min/4 °C: CD4-PE/Cy5 (1:1000; 130312, BioLegend, San Diego, USA), CD25-biotin (1:200; 553070, BD-Biosciences, San Jose, CA, USA) plus FITC Streptavidin (1:200; 405202, BioLegend). Filtered samples were acquired on a FACSAria Sorp (BD-Biosciences), and data analyzed by FlowJo software (BD-Biosciences).

CTLA4 confirmation by immunocytochemistry

Single-cell suspension was prepared from spleen (C57BL/6). After washing with HBSS, cells were fixed, permeabilized, and stained with CTLA4-SeTau647 (1:100) and FoxP3-PE (1:100) antibodies (FoxP3 kit, 72-5775, ThermoFisher). Nuclei were stained with DAPI for 5 min (1:5000; D9542, Sigma-Aldrich, St. Louis, USA) at room temperature (RT). After washing twice with 1 × permeabilization buffer, cells were spotted on slides (cytospin, ROTOFIX 32A, Hettich, Kirchlengern, Germany), 1200 rpm/7 min, dried overnight, and mounted with Aqua-Poly/Mount (18606-20, Polysciences, Warrington, USA). Representative images (2048 × 2048) were taken with Leica-TCS-SP5 confocal-microscope (63 × glycerol-immersion objective, 0.5 µm intervals, Leica-Microsystems, Mannheim, Germany), then processed with FIJI-ImageJ-software (https://fiji.sc/).

CTLA4-AB mouse study

Female C57BL/6N mice ($N = 41$) were used (details in Fig. 2e). Based on baseline NMDAR1-AB seropositivity, mice were equally distributed into groups receiving CTLA4-AB ($N = 21$) or isotype-control IgG ($N = 20$; BE0091, Bio X Cell, West Lebanon, USA) intraperitoneally.

cFos immunohistochemistry

For stress pilot experiment (Fig. 3a), mice were anesthetized (Avertin, 2,2,2-Tribromoethanol; T48402, Sigma-Aldrich), transcardially perfused with Ringer (Braun-Melsungen,

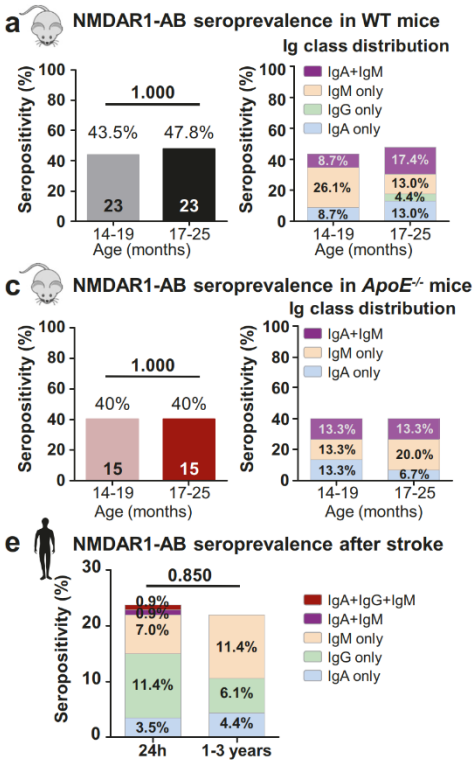

b Course of serum NMDAR1-AB in WT mice
(N=23; intraindividual follow-up)

14-19 to 17-25 months	N number	Percentage
Stayed seronegative	6	26.1%
Stayed seropositive (any Ig class)	2	8.7%
Acquired any Ig class	8	34.8%
Lost any Ig class	7	30.4%

d Course of serum NMDAR1-AB in *ApoE*$^{-/-}$ mice
(N=15; intraindividual follow-up)

14-19 to 17-25 months	N number	Percentage
Stayed seronegative	5	33.3%
Stayed seropositive (any Ig class)	1	6.7%
Acquired any Ig class	5	41.7%
Lost any Ig class	4	33.3%

f Course of serum NMDAR1-AB post-stroke
(N=114; intraindividual follow-up of patients)

24h to 1-3 years	N number	Percentage
Stayed seronegative	74	64.9%
Stayed seropositive (any Ig class)	10	8.8%
Acquired any Ig class	13	11.4%
Lost any Ig class	17	14.9%

Fig. 1 Fluctuation of NMDAR1-AB in mice and human upon longitudinal observation, independent of BBB perturbation. **a** Intraindividual comparison of NMDAR1-AB seropositivity and Ig-class distribution in aged WT mice at two different time points. **b** Course of serum NMDAR1-AB in WT mice. **c** Intraindividual comparison of NMDAR1-AB seropositivity and Ig-class distribution in aged *ApoE*$^{-/-}$ mice at two different time points. **d** Course of serum NMDAR1-AB in *ApoE*$^{-/-}$ mice. **e** Intraindividual follow-up of NMDAR1-AB seropositivity in stroke patients at two different time points after stroke. **f** Course of serum NMDAR1-AB in stroke patients. **a**, **c**, **e** *N* numbers/percentage displayed in bars; McNemar's test.

Germany) for 2 min and 4% formaldehyde for 10 min. Brains were 24 h post-fixed in 4% formaldehyde, cryoprotected in 30% sucrose, frozen and embedded in Tissue-Tek (4583, Sakura-Finetek-Europe, Netherlands). Coronal 30 µm-thick sections (cryostat; Leica-CM1950; Leica-Microsystems, Buffalo Grove, IL, USA) were kept in 25% ethylene glycol and 25% glycerol/PBS. Free-floating sections were blocked (1 h/RT) in 5% normal horse serum (NHS) in PBST (1 × PBS + 0.3% Triton X-100) and incubated with rabbit anti-cFos (226003; Synaptic Systems, Göttingen, Germany) 1:1000 in PBST + 5% NHS overnight/4 °C. After washing with PBS, secondary antibody donkey anti-rabbit IgG-Alexa Fluor 647 (A-31573, ThermoFisher) 1:500 in PBST + 3% NHS was incubated for 2 h/RT. Nuclei were visualized with DAPI (Sigma-Aldrich) 1:5000 for 10 min. Sections were mounted using Aqua-Poly/Mount (Polysciences). Tile scans of hippocampus/hypothalamus were acquired using the 20× air-objective from Nikon-Ti2 Eclipse (Nikon, Tokyo, Japan) and cFos+ cells counted using cell-counter-plugin of FIJI-ImageJ-software. Representative images (1024 × 1024; 1 µm intervals) were taken with Leica-TCS-SP5, then processed with FIJI-ImageJ.

Chronic stress study

Details of the experimental setup are given in Fig. 3. All mice were housed in standard laboratory conditions (22 ± 1 °C, 55% humidity, food/water ad libitum), and after moving kept in cages with simple top lid to allow direct contact with environment air. Blood was collected from orbital sinus at indicated time points for FACS and NMDAR1-AB determination.

Behavioral tests

Tail-suspension test Mice were gently fixed with adhesive tape 20 mm from the tail tip, and time spent immobile recorded for 6 min with a digital camera [30].

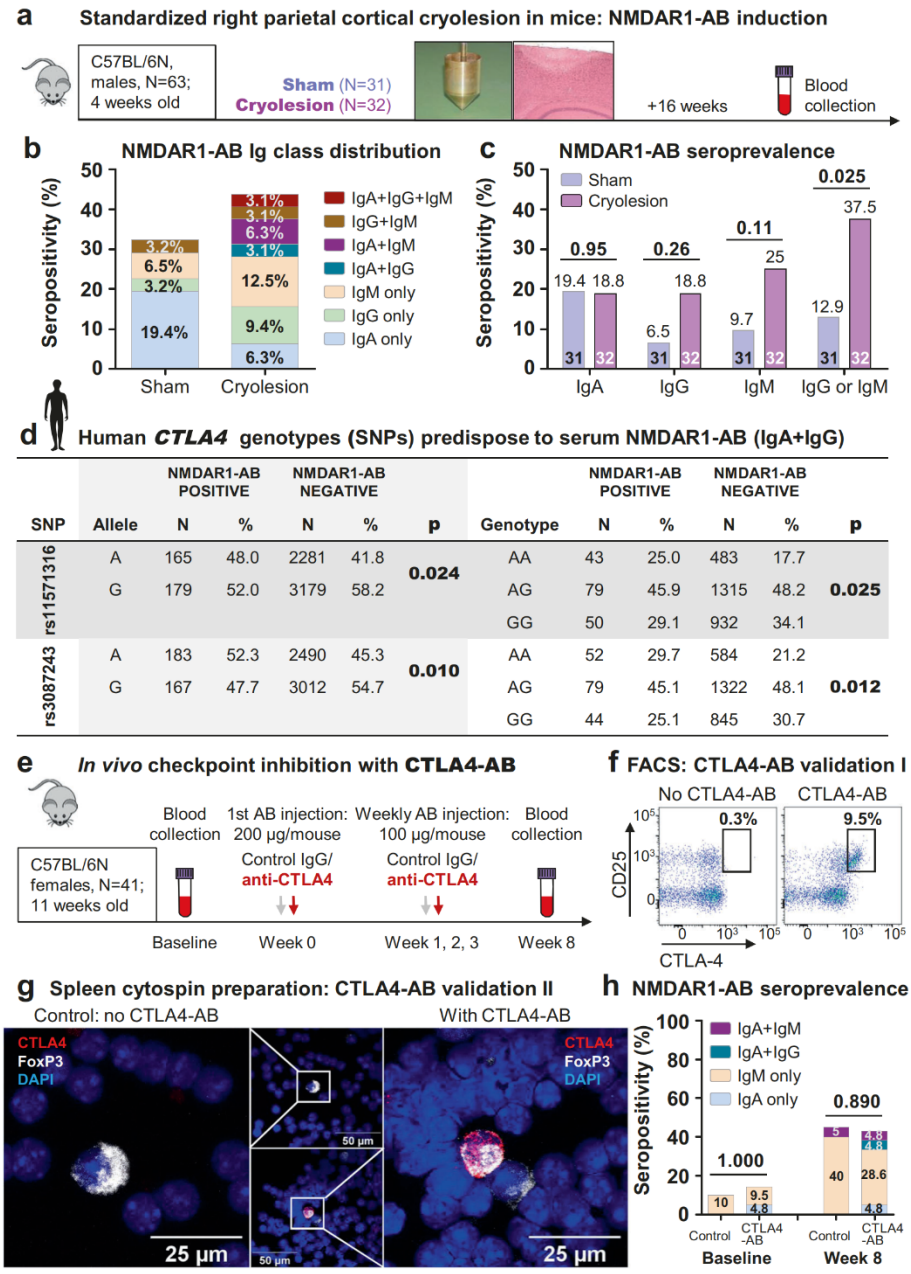

SNP	Allele	NMDAR1-AB POSITIVE N	%	NMDAR1-AB NEGATIVE N	%	p	Genotype	NMDAR1-AB POSITIVE N	%	NMDAR1-AB NEGATIVE N	%	p
rs11571316	A	165	48.0	2281	41.8	**0.024**	AA	43	25.0	483	17.7	
	G	179	52.0	3179	58.2		AG	79	45.9	1315	48.2	**0.025**
							GG	50	29.1	932	34.1	
rs3087243	A	183	52.3	2490	45.3	**0.010**	AA	52	29.7	584	21.2	
	G	167	47.7	3012	54.7		AG	79	45.1	1322	48.1	**0.012**
							GG	44	25.1	845	30.7	

Fig. 2 Inducers/boosters of serum NMDAR1-AB. a Experimental outline of the cryolesion experiment (cryolesion according to Sirén et al. [29]). **b** Higher Ig-class diversity of serum NMDAR1-AB at 4 months after cryolesion versus sham operation. **c** Increased percentage of serum NMDAR1-AB upon cryolesion is due to IgG and IgM. *N* numbers/percentage displayed in bars; chi-square test (IgA, IgM, and IgG + IgM) or Fisher's exact test (IgG), two sided. **d** Human *CTLA4* SNPs predispose to serum NMDAR1-AB (IgA + IgG) as seen in both allelic and genotypic analyses (minor variation in *N* numbers due to missing information). **e** Experimental outline of CTLA4-AB treatment of mice. **f** CTLA4-AB validation by flow cytometry on cells from murine lymph nodes (FACS): left, control staining (without CTLA4-AB), right, CTLA4-AB staining; cells pre-gated on CD4+. **g** Representative images of FoxP3 ± CTLA4-AB staining of murine spleen cells, demonstrating specific double labeling of regulatory T-cells. **h** Intraindividual follow-up of NMDAR1-AB seropositivity upon CTLA4-AB versus isotype-control IgG treatment. *N* numbers displayed in bars; Cochran–Armitage test for trend or chi-square test, two sided.

Baseline and post-MK-801 locomotion in open field this test using the non-competitive NMDAR antagonist MK-801 (M107, Sigma-Aldrich), intraperitoneally injected (0.3 µg/10 µl of PBS/g body weight), was performed as described previously [17, 20].

Flow cytometry

Blood

50 µl of blood was 1:1 diluted in PBS; lymphocytes were separated using 100 µl Lymphocyte Separation Medium 1077 (C-44010, PromoCell, Heidelberg, Germany). Cells were stained for 30 min/4 °C with: CD4-PE/Cy5 (1:1000; 130312), CD8a-PE/Cy7 (1:500; 100722), B220-BV510 (1:300; 103248), Gr-1-PE (1:1000; 108408), CD11b-PerCP/Cy5.5 (1:1000; 101227), F4/80-FITC (1:1000; 123107, all from BioLegend). Filtered samples were acquired on FACSAria Sorp (BD-Biosciences), and data analyzed by FlowJo software (BD-Biosciences).

Lung and small intestine

Tissue was collected in RPMI-1640 containing 10% FBS on ice to maximize cell viability. Isolation/analysis of immune cells was performed according to Li et al. [31]. *T-/B-cell panel*: CD45-FITC (103108), CD45R/B220-PerCP/Cy5.5 (103235), CD138-PE (142503), CD4-APC/Cy7 (100525), CD8a-APC (100712), and Zombie Aqua (423101), all from BioLegend, 1:200 dilutions; *myeloid panel*: CD45-PerCP/Cy5.5 (103132), Ly6C-APC (128016), Ly6G-BV421 (127628), F4/80-FITC (123107), and Zombie NIR (423105), all from BioLegend, 1:200 dilutions, and CD11b-PE (1:200; 12-0112-81, eBioscience, San Diego, USA). Filtered samples were acquired on FACSAria-I (BD-Biosciences), data analyzed by FlowJo software (BD-Biosciences).

Statistical analysis

Statistical analyses were performed using SPSSv.17 (IBM-Deutschland-GmbH, Munich, Germany) or Prism5 (GraphPad-Software, San Diego, California, USA). Allelic and genotypic association tests were done in PLINKv1.90 (www.cog-genomics.org/plink/1.9/) [32]. Group differences in categorical/continuous variables were assessed using Cochran–Armitage test for trend, chi-square, Fisher's exact, McNemar's, Mann–Whitney *U*, or Student *t* tests, dependent on data distribution/variance homogeneity, ANOVA, or generalized estimating equation employed as indicated in the figures. All *p* values are two tailed unless stated otherwise; significance threshold set to $p < 0.05$; mean ± SEM presented. Based on previous work, sample sizes (humans, mice) were selected to have statistical power to detect differences. Care was taken to use a minimum number of animals (RRR principle). Datasets were routinely screened for statistical outliers to be excluded if indicated.

Results

Analysis across species of the spontaneous course of NMDAR1-AB in serum reveals intraindividual fluctuations

We investigated the spontaneous intraindividual course of serum NMDAR1-AB in long-term observational studies in humans and mice. Older mice have a high probability to be seropositive [20]. Therefore, cohorts of WT and $ApoE^{-/-}$ mice were screened for seroprevalence at age 14–19 months. Testing was repeated for all individuals 3–6 months after the first sampling. As illustrated in Fig. 1a–d, genotype groups showed an average of ≥40% seropositivity at both time points without considerable changes in overall Ig-class distribution. Analyzing the intraindividual course of serum NMDAR1-AB, remarkable fluctuations became obvious, comparable for both genotypes, with individual mice acquiring or losing NMDAR1-AB, others remaining seronegative or seropositive (Fig. 1b, d). Translating to older humans, a stroke population could be evaluated at 24 h post stroke and again 1–3 years thereafter. Here, a similarly undulating picture arose, with no change in absolute percentage of seropositivity or Ig-class distribution but obvious intraindividual shifts. Acquisition or loss amounted to lower overall percentages (<15%) as compared with mice (>30%) (Fig. 1e, f). Total plasma IgG, IgM, IgA, albumin, and CRP at 24 h after stroke did not differ between NMDAR1-AB carriers and non-carriers (all $p > 0.3$). In addition, we analyzed consecutive samples of non-human primates (baboons, rhesus macaques) showing equivalent fluctuations (data not shown). Together, these data across species reveal "oscillations" of serum NMDAR1-AB over time, and additionally, show that chronic BBB permeability in $ApoE^{-/-}$ mice and poststroke patients does not seem to measurably influence serum NMDAR1-AB. The slightly (non-significantly) lower overall seropositivity in $ApoE^{-/-}$ compared with WT mice may point to NMDAR1-AB continuously being trapped in brain [18] (see also below).

Small cortical brain lesion in juvenile mice enhances NMDAR1-AB seroprevalence and Ig-class diversity

We next wondered whether a brain lesion at young age would induce NMDAR1-AB formation, possibly due to early accessibility of the brain to immune cells via BBB

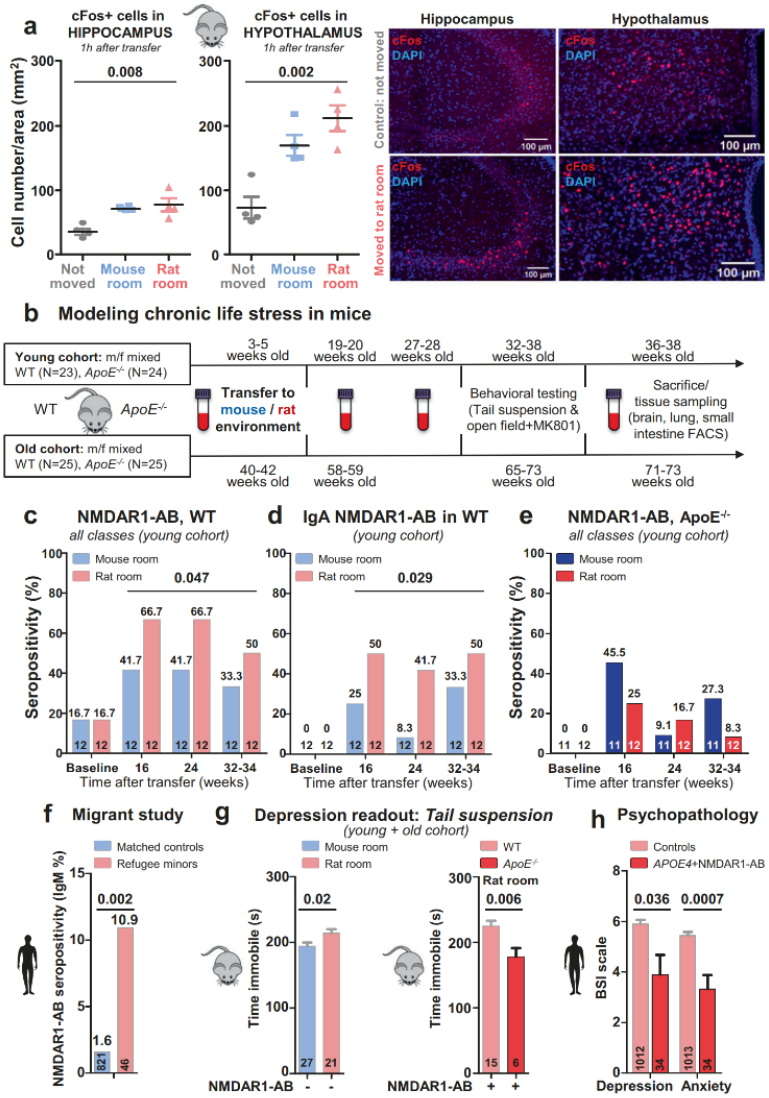

Fig. 3 NMDAR1-AB are induced by chronic life stress and exert antidepressive effects in mice and human. a Pilot experiment comparatively evaluating cFos expression in mouse brain as acute stress marker at 1 h after either moving within the mouse room, or moving to the rat room, or controls, staying without moving. Left: quantification of cFos + cells in the hippocampus and hypothalamus of C57BL/6N WT males, 4 weeks old, $n = 4$/group, 2–3 sections/mouse quantified; Jonckheere's trend test; right: representative images of cFos staining in the hippocampus and hypothalamus under control versus transfer to rat room conditions. **b** Experimental outline for modeling of chronic life stress in mice. *Young cohort*: mouse environment: $N = 23$, 11 $ApoE^{-/-}$ (eight males, three females), 12 WT (eight males, four females); rat environment: $N = 24$, 12 $ApoE^{-/-}$ (eight males, four females), 12 WT (four males, eight females); *old cohort*: mouse environment: $N = 24$, 12 $ApoE^{-/-}$ (six males, six females), 12 WT (three males, nine females); rat environment: $N = 26$, 13 $ApoE^{-/-}$ (six males, seven females), 13 WT (three males, ten females). **c** NMDAR1-AB overall seroprevalence of WT is higher in mice housed in the rat compared with the mouse room (young cohort displayed; old cohort similar—not shown). **d** This increased seroprevalence in WT is due to NMDAR1-AB of the IgA class. **e** In contrast, $ApoE^{-/-}$ mice lack the "organized pattern" seen in WT mice over time. *N* numbers given in the bars; generalized estimating equation, one sided. **f** NMDAR1-AB seroprevalence (IgM) is higher in prospectively recruited young migrants compared with age-matched controls of the GRAS data collection; *N* numbers given in the bars; Fisher's exact test, two sided. **g** Left: higher depressive-like behavior of seronegative mice housed in rat as compared with mouse environment (both genotypes pooled); right: comparison of seropositive mice housed in rat environment reveals an antidepressive effect of NMDAR1-AB dependent on BBB function, i.e., in $ApoE^{-/-}$ mice. *N* numbers given in the bars; unpaired *t* test, two sided. **h** Translation to humans using the GRAS data collection: NMDAR1-AB carriers with permeable BBB (*APOE4*+) are less depressed and anxious (BSI-scale scores) compared with controls; *N* numbers given in the bars; depression, unpaired *t* test, two sided; anxiety, Welch test, two sided.

breakdown [29]. Indeed, stereotactic application of a small standardized cryolesion to the right parietal cortex of mice at age 28 days, leading to BBB leakiness as described in detail before [29], induces higher overall Ig-class diversity as well as increased NMDAR1-AB seroprevalence (IgM or IgG, but not IgA), compared with the skin-only lesion (scalp incision) of sham-operated mice (Fig. 2a–c). This is in some contrast to human stroke (an "old-age lesion", also with compromised BBB) and perhaps explained by species differences or—more likely—the different responsiveness of the immune system at young age [33, 34]. It cannot be excluded at this point and may be interesting to explore in the future, whether lesions of other organs in young mice, e.g., the gut, would result in similar increases in NMDAR1-AB seroprevalence.

Immune-checkpoint *CTLA4* SNPs predispose to the presence of serum NMDAR1-AB in humans

The SNPs rs3087243 (A/G) and rs11571316 (A/G) of the human *CTLA4* (cytotoxic T-lymphocyte antigen4) gene on chromosome 2q33 have been associated with susceptibility to autoimmune disease, e.g., type 1 diabetes, Graves' disease, autoimmune hypothyroidism, systemic lupus, and Addison's disease [35–42]. Interestingly, this allelic variation can alter regulatory T-cell frequency and the signaling threshold of CD4+ T-cells [35, 39]. We therefore asked whether also NMDAR1-AB as components of the mammalian autoimmune repertoire would be associated with these immune-checkpoint *CTLA4* variants. Indeed, we obtained significant associations upon screening of $N =$ 2934 human subjects (healthy or suffering from neuropsychiatric diseases) of our GRAS database (Fig. 2d). Would this finding bring us closer to understanding autoimmune mechanisms regarding NMDAR1-AB?

Checkpoint-inhibitor treatment (anti-CTLA4-AB) of healthy adult mice does not further enhance their already high NMDAR1-AB seroprevalence

Since treatment of cancer patients with checkpoint-inhibitors (anti-CTLA4) has led to autoimmune diseases as serious adverse events [43–46], we next treated healthy female WT mice with CTLA4-AB, starting at age 11 weeks (Fig. 2e). Whereas the CTLA4-AB used (purified from monoclonal AB-producing UC10-4F10-11 hybridoma line [47]) proved functional in lymph node FACS and spleen cytospin preparation (double labeling with CD25 or FoxP3, Fig. 2f, g), there were no increased serum NMDAR1-AB at 4 weeks after 1 month of weekly injections (week 8 after treatment start, Fig. 2h). Seropositivity, also in controls at that time point, however, was already >40%. To summarize, *CTLA4* (immune-checkpoint) SNPs and CTLA4-AB treatment, previously associated with autoimmune disease, predispose in humans, as uncovered here, also to NMDAR1-AB, while checkpoint-inhibitor treatment (CTLA4-AB) of healthy adult mice without additional immune stimulation does not further enhance their already high NMDAR1-AB seroprevalence.

Modeling chronic life stress in WT mice leads to stress-induced enhancement of NMDAR1-AB seroprevalence mainly of the IgA class

Previously, we reported high early seroprevalence of NMDAR1-AB in non-human primates in captivity and human migrants, determined retrospectively, and interpreted these findings as a reflection of persistent life stress as potential inducer of NMDAR1-AB [20]. Searching now for a chronic stress paradigm that would not require too much interference with daily life in the cage, e.g., by handling, we developed the idea to expose mice to housing in close vicinity of their natural enemy/predator, the rat [48]. In order to evaluate the reaction of mice to this new environment, we compared the number of cFos+ cells (immediate early-gene expression as stress marker) [48] in hippocampus and hypothalamus of three subgroups of male animals, namely, mice 1 h after moving either to a rat room (cage surrounded by rat cages), or within a mouse room, or not moving at all. Figure 3a illustrates the clear stair pattern for both brain regions, with moving to the rat room reaching the highest values. We therefore chose this stress paradigm and exposed two cohorts of WT versus $ApoE^{-/-}$ mice (young and old; groups balanced for gender), to either mouse or rat environment. Blood samples for NMDAR1-AB determinations were drawn at baseline and after 16, 24, and ~33 weeks of transfer (Fig. 3b). This prospective experimental stress study yielded in WT mice, living in rat environment, an overall increase in serum NMDAR1-AB, dominated by NMDAR1-AB of the IgA class (young cohort shown in Fig. 3c, d; old cohort similar—not shown). In contrast, the serum pattern obtained in $ApoE^{-/-}$ mice with their leaky BBB looks "less organized" and seems not clearly interpretable, most likely due to irregular transfer to and massive trapping of NMDAR1-AB in brain (Fig. 3e) [18, 49]. This binding to brain tissue on the other hand explains the distinct behavioral effects observed in $ApoE^{-/-}$ mice. In fact, the MK-801 open-field test resulted, as expected from our previous work [17, 20], in a clear distinction between NMDAR1-AB carriers with or without compromised BBB. Seropositive $ApoE^{-/-}$ mice showed increased locomotion after MK-801 compared with seropositive WT, independent of environment (mouse versus rat room) and age group (young as well as old cohort). While these results indicate functionality of the NMDAR1-AB upon access to brain, immunohistochemistry did not

yield differences dependent on NMDAR1-AB seropositivity regarding microglia or T-cell numbers as readouts of brain inflammation. This is less surprising when considering the complete lack of any quantifiable cellular response of that kind in the brain even upon immunization against NMDAR1 peptides, leading to extremely high circulating titers of functional NMDAR1-AB of the IgG class [20]. In addition, extensive repeated FACS of blood as well as terminal FACS of lung and gut did not reveal any considerable changes in major immune cell composition (data not shown).

Chronic life stress in humans: replication of our previous findings of enhanced NMDAR1-AB seroprevalence in young migrants

We next tried in humans to further consolidate, in a straightforward, hypothesis-driven fashion, the stress association of NMDAR1-AB seroprevalence. This had previously been suspected for non-human primates in captivity and human migrants [20], and has now experimentally been confirmed here in mice, housed close to their natural enemies. Thus, we prospectively recruited young migrants ($N = 46$) from different countries/ethnicities (Africa/Middle East/Europe). They were 18.7 ± 4.6 years old at the time of flight as war or political refugees, many as unaccompanied refugee minors. The NMDAR1-AB seroprevalence of these refugees, determined on average 2.5 years later and compared with that of $N = 821$ age-matched individuals of the GRAS data collection without migration background, revealed again a highly significant increase. This increase consisted in this very young population still of IgM, likely before the expected class switch to IgA (Fig. 3f).

Novel antidepressive, ketamine-like role of NMDAR1-AB upon access to the brain in humans and mice

We next wondered whether housing in a rat environment would result in a depressive-like phenotype in mice as determined by an established depression measure, the tail-suspension test [50]. Indeed, pooling all NMDAR1-AB seronegative WT and *ApoE*$^{-/-}$ mice, and comparing individuals in mouse environment with those in rat neighborhood, showed a significant increase in immobility of the latter. Strikingly, NMDAR1-AB seropositive *ApoE*$^{-/-}$ mice with their permeable BBB exhibited in the rat environment a clearly lower depressive-like phenotype compared with seropositive WT (Fig. 3g). Would we be able to see similar effects in humans? To address this question, we again employed deeply phenotyped subjects of the GRAS data collection. As shown in Fig. 3h, NMDAR1-AB seropositive *APOE4* carriers ($N = 34$; permeable BBB [51–53]) had significantly lower depression and anxiety ratings as compared with all controls ($N = 1013$) that do not combine both markers (APOE4+ and NMDAR1-AB+).

Discussion

The present study addressed several yet unclear topics in the NMDAR1-AB field, which are relevant for basic and clinical research and practice, but likely also for our understanding of (patho)physiological autoimmunity beyond NMDAR1-AB.

In older subjects, mice and humans, the course of serum NMDAR1-AB fluctuates remarkably, independent of BBB intactness. Similar fluctuations have been observed previously with other autoantibodies, determined as predictors of disease probability, e.g., in type I diabetes [54]. Assuming that NMDAR1-AB are part of the normal autoimmune repertoire, the detected fluctuations might be due to just periodical boosting of the respective B cells by various possible inducers [13, 17, 21, 55], in sum adding up to the age-dependently increasing total numbers. In absence of any persistent or reappearing inducers/boosters, levels would probably rather decline over time. Another potential mechanism of fast fluctuations or rapid decrease may be the trapping of NMDAR1-AB in brain upon BBB perturbation [21], which may lead to disappearance of previously measurable serum titers. In fact, since NMDAR1-AB serum levels decreased 2 days after stroke [16], we hypothesized earlier that brain tissue with its densely expressed NMDAR1 (acutely accessible after BBB breakdown due to stroke) may "extract" circulating NMDAR1-AB [16, 21]. Indeed, we could experimentally prove in mice that the brain acts as "immunoprecipitator" [21].

Despite the well-known continued BBB leakiness after stroke, and the accessibility of immune cells to the brain, we did not find evidence of stroke to induce further serum NMDAR1-AB. This apparent lack of an effect may be due, at least in part, to stroke lesion-induced neuropathology, which often continues to progress over time from the point of the initial lesion, especially in the elderly, once again serving as an "immunoprecipitator" [21]. This could potentially veil increased amounts of NMDAR1-AB. Further stroke follow-up work will be needed to test this possibility.

In contrast to stroke (as a brain lesion of old age), a small standardized cryolesion of the right parietal cortex in juvenile mice enhanced seroprevalence and Ig-class diversity of NMDAR1-AB. Strikingly, when comparing NMDAR1-AB Ig-classes post cryolesion (physical brain damage) with those induced by chronic life stress ("only" psychological brain trauma), we see IgG/IgM prevailing in

the former, IgA in the latter condition. While we already suggested an association of stress with NMDAR1-AB of the IgA class in previous work on monkeys and migrants [20], the increase in IgG/IgM (but not IgA) NMDAR1-AB seroprevalence upon brain lesion was unexpected and will require experimental and clinical follow-up studies to further confirm and explore the mechanisms underlying this highly interesting class-specific response. Since IgA is seen as "mucosal Ig", we wondered whether chronic life stress, known to be commonly associated with an abnormal breathing pattern or with a tendency to develop diarrhea or constipation, would reveal an altered immune cell composition in lung [56] and/or gut [57] of our experimental animals. However, neither FACS of these organs nor of blood uncovered any appreciable changes in the proportion of the main immune cell subsets. Therefore, numerical alterations do not aid in explaining the here-observed Ig-class-specific response, and future work on NMDAR1-AB formation will have to explore the mechanisms prompting inducer-specific Ig-class formation.

In a first search of cellular mechanisms relevant for (patho)physiological autoimmunity in general, and NMDAR1-AB in particular, we focused here on the gene encoding *CTLA4*, an Ig-superfamily member and dampener of T-cell activation, with recognized susceptibility to various autoimmune diseases [35–42]. Correspondingly, anti-CTLA4 treatment of cancer patients can result in autoimmune disease as serious adverse event [43–46]. CTLA4 is an important regulator of the immune response, exerting its influence on reactivity to both foreign and self-antigens. Allelic variation of *CTLA4* as well as CTLA4 blockade/anti-CTLA4 treatment influences the signaling threshold of CD4 T-cells [39, 45], thereby augmenting antitumor immunity but also exacerbating/inducing autoimmune disease. Would NMDAR1-AB as components of the natural autoimmune repertoire follow the rules observed for autoimmune diseases? While we could demonstrate an association of *CTLA4* SNPs with NMDAR1-AB seroprevalence in humans, our first treatment approach in mice did not yield the expected increased NMDAR1-AB seroprevalence. This negative result may be explained by the here performed anti-CTLA4 treatment under basal housing and cage-life conditions and, accordingly, a lack of particular immune stimulation that would have led to the necessary threshold of T-cell activation. Another factor to be changed in a follow-up study might be the relatively old age of mice at treatment start with an already high percentage of NMDAR1-AB carriers at the time point of analysis.

Finally, the perhaps most intriguing finding of the present study is the antidepressive action of circulating NMDAR1-AB, induced upon experimental chronic life stress in mice, and analogously demonstrated in human NMDAR1-AB carriers. The presence of NMDAR1-AB in serum, together with a compromised BBB, allowing their access to brain, reduces depression and anxiety. The antidepressive effect of the NMDAR antagonist ketamine is well established and increasingly applied in the clinical setting [58–61]. Our across-species findings with NMDAR1-AB as "endogenous antagonists" do not only replicate in vivo functionality of NMDAR1-AB, but also raise the intriguing possibility that the body can, under certain circumstances, produce its own antidepressants. Recent work reports sustained rescue of prefrontal circuit dysfunction by ketamine-induced spine formation as potential antidepressive mechanism [62, 63]. The question of whether NMDAR1-AB as endogenous antidepressants act in a similar fashion will have to be pursued in follow-up studies, searching for further mechanistic insight.

To summarize, the present translational work demonstrates that the abundantly detected NMDAR1-AB in serum of mammals fluctuate spontaneously, are Ig-class specifically induced by brain lesion or chronic life stress, particularly at young age, and can act in an antidepressive fashion upon brain access. Building here on the highly frequent NMDAR1-AB as a convenient research tool, these findings may extend beyond NMDAR1-AB, indicate general modulatory roles of autoantibodies regarding a wide range of biological functions, and inspire a broader perspective on (patho)physiological autoimmunity.

Acknowledgements This study was supported by the Max Planck Society and the DFG Research Center for Nanoscale Microscopy and Molecular Physiology of the Brain (CNMPB) as well as the DFG CRC TRR 274. The authors thank Angelika Mönnich for helping with CTLA4 antibody purification. Open access funding provided by Projekt DEAL.

Author contributions Concept, study design, and supervision: HE, together with FL. Experimental design and interpretation: HP, HE, and FL. Data acquisition and analysis: HP, AAS-K, AS, ND, AR, DT, NvA, MM, HW, RT, CK-S, NS, KR, MB, JW, WS, KW, MH, K-AN, FL, and HE. Drafting the paper: HE, together with HP. Drafting display items: HP, AAS-K, and HE. All authors read and approved the final version of the paper.

Compliance with ethical standards

Conflict of interest WS is a member of the board and holds stocks in Euroimmun AG. KR is a full-time employee of Euroimmun AG. All other authors declare no competing financial or other interests.

Publisher's note Springer Nature remains neutral with regard to jurisdictional claims in published maps and institutional affiliations.

References

1. Li F, Tsien JZ. Memory and the NMDA receptors. N Engl J Med. 2009;361:302–3.
2. Dzamba D, Honsa P, Anderova M. NMDA receptors in glial cells: pending questions. Curr Neuropharmacol. 2013;11:250–62.
3. Lau CG, Zukin RS. NMDA receptor trafficking in synaptic plasticity and neuropsychiatric disorders. Nat Rev Neurosci. 2007;8:413–26.
4. Reijerkerk A, Kooij G, van der Pol SM, Leyen T, Lakeman K, van Het Hof B, et al. The NR1 subunit of NMDA receptor regulates monocyte transmigration through the brain endothelial cell barrier. J Neurochem. 2010;113:447–53.
5. Saab AS, Tzvetavona ID, Trevisiol A, Baltan S, Dibaj P, Kusch K, et al. Oligodendroglial NMDA receptors regulate glucose import and axonal energy metabolism. Neuron. 2016;91:119–32.
6. Du J, Li XH, Li YJ. Glutamate in peripheral organs: biology and pharmacology. Eur J Pharm. 2016;784:42–8.
7. Dalmau J, Tuzun E, Wu HY, Masjuan J, Rossi JE, Voloschin A, et al. Paraneoplastic anti-N-methyl-D-aspartate receptor encephalitis associated with ovarian teratoma. Ann Neurol. 2007;61:25–36.
8. Dalmau J, Gleichman AJ, Hughes EG, Rossi JE, Peng X, Lai M, et al. Anti-NMDA-receptor encephalitis: case series and analysis of the effects of antibodies. Lancet Neurol. 2008;7:1091–8.
9. Dalmau J, Lancaster E, Martinez-Hernandez E, Rosenfeld MR, Balice-Gordon R. Clinical experience and laboratory investigations in patients with anti-NMDAR encephalitis. Lancet Neurol. 2011;10:63–74.
10. Titulaer MJ, McCracken L, Gabilondo I, Armangué T, Glaser C, Iizuka T, et al. Treatment and prognostic factors for long-term outcome in patients with anti-NMDA receptor encephalitis: an observational cohort study. Lancet Neurol. 2013;12:157–65.
11. Hughes EG, Peng X, Gleichman AJ, Lai M, Zhou L, Tsou R, et al. Cellular and synaptic mechanisms of anti-NMDA receptor encephalitis. J Neurosci. 2010;30:5866–75.
12. Choe CU, Karamatskos E, Schattling B, Leypoldt F, Liuzzi G, Gerloff C, et al. A clinical and neurobiological case of IgM NMDA receptor antibody associated encephalitis mimicking bipolar disorder. Psychiatry Res. 2013;208:194–6.
13. Prüss H, Finke C, Holtje M, Hofmann J, Klingbeil C, Probst C, et al. N-methyl-D-aspartate receptor antibodies in herpes simplex encephalitis. Ann Neurol. 2012;72:902–11.
14. Prüss H, Holtje M, Maier N, Gomez A, Buchert R, Harms L, et al. IgA NMDA receptor antibodies are markers of synaptic immunity in slow cognitive impairment. Neurology. 2012;78:1743–53.
15. Steiner J, Walter M, Glanz W, Sarnyai Z, Bernstein HG, Vielhaber S, et al. Increased prevalence of diverse N-methyl-D-aspartate glutamate receptor antibodies in patients with an initial diagnosis of schizophrenia: specific relevance of IgG NR1a antibodies for distinction from N-methyl-D-aspartate glutamate receptor encephalitis. JAMA Psychiatry. 2013;70:271–8.
16. Zerche M, Weissenborn K, Ott C, Dere E, Asif AR, Worthmann H, et al. Preexisting serum autoantibodies against the NMDAR subunit NR1 modulate evolution of lesion size in acute ischemic stroke. Stroke. 2015;46:1180–6.
17. Hammer C, Stepniak B, Schneider A, Papiol S, Tantra M, Begemann M, et al. Neuropsychiatric disease relevance of circulating anti-NMDA receptor autoantibodies depends on blood-brain barrier integrity. Mol Psychiatry. 2014;19:1143–9.
18. Castillo-Gomez E, Oliveira B, Tapken D, Bertrand S, Klein-Schmidt C, Pan H, et al. All naturally occurring autoantibodies against the NMDA receptor subunit NR1 have pathogenic potential irrespective of epitope and immunoglobulin class. Mol Psychiatry. 2017;22:1776–84.
19. Hammer C, Zerche M, Schneider A, Begemann M, Nave KA, Ehrenreich H. Apolipoprotein E4 carrier status plus circulating anti-NMDAR1 autoantibodies: association with schizoaffective disorder. Mol Psychiatry. 2014;19:1054–6.
20. Pan H, Oliveira B, Saher G, Dere E, Tapken D, Mitjans M, et al. Uncoupling the widespread occurrence of anti-NMDAR1 autoantibodies from neuropsychiatric disease in a novel autoimmune model. Mol Psychiatry. 2019;24:1489–501.
21. Castillo-Gomez E, Kastner A, Steiner J, Schneider A, Hettling B, Poggi G, et al. The brain as immunoprecipitator of serum autoantibodies against N-Methyl-D-aspartate receptor subunit NR1. Ann Neurol. 2016;79:144–51.
22. Dahm L, Ott C, Steiner J, Stepniak B, Teegen B, Saschenbrecker S, et al. Seroprevalence of autoantibodies against brain antigens in health and disease. Ann Neurol. 2014;76:82–94.
23. Steiner J, Teegen B, Schiltz K, Bernstein HG, Stoecker W, Bogerts B. Prevalence of N-methyl-D-aspartate receptor autoantibodies in the peripheral blood: healthy control samples revisited. JAMA Psychiatry. 2014;71:838–9.
24. Begemann M, Grube S, Papiol S, Malzahn D, Krampe H, Ribbe K, et al. Modification of cognitive performance in schizophrenia by complexin 2 gene polymorphisms. Arch Gen Psychiatry. 2010;67:879–88.
25. Ribbe K, Friedrichs H, Begemann M, Grube S, Papiol S, Kastner A, et al. The cross-sectional GRAS sample: a comprehensive phenotypical data collection of schizophrenic patients. BMC Psychiatry. 2010;10:91.
26. Stepniak B, Kastner A, Poggi G, Mitjans M, Begemann M, Hartmann A, et al. Accumulated common variants in the broader fragile X gene family modulate autistic phenotypes. EMBO Mol Med. 2015;7:1565–79.
27. Franke GH, Heemann U, Kohnle M, Luetkes P, Maehner N, Reimer J. Quality of life in patients before and after kidney transplantation. Psychol Health. 2000;14:1037–49.
28. Wandinger KP, Saschenbrecker S, Stoecker W, Dalmau J. Anti-NMDA-receptor encephalitis: a severe, multistage, treatable disorder presenting with psychosis. J Neuroimmunol. 2011;231:86–91.
29. Sirén AL, Radyushkin K, Boretius S, Kammer D, Riechers CC, Natt O, et al. Global brain atrophy after unilateral parietal lesion and its prevention by erythropoietin. Brain. 2006;129:480–9.
30. Cryan JF, Mombereau C, Vassout A. The tail suspension test as a model for assessing antidepressant activity: review of pharmacological and genetic studies in mice. Neurosci Biobehav Rev. 2005;29:571–625.
31. Li Q, Li D, Zhang X, Wan Q, Zhang W, Zheng M, et al. E3 Ligase VHL promotes group 2 innate lymphoid cell maturation and function via glycolysis inhibition and induction of interleukin-33 receptor. Immunity. 2018;48:258–70.
32. Chang CC, Chow CC, Tellier LC, Vattikuti S, Purcell SM, Lee JJ. Second-generation PLINK: rising to the challenge of larger and richer datasets. Gigascience. 2015;4:7.
33. Dorshkind K, Montecino-Rodriguez E, Signer RA. The ageing immune system: is it ever too old to become young again? Nat Rev Immunol. 2009;9:57–62.
34. Nikolich-Zugich J. The twilight of immunity: emerging concepts in aging of the immune system. Nat Immunol. 2018;19:10–9.
35. Atabani SF, Thio CL, Divanovic S, Trompette A, Belkaid Y, Thomas DL, et al. Association of CTLA4 polymorphism

with regulatory T cell frequency. Eur J Immunol. 2005; 35:2157–62.
36. Birlea SA, Laberge GS, Procopciuc LM, Fain PR, Spritz RA. CTLA4 and generalized vitiligo: two genetic association studies and a meta-analysis of published data. Pigment Cell Melanoma Res. 2009;22:230–4.
37. Blomhoff A, Lie BA, Myhre AG, Kemp EH, Weetman AP, Akselsen HE, et al. Polymorphisms in the cytotoxic T lymphocyte antigen-4 gene region confer susceptibility to Addison's disease. J Clin Endocrinol Metab. 2004;89:3474–6.
38. Howson JM, Dunger DB, Nutland S, Stevens H, Wicker LS, Todd JA. A type 1 diabetes subgroup with a female bias is characterised by failure in tolerance to thyroid peroxidase at an early age and a strong association with the cytotoxic T-lymphocyte-associated antigen-4 gene. Diabetologia. 2007;50:741–6.
39. Maier LM, Anderson DE, De Jager PL, Wicker LS, Hafler DA. Allelic variant in CTLA4 alters T cell phosphorylation patterns. Proc Natl Acad Sci USA. 2007;104:18607–12.
40. Torres B, Aguilar F, Franco E, Sanchez E, Sanchez-Roman J, Jimenez Alonso J, et al. Association of the CT60 marker of the CTLA4 gene with systemic lupus erythematosus. Arthritis Rheum. 2004;50:2211–5.
41. Ueda H, Howson JM, Esposito L, Heward J, Snook H, Chamberlain G, et al. Association of the T-cell regulatory gene CTLA4 with susceptibility to autoimmune disease. Nature. 2003;423: 506–11.
42. Walker EJ, Hirschfield GM, Xu C, Lu Y, Liu X, Lu Y, et al. CTLA4/ICOS gene variants and haplotypes are associated with rheumatoid arthritis and primary biliary cirrhosis in the Canadian population. Arthritis Rheum. 2009;60:931–7.
43. Bartels F, Stronisch T, Farmer K, Rentzsch K, Kiecker F, Finke C. Neuronal autoantibodies associated with cognitive impairment in melanoma patients. Ann Oncol. 2019;30:823–9.
44. de Moel EC, Rozeman EA, Kapiteijn EH, Verdegaal EME, Grummels A, Bakker JA, et al. Autoantibody development under treatment with immune-checkpoint inhibitors. Cancer Immunol Res. 2019;7:6–11.
45. Lühder F, Hoglund P, Allison JP, Benoist C, Mathis D. Cytotoxic T lymphocyte-associated antigen 4 (CTLA-4) regulates the unfolding of autoimmune diabetes. J Exp Med. 1998;187: 427–32.
46. June CH, Warshauer JT, Bluestone JA. Is autoimmunity the Achilles' heel of cancer immunotherapy? Nat Med. 2017;23:540–7.
47. Walunas TL, Lenschow DJ, Bakker CY, Linsley PS, Freeman GJ, Green JM, et al. CTLA-4 can function as a negative regulator of T cell activation. Immunity. 1994;1:405–13.
48. Martinez RC, Carvalho-Netto EF, Amaral VC, Nunes-de-Souza RL, Canteras NS. Investigation of the hypothalamic defensive system in the mouse. Behav Brain Res. 2008;192:185–90.
49. Diamond B, Huerta PT, Mina-Osorio P, Kowal C, Volpe BT. Losing your nerves? Maybe it's the antibodies. Nat Rev Immunol. 2009;9:449–56.
50. Ferreira MF, Castanheira L, Sebastiao AM, Telles-Correia D. Depression assessment in clinical trials and pre-clinical tests: a critical review. Curr Top Med Chem. 2018;18:1677–703.
51. Bell RD, Winkler EA, Singh I, Sagare AP, Deane R, Wu Z, et al. Apolipoprotein E controls cerebrovascular integrity via cyclophilin A. Nature. 2012;485:512–6.
52. Halliday MR, Pomara N, Sagare AP, Mack WJ, Frangione B, Zlokovic BV. Relationship between cyclophilin a levels and matrix metalloproteinase 9 activity in cerebrospinal fluid of cognitively normal apolipoprotein e4 carriers and blood-brain barrier breakdown. JAMA Neurol. 2013;70:1198–1200.
53. Zlokovic BV. Cerebrovascular effects of apolipoprotein E: implications for Alzheimer disease. JAMA Neurol. 2013;70:440–4.
54. Endesfelder D, Zu Castell W, Bonifacio E, Rewers M, Hagopian WA, She JX, et al. Time-resolved autoantibody profiling facilitates stratification of preclinical type 1 diabetes in children. Diabetes. 2019;68:119–30.
55. Bechter K. Mild encephalitis underlying psychiatric disorder—a reconsideration and hypothesis exemplified on Borna disease. Neurol Psychiat Br. 2001;9:55–70.
56. Salvi S, Holgate ST. Could the airway epithelium play an important role in mucosal immunoglobulin A production? Clin Exp Allergy. 1999;29:1597–605.
57. Tezuka H, Ohteki T. Regulation of IgA production by intestinal dendritic cells and related cells. Front Immunol. 2019;10:1891.
58. Zanos P, Moaddel R, Morris PJ, Riggs LM, Highland JN, Georgiou P, et al. Ketamine and Ketamine Metabolite Pharmacology: insights into therapeutic mechanisms. Pharm Rev. 2018;70:621–60.
59. Peltoniemi MA, Hagelberg NM, Olkkola KT, Saari TI. Ketamine: a review of clinical pharmacokinetics and pharmacodynamics in anesthesia and pain therapy. Clin Pharmacokinet. 2016;55:1059–77.
60. Aleksandrova LR, Phillips AG, Wang YT. Antidepressant effects of ketamine and the roles of AMPA glutamate receptors and other mechanisms beyond NMDA receptor antagonism. J Psychiatry Neurosci. 2017;42:222–9.
61. Molero P, Ramos-Quiroga JA, Martin-Santos R, Calvo-Sanchez E, Gutierrez-Rojas L, Meana JJ. Antidepressant efficacy and tolerability of ketamine and esketamine: a critical review. CNS Drugs. 2018;32:411–20.
62. Moda-Sava RN, Murdock MH, Parekh PK, Fetcho RN, Huang BS, Huynh TN, et al. Sustained rescue of prefrontal circuit dysfunction by antidepressant-induced spine formation. Science. 2019;364:pii: eaat8078.
63. Beyeler A. Do antidepressants restore lost synapses? Science. 2019;364:129–30.

Chapter 4
Summary and outlook

Summary and outlook

From the previous work of our group in this field, we found comparable seroprevalence of NMDAR1-AB in human across healthy and disease groups, increasing with age. The NMDAR1-AB in those individuals are also functional confirmed by internalization test, electrophysiology test, and they share similar epitopes among different Ig classes (IgA, IgG and IgM) (Castillo-Gomez et al., 2017; Dahm et al., 2014; Ehrenreich, 2017, 2018; Hammer et al., 2014).

In the 1st project, we explored the seroprevalence in non-human mammals, and studied the effects of NMDAR1-AB in mice by an immunization model.

(I) The seroprevalence of NMDAR1-AB in non-human mammals. We detected the NMDAR1-AB in dogs, cats, mice, rats in an age-dependent pattern. The NMDAR1-AB in baboons and rhesus macaques are exceptional, as they already had a high seroprevalence at an early age. Thus, we hypothesized that chronic life stress maybe related to the NMDAR1-AB production. Driven by this hypothesis, we tested human migrants who also had chronic life stress and found a high seroprevalence of NMDAR1-AB (prominent IgA class) at an early age too.

(II) We used an active immunization mouse model to study the effect of carrying NMDAR1-AB. We immunized both *ApoE*$^{-/-}$ and WT mice with GluN1 antigen cocktail containing 4 different peptides against NMDA receptor extracellular structure. We confirmed the high titer of NMDAR1-AB IgG class by ELISA, and the kinetics of NMDAR1-AB production is similar to ovalbumin. In addition, the *ApoE*$^{-/-}$ mice who also carried the NMDAR1-AB showed higher locomotion in open field after MK801 challenge compared to the WT mice AB carriers. This result confirmed the functionality of the endogenously produced NMDAR1-AB in terms of hypofunction hypothesis of NMDA receptors (Hammer et al., 2014; Vishnoi et al., 2015). However, the mice did not develop anti-NMDAR encephalitis although there were high titers of NMDAR1-AB IgG class produced endogenously, which is contradictory to the findings of Dalmau (Dalmau et al., 2008; Dalmau et al., 2018; Dalmau et al., 2011; Dalmau et al., 2007). In our mouse model, circulating NMDAR1-AB (IgG class) in healthy mice does not result in anti-NMDAR encephalitis.

Jones et al. published an immunization mouse model in July 2019 with NMDA receptor holoprotein, and they reported that the mice developed fulminant anti-NMDAR encephalitis (Jones et al., 2019). Although we found the immunization strategy is elegant, there are still some questions remaining to be addressed in this study. For example, saline or empty liposome was used as controls which may not be adequate to control for the liposome-embedded native NMDA receptors. It would be interesting to add an additional liposome-embedded protein (e.g. GABA receptor) as controls (Ehrenreich et al., 2019). Our hypothesis remains that pre-existing encephalitis plus the circulating NMDAR1-AB will cause the typical Dalmau anti-NMDAR encephalitis model. The project aiming to prove the hypothesis is currently running in our group, we hope to uncover the mechanism behind the disease soon.

The 2nd project aimed to find the potential inducers of the NMDAR1-AB.

(I) We observed the spontaneous NMDAR1-AB course in a longitudinal study both in mice and humans. We found the fluctuation of the NMDAR1-AB in both *ApoE*$^{-/-}$ and WT mice, which means that we saw one can gain or lose the AB, or stay positive or negative over a 3-6 months' time period. The same phenomenon was seen in human ischemic stroke patients from 24h of the symptom onset till 1-3 years after stroke. These findings indicated that NMDAR1-AB belong to the normal autoantibody repertoire, and the specific B cell clone can be stimulated under certain circumstances, e.g. infection or trauma, etc. Similar fluctuation of autoantibodies were seen in other studies, for instance for type 1 diabetes (Endesfelder et al., 2019); or SLE (Arbuckle et al., 2003).

In type 1 diabetes, Endesfelder et al performed a longitudinal study in children who were at risk genetically for developing type 1 diabetes, which was published in 2019. The authors reported the children were stable-positive for insulin autoantibodies (IAA) and insulinoma-associated antigen 2 autoantibodies (IA-2A) on follow up had the highest risk of diabetes compared to those who were transitionally positive or negative (Endesfelder et al., 2019). In SLE, autoantibodies including antinuclear antibodies (ANAs), anti–double-stranded DNA antibodies, etc. are typically present many years before the diagnosis (Arbuckle et al., 2003). It's also common to find ANA positivity in the general population, also supporting the fact that autoantibodies are part of a healthy

immune response supported together with our findings (Castillo-Gomez et al., 2017; Dahm et al., 2014; Hammer et al., 2014; Pan et al., 2019). Thus detecting of autoantibodies is not sufficient to predict diseases, it remains a challenge to uncover the mechanism of the transition from health to disease (Olsen et al., 2014).

(II) We conducted cryolesion surgery (brain injury model) in mice as a potential inducer, and a higher diversity of NMDAR1-AB in the lesion mice was observed compared to the sham mice. The cryolesion mice also had more IgG and IgM classes compared to the sham mice, however, the IgA class stays comparable between the two groups. This is an interesting finding, as we observed that brain lesion had an effect on the young mice, but not in the stroke patients (relatively old) who also had a lesion in the brain. This could probably be explained by the efficacy of the immune system at young and old age (Linton et al., 2004; Nikolich-Zugich, 2018).

(III) We tried the immune check point inhibitor CTLA4-AB as a potential inducer, as we found *CTLA4* SNPs (rs3087243 and rs11571316) were associated with NMDAR1-AB in human. However, in our experimental setup, no increase of NMDAR1-AB in mice treated with CTLA4-AB was observed compared to the control IgG treated mice.

CTLA4 is cytotoxic T lymphocyte associated protein 4, exclusively expressed on T lymphocytes, constitutively by Treg cells and transiently on activated T cells. It works as a co-inhibitory signal, and it is an essential immune checkpoint to maintain self-tolerance and protecting the host form tissue damage (Murphy, 2012). Checkpoint inhibitors are used for treating cancers, and the findings were awarded for Nobel Prize in 2018. The antibody against CTLA4 (ipilimumab) was approved for treating metastatic melanoma by the Food and Drug Administration (FDA) in 2011. The treatment mechanism is by blocking CTLA4 (competing with CD28 to bind with B7 ligand), CD28 on the T cell surface could to bind with B7 ligand on the antigen presenting cells (APCs), thus T cells can be activated, and migrate to the cancer tissue, resulting in attacking cancer cells (Abril-Rodriguez et al., 2017). There were studies showed that melanoma patients after treatment with ipilimumab often developed autoantibodies (Bartels et al., 2019), and many autoimmune diseases such as colitis, dermatitis, hepatitis etc. (de Moel et al.,

2019; June et al., 2017). There were also studies reporting that the CTLA4 expression increase with aging in both humans and mice (Channappanavar et al., 2009; Leng et al., 2002), and we reported that the NMDAR1-AB increase with aging in both human and animals (Castillo-Gomez et al., 2017; Dahm et al., 2014; Hammer et al., 2014; Pan et al., 2019). We still cannot exclude the probability that CTLA4-AB being an inducer of NMDAR1-AB formation. Therefore, we updated our hypothesis: to stimulate NMDAR1-AB production by the treatment of CTLA4-AB, additional immune challenges need to be considered. The project driven by this hypothesis is also running in our group currently.

(IV) We used a chronic stress mouse model to prove our hypothesis from project 1: Chronic life stress may relates to NMDAR1-AB production. We designed a mouse model that allowed us to apply chronic stress in mice without interfering in their daily lives. The mice were transferred to the rat (predator of mice) environment. They did not have direct contact with rats, but they had direct access to the same environment air. We observed an increase of NMDAR1-AB especially IgA class in the WT mice housed in the rat environment compared to the mice housed in the mouse environment as controls. However, we did not observe NMDAR1-AB changes in ApoE-/- mice. The possible explanation is that the NMDAR1-AB could reach the brain through the compromised BBB and bind to the NMDA receptors, thus there was no difference in the periphery (Castillo-Gomez E, 2016; Zerche et al., 2015). Meanwhile, the mice in the rat environment showed depression signs as compared to the controls in the tail suspension test. Moreover, the *ApoE*$^{-/-}$ mice who had a compromised BBB and also carried the NMDAR1-AB showed less depressive phenotype compared the WT mice who carried NMDAR1-AB. In our human study, we observed that individuals who had a compromised BBB (*APOE4*+) and were NDMAR1-AB carriers had less depression and anxiety score.

We proved that the rat environment is stressful for the mice by cFos quantification in the hippocampus and hypothalamus in the mouse brains. cFos is an immediate early gene, it was used as a stress marker as it reflects the activity of the cells (Canteras et al., 2008; Cullinan et al., 1995; Hoffman GE, 1993; Martinez et al., 2008). However, we did not have a good chronic stress marker, as it was a mild chronic stress paradigm over 30 weeks. The classical stress marker corticosterone is frequently used in acute stress paradigms (Sapolsky et al., 2000)

or reported reflecting variation in metabolic rate independent of stress (Jimeno et al., 2018), we did not see any difference in a chronic period (data not shown). Besides, the blood sampling methods seem also to have an impact on the level of plasma corticosterone, the samples obtained from retro-orbital (our strategy) have a much higher level of corticosterone compared to other methods, e.g. via tail snip. (Kim, S. et al., 2018). However, we did not have other choices as we need sufficient amount of blood samples (minimizing invasion to the mice) for both flow cytometry and NMDAR1-AB determination in the plasma. We also tried with another marker: ghrelin. Ghrelin is a hormone produced in gastrointestinal tract, it regulated food intake and body weight, also controls glucose metabolism (Sakata et al., 2010; Wiedmer et al., 2007). It was proposed to be related to stress response and used as a stress marker (Sominsky et al., 2017; Yousufzai et al., 2018). However, we did not observe any difference between the mice house in the mouse and rat environment at the end of the study (data not shown). We also did not observe any difference regarding food intake and body weight (data not shown) between the mice in mouse and rat environment, which fits to the ghrelin results. The possible explanation could be that our stress paradigm is too mild to induce the endocrine hormone changes, or the mice slowly adapt to the rat environment so that we could not detect the differences at these time points. As we observed the depressive behavior in the mice in the rat environment by tail suspension test, we believe the paradigm is valid enough to study the impact of chronic stress on NMDAR1-AB formation. Indeed, we observed there was an increased NMDAR1-AB seropositivity in the mice housed in the rat environment, especially IgA class, which fits to our hypothesis. Compared to the results from the cryolesion mice where we observed IgG+IgM increase instead of IgA; it became very interesting. So far, there were no studies reporting the Ig class specificity by the inducers, and the mechanism behind needs to be pursed further.

As IgA is secreted by the mucosal membrane, we wondered whether there is a difference regarding the immune system in the lung and small intestine. However, we did not observe considerable changes in the major immune cells composition neither between the two environments, nor seropositive and seronegative mice in flow cytometry analysis in blood, lung and small intestine. These results suggested that there is no inflammation in the periphery in the mice

from the chronic stress study. In addition, we are still analyzing the inflammation markers in the brain in the mice from the chronic stress study.

Besides discussed above, there are still a lot of questions which need to be addressed in the future work. For example, under which circumstances, the specific B/T cell clone will be activated? As B1 cells were thought to be associated with autoimmune disease (Linton et al., 2004), are they also involved in the NMDAR1-AB production? Some of the questions are integrated in current running projects in our group. We hope to uncover the mechanism of the anti-NMDAR encephalitis induction and NMDAR1-AB production.

Chapter 5
Bibliography

Bibliography

Abril-Rodriguez, G., & Ribas, A. (2017). SnapShot: Immune Checkpoint Inhibitors. *Cancer Cell, 31*(6), 848-848 e841. doi:10.1016/j.ccell.2017.05.010

Akazawa, C., Shigemoto, R., Bessho, Y., Nakanishi, S., & Mizuno, N. (1994). Differential expression of five N-methyl-D-aspartate receptor subunit mRNAs in the cerebellum of developing and adult rats. *J Comp Neurol, 347*(1), 150-160. doi:10.1002/cne.903470112

Arbuckle, M. R., McClain, M. T., Rubertone, M. V., Scofield, R. H., Dennis, G. J., James, J. A., & Harley, J. B. (2003). Development of autoantibodies before the clinical onset of systemic lupus erythematosus. *N Engl J Med, 349*(16), 1526-1533. doi:10.1056/NEJMoa021933

Bartels, F., Stronisch, T., Farmer, K., Rentzsch, K., Kiecker, F., & Finke, C. (2019). Neuronal autoantibodies associated with cognitive impairment in melanoma patients. *Ann Oncol, 30*(5), 823-829. doi:10.1093/annonc/mdz083

Begemann, M., Grube, S., Papiol, S., Malzahn, D., Krampe, H., Ribbe, K., . . . Ehrenreich, H. (2010). Modification of cognitive performance in schizophrenia by complexin 2 gene polymorphisms. *Arch Gen Psychiatry, 67*(9), 879-888. doi:10.1001/archgenpsychiatry.2010.107

Bell, R. D., Winkler, E. A., Singh, I., Sagare, A. P., Deane, R., Wu, Z., . . . Zlokovic, B. V. (2012). Apolipoprotein E controls cerebrovascular integrity via cyclophilin A. *Nature, 485*(7399), 512-516. doi:10.1038/nature11087

Canteras, N. S., Kroon, J. A., Do-Monte, F. H., Pavesi, E., & Carobrez, A. P. (2008). Sensing danger through the olfactory system: the role of the hypothalamic dorsal premammillary nucleus. *Neurosci Biobehav Rev, 32*(7), 1228-1235. doi:10.1016/j.neubiorev.2008.05.009

Castillo-Gomez E, K. A., Steiner J, Schneider A, Hettling B, Poggi G, Ostehr K, Uhr M, Asif AR, Matzke M, Schmidt U, Pfander V, Hammer C, Schulz TF, Binder L, Stöcker W, Weber F, Ehrenreich H. (2016). The brain as immunoprecipitator of serum autoantibodies against N-Methyl-D-aspartate receptor subunit NR1. *Ann Neurol., 79*(1). doi:10.1002/ana.24545

Castillo-Gomez, E., Oliveira, B., Tapken, D., Bertrand, S., Klein-Schmidt, C., Pan, H., . . . Hollmann, M. (2017). All naturally occurring autoantibodies against the NMDA receptor subunit NR1 have pathogenic potential irrespective of epitope and immunoglobulin class. *Mol Psychiatry, 22*(12), 1776-1784. doi:10.1038/mp.2016.125

Channappanavar, R., Twardy, B. S., Krishna, P., & Suvas, S. (2009). Advancing age leads to predominance of inhibitory receptor expressing CD4 T cells. *Mech Ageing Dev, 130*(10), 709-712. doi:10.1016/j.mad.2009.08.006

Correale, J., Gaitan, M. I., Ysrraelit, M. C., & Fiol, M. P. (2017). Progressive multiple sclerosis: from pathogenic mechanisms to treatment. *Brain, 140*(3), 527-546. doi:10.1093/brain/aww258

Crupi, R., Impellizzeri, D., & Cuzzocrea, S. (2019). Role of Metabotropic Glutamate Receptors in Neurological Disorders. *Front Mol Neurosci, 12*, 20. doi:10.3389/fnmol.2019.00020

Cullinan, W. E., Herman, J. P., Battaglia, D. F., Akil, H., & Watson, S. J. (1995). Pattern and time course of immediate early gene expression in rat brain following acute stress. *Neuroscience, 64*(2), 477-505. doi:10.1016/0306-4522(94)00355-9

Cyster, J. G., Hartley, S. B., & Goodnow, C. C. (1994). Competition for follicular niches excludes self-reactive cells from the recirculating B-cell repertoire. *Nature, 371*(6496), 389-395. doi:10.1038/371389a0

Dahm, L., Ott, C., Steiner, J., Stepniak, B., Teegen, B., Saschenbrecker, S., . . . Ehrenreich, H. (2014). Seroprevalence of autoantibodies against brain antigens in health and disease. *Ann Neurol, 76*(1), 82-94. doi:10.1002/ana.24189

Dalmau, J., Gleichman, A. J., Hughes, E. G., Rossi, J. E., Peng, X., Lai, M., . . . Lynch, D. R. (2008). Anti-NMDA-receptor encephalitis: case series and analysis of the effects of antibodies. *Lancet Neurol, 7*(12), 1091-1098. doi:10.1016/S1474-4422(08)70224-2

Dalmau, J., & Graus, F. (2018). Antibody-Mediated Encephalitis. *N Engl J Med, 378*(9), 840-851. doi:10.1056/NEJMra1708712

Dalmau, J., Lancaster, E., Martinez-Hernandez, E., Rosenfeld, M. R., & Balice-Gordon, R. (2011). Clinical experience and laboratory investigations in patients with anti-NMDAR encephalitis. *Lancet Neurol, 10*(1), 63-74. doi:10.1016/S1474-4422(10)70253-2

Dalmau, J., Tuzun, E., Wu, H. Y., Masjuan, J., Rossi, J. E., Voloschin, A., . . . Lynch, D. R. (2007). Paraneoplastic anti-N-methyl-D-aspartate receptor encephalitis associated with ovarian teratoma. *Ann Neurol, 61*(1), 25-36. doi:10.1002/ana.21050

de Moel, E. C., Rozeman, E. A., Kapiteijn, E. H., Verdegaal, E. M. E., Grummels, A., Bakker, J. A., . . . van der Woude, D. (2019). Autoantibody Development under Treatment with Immune-Checkpoint Inhibitors. *Cancer Immunol Res, 7*(1), 6-11. doi:10.1158/2326-6066.CIR-18-0245

Ehrenreich. (2017). Autoantibodies against the N-Methyl-d-Aspartate Receptor Subunit NR1: Untangling Apparent Inconsistencies for Clinical Practice. *Front Immunol, 8*, 181. doi:10.3389/fimmu.2017.00181

Ehrenreich. (2018). Autoantibodies against N-methyl-d-aspartate receptor 1 in health and disease. *Current Opinion in Neurology*. doi:10.1097/wco.0000000000000546

Ehrenreich, Pan, & Hollmann. (2019). Active immunization, autoimmunity and encephalitis: The missing links. Retrieved from https://stm.sciencemag.org/content/11/500/eaaw0044/tab-e-letters

Elkon, K., & Casali, P. (2008). Nature and functions of autoantibodies. *Nat Clin Pract Rheumatol, 4*(9), 491-498. doi:10.1038/ncprheum0895

Endesfelder, D., Zu Castell, W., Bonifacio, E., Rewers, M., Hagopian, W. A., She, J. X., . . . Group, T. S. (2019). Time-Resolved Autoantibody Profiling Facilitates Stratification of Preclinical Type 1 Diabetes in Children. *Diabetes, 68*(1), 119-130. doi:10.2337/db18-0594

Goodnow, C. C., Crosbie, J., Jorgensen, H., Brink, R. A., & Basten, A. (1989). Induction of self-tolerance in mature peripheral B lymphocytes. *Nature, 342*(6248), 385-391. doi:10.1038/342385a0

Goodnow, C. C., Sprent, J., Fazekas de St Groth, B., & Vinuesa, C. G. (2005). Cellular and genetic mechanisms of self tolerance and autoimmunity. *Nature, 435*(7042), 590-597. doi:10.1038/nature03724

Hafezi-Moghadam, A., Thomas, K. L., & Wagner, D. D. (2007). ApoE deficiency leads to a progressive age-dependent blood-brain barrier leakage. *Am J Physiol Cell Physiol, 292*(4), C1256-1262. doi:10.1152/ajpcell.00563.2005

Halterman, M. W. (2005). *Neuroscience, 3rd Edition*: Sinauer Associates, Inc.

Hammer, C., Stepniak, B., Schneider, A., Papiol, S., Tantra, M., Begemann, M., . . . Ehrenreich, H. (2014). Neuropsychiatric disease relevance of circulating anti-NMDA receptor autoantibodies depends on blood-brain barrier integrity. *Mol Psychiatry, 19*(10), 1143-1149. doi:10.1038/mp.2013.110

Henson, M. A., Roberts, A. C., Perez-Otano, I., & Philpot, B. D. (2010). Influence of the NR3A subunit on NMDA receptor functions. *Prog Neurobiol, 91*(1), 23-37. doi:10.1016/j.pneurobio.2010.01.004

Hoffman GE, S. M., Verbalis JG. (1993). c-Fos and related immediate early gene products as markers of activity in neuroendocrine systems. *Frontiers Neuroendocrinology*. doi:10.1006/frne.1993.1006

Hogquist, K. A., Baldwin, T. A., & Jameson, S. C. (2005). Central tolerance: learning self-control in the thymus. *Nat Rev Immunol, 5*(10), 772-782. doi:10.1038/nri1707

Ikegami, H., Awata, T., Kawasaki, E., Kobayashi, T., Maruyama, T., Nakanishi, K., . . . Ogihara, T. (2006). The association of CTLA4 polymorphism with type 1 diabetes is concentrated in patients complicated with autoimmune thyroid disease: a multicenter collaborative study in Japan. *J Clin Endocrinol Metab, 91*(3), 1087-1092. doi:10.1210/jc.2005-1407

Jimeno, B., Hau, M., & Verhulst, S. (2018). Corticosterone levels reflect variation in metabolic rate, independent of 'stress'. *Sci Rep, 8*(1), 13020. doi:10.1038/s41598-018-31258-z

Jones, B. E., Tovar, K. R., Goehring, A., Jalali-Yazdi, F., Okada, N. J., Gouaux, E., & Westbrook, G. L. (2019). Autoimmune receptor encephalitis in mice induced by active immunization with conformationally stabilized holoreceptors. *Sci Transl Med, 11*(500). doi:10.1126/scitranslmed.aaw0044

Joyce, J. A., & Fearon, D. T. (2015). T cell exclusion, immune privilege, and the tumor microenvironment. *Science, 348*(6230), 74-80. doi:10.1126/science.aaa6204

June, C. H., Warshauer, J. T., & Bluestone, J. A. (2017). Is autoimmunity the Achilles' heel of cancer immunotherapy? *Nat Med, 23*(5), 540-547. doi:10.1038/nm.4321

Kew, J. N., & Kemp, J. A. (2005). Ionotropic and metabotropic glutamate receptor structure and pharmacology. *Psychopharmacology (Berl), 179*(1), 4-29. doi:10.1007/s00213-005-2200-z

Kim, K. S. (2008). Mechanisms of microbial traversal of the blood-brain barrier. *Nat Rev Microbiol, 6*(8), 625-634. doi:10.1038/nrmicro1952

Kim, S., Foong, D., Cooper, M. S., Seibel, M. J., & Zhou, H. (2018). Comparison of blood sampling methods for plasma corticosterone measurements in mice associated with minimal stress-related artefacts. *Steroids, 135*, 69-72. doi:10.1016/j.steroids.2018.03.004

Knowland, D., Arac, A., Sekiguchi, K. J., Hsu, M., Lutz, S. E., Perrino, J., . . . Agalliu, D. (2014). Stepwise recruitment of transcellular and paracellular pathways underlies blood-brain barrier breakdown in stroke. *Neuron, 82*(3), 603-617. doi:10.1016/j.neuron.2014.03.003

Lee, D. M., & Weinblatt, M. E. (2001). Rheumatoid arthritis. *The Lancet, 358*(9285), 903-911. doi:10.1016/s0140-6736(01)06075-5

Lee, G., & Zhou, Y. (2019). NMDAR Hypofunction Animal Models of Schizophrenia. *Front Mol Neurosci, 12*, 185. doi:10.3389/fnmol.2019.00185

Leng, Q., Bentwich, Z., & Borkow, G. (2002). CTLA-4 upregulation during aging. *Mechanisms of Ageing and Development, 123*(10), 1419-1421. doi:10.1016/s0047-6374(02)00077-5

Li, W., Huang, E., & Gao, S. (2017). Type 1 Diabetes Mellitus and Cognitive Impairments: A Systematic Review. *J Alzheimers Dis, 57*(1), 29-36. doi:10.3233/JAD-161250

Linton, P. J., & Dorshkind, K. (2004). Age-related changes in lymphocyte development and function. *Nat Immunol, 5*(2), 133-139. doi:10.1038/ni1033

Lynch, G., Larson, J., Kelso, S., Barrionuevo, G., & Schottler, F. (1983). Intracellular injections of EGTA block induction of hippocampal long-term potentiation. *Nature, 305*(5936), 719-721. doi:10.1038/305719a0

Marshak-Rothstein, A. (2006). Toll-like receptors in systemic autoimmune disease. *Nat Rev Immunol, 6*(11), 823-835. doi:10.1038/nri1957

Martinez, R. C., Carvalho-Netto, E. F., Amaral, V. C., Nunes-de-Souza, R. L., & Canteras, N. S. (2008). Investigation of the hypothalamic defensive system in the mouse. *Behav Brain Res, 192*(2), 185-190. doi:10.1016/j.bbr.2008.03.042

Methia N, André P, Hafezi-Moghadam A, Economopoulos M, Thomas KL, & DD, W. (2001). ApoE deficiency compromises the blood brain barrier especially after injury. *Molecular Medicine*.

Miller, K. D., Schnell, M. J., & Rall, G. F. (2016). Keeping it in check: chronic viral infection and antiviral immunity in the brain. *Nat Rev Neurosci, 17*(12), 766-776. doi:10.1038/nrn.2016.140

Monyer, H., Burnashev, N., Laurie, D. J., Sakmann, B., & Seeburg, P. H. (1994). Developmental and regional expression in the rat brain and functional properties of four NMDA receptors. *Neuron, 12*(3), 529-540. doi:10.1016/0896-6273(94)90210-0

Murphy, K. (2012). *Janeway's Immunobiology - 8th edition*: Garland Publishing.

Nemazee, D. (2006). Receptor editing in lymphocyte development and central tolerance. *Nat Rev Immunol, 6*(10), 728-740. doi:10.1038/nri1939

Nemazee, D. (2017). Mechanisms of central tolerance for B cells. *Nat Rev Immunol, 17*(5), 281-294. doi:10.1038/nri.2017.19

Niciu, M. J., Kelmendi, B., & Sanacora, G. (2012). Overview of glutamatergic neurotransmission in the nervous system. *Pharmacol Biochem Behav, 100*(4), 656-664. doi:10.1016/j.pbb.2011.08.008

Nicoll, R. A. (2017). A Brief History of Long-Term Potentiation. *Neuron, 93*(2), 281-290. doi:10.1016/j.neuron.2016.12.015

Nikolich-Zugich, J. (2018). The twilight of immunity: emerging concepts in aging of the immune system. *Nat Immunol, 19*(1), 10-19. doi:10.1038/s41590-017-0006-x

Olsen, N. J., & Karp, D. R. (2014). Autoantibodies and SLE: the threshold for disease. *Nat Rev Rheumatol, 10*(3), 181-186. doi:10.1038/nrrheum.2013.184

Pan, H., Oliveira, B., Saher, G., Dere, E., Tapken, D., Mitjans, M., . . . Ehrenreich, H. (2019). Uncoupling the widespread occurrence of anti-NMDAR1 autoantibodies from neuropsychiatric disease in a novel autoimmune model. *Mol Psychiatry, 24*(10), 1489-1501. doi:10.1038/s41380-017-0011-3

Paoletti, P., Bellone, C., & Zhou, Q. (2013). NMDA receptor subunit diversity: impact on receptor properties, synaptic plasticity and disease. *Nat Rev Neurosci, 14*(6), 383-400. doi:10.1038/nrn3504

Platt, M. P., Agalliu, D., & Cutforth, T. (2017). Hello from the Other Side: How Autoantibodies Circumvent the Blood-Brain Barrier in Autoimmune Encephalitis. *Front Immunol, 8*, 442. doi:10.3389/fimmu.2017.00442

Plenge, R. M., Padyukov, L., Remmers, E. F., Purcell, S., Lee, A. T., Karlson, E. W., . . . Rioux, J. D. (2005). Replication of putative candidate-gene associations with rheumatoid arthritis in >4,000 samples from North America and Sweden: association of susceptibility with PTPN22, CTLA4, and PADI4. *Am J Hum Genet, 77*(6), 1044-1060. doi:10.1086/498651

Plotz, P. H. (2003). The autoantibody repertoire: searching for order. *Nat Rev Immunol, 3*(1), 73-78. doi:10.1038/nri976

Prüss, H., Finke, C., Holtje, M., Hofmann, J., Klingbeil, C., Probst, C., . . . Wandinger, K. P. (2012). N-methyl-D-aspartate receptor antibodies in herpes simplex encephalitis. *Ann Neurol, 72*(6), 902-911. doi:10.1002/ana.23689

Prüss, H., Leubner, J., Wenke, N. K., Czirjak, G. A., Szentiks, C. A., & Greenwood, A. D. (2015). Anti-NMDA Receptor Encephalitis in the Polar Bear (Ursus maritimus) Knut. *Sci Rep, 5*, 12805. doi:10.1038/srep12805

Rahman, A., & Isenberg, D. A. (2008). Systemic lupus erythematosus. *N Engl J Med, 358*(9), 929-939. doi:10.1056/NEJMra071297

Ribbe, K., Friedrichs, H., Begemann, M., Grube, S., Papiol, S., Kastner, A., . . . Ehrenreich, H. (2010). The cross-sectional GRAS sample: a comprehensive phenotypical data collection of schizophrenic patients. *BMC Psychiatry, 10*, 91. doi:10.1186/1471-244X-10-91

Rioux, J. D., & Abbas, A. K. (2005). Paths to understanding the genetic basis of autoimmune disease. *Nature, 435*(7042), 584-589. doi:10.1038/nature03723

Rose, N. R. (2001). Infection, mimics, and autoimmune disease. *J Clin Invest, 107*(8), 943-944. doi:10.1172/JCI12673

Russell, D. M., Dembic, Z., Morahan, G., Miller, J. F., Burki, K., & Nemazee, D. (1991). Peripheral deletion of self-reactive B cells. *Nature, 354*(6351), 308-311. doi:10.1038/354308a0

Sakata, I., & Sakai, T. (2010). Ghrelin Cells in the Gastrointestinal Tract. *International Journal of Peptides, 2010*, 1-7. doi:10.1155/2010/945056

Sapolsky, R. M., Romero, L. M., & Munck, A. U. (2000). How do glucocorticoids influence stress responses? Integrating permissive, suppressive, stimulatory, and preparative actions. *Endocr Rev, 21*(1), 55-89. doi:10.1210/edrv.21.1.0389

Shlomchik, M. J. (2008). Sites and stages of autoreactive B cell activation and regulation. *Immunity, 28*(1), 18-28. doi:10.1016/j.immuni.2007.12.004

Sirén, A. L., Radyushkin, K., Boretius, S., Kammer, D., Riechers, C. C., Natt, O., . . . Ehrenreich, H. (2006). Global brain atrophy after unilateral parietal lesion and its prevention by erythropoietin. *Brain, 129*(Pt 2), 480-489. doi:10.1093/brain/awh703

Sominsky, L., Hodgson, D. M., McLaughlin, E. A., Smith, R., Wall, H. M., & Spencer, S. J. (2017). Linking Stress and Infertility: A Novel Role for Ghrelin. *Endocr Rev, 38*(5), 432-467. doi:10.1210/er.2016-1133

Steinman, M. D. L. (1996). Multiple Sclerosis: A Coordinated Immunological Attack against Myelin in the Central Nervous System. *Cell, 85*(3), 299-302. doi:10.1016/s0092-8674(00)81107-1

Stepniak, B., Kastner, A., Poggi, G., Mitjans, M., Begemann, M., Hartmann, A., . . . Ehrenreich, H. (2015). Accumulated common variants in the broader fragile X gene family modulate autistic phenotypes. *EMBO Mol Med, 7*(12), 1565-1579. doi:10.15252/emmm.201505696

Vishnoi, S., Raisuddin, S., & Parvez, S. (2015). Modulatory effects of an NMDAR partial agonist in MK-801-induced memory impairment. *Neuroscience, 311*, 22-33. doi:10.1016/j.neuroscience.2015.10.008

Wiedmer, P., Nogueiras, R., Broglio, F., D'Alessio, D., & Tschop, M. H. (2007). Ghrelin, obesity and diabetes. *Nat Clin Pract Endocrinol Metab, 3*(10), 705-712. doi:10.1038/ncpendmet0625

Wildbaum, G., Nahir, M. A., & Karin, N. (2003). Beneficial Autoimmunity to Proinflammatory Mediators Restrains the Consequences of Self-Destructive Immunity. *Immunity, 19*(5), 679-688. doi:10.1016/s1074-7613(03)00291-7

Yousufzai, M., Harmatz, E. S., Shah, M., Malik, M. O., & Goosens, K. A. (2018). Ghrelin is a persistent biomarker for chronic stress exposure in adolescent rats and humans. *Transl Psychiatry, 8*(1), 74. doi:10.1038/s41398-018-0135-5

Zerche, M., Weissenborn, K., Ott, C., Dere, E., Asif, A. R., Worthmann, H., . . . Ehrenreich, H. (2015). Preexisting Serum Autoantibodies Against the NMDAR Subunit NR1 Modulate Evolution of Lesion Size in Acute Ischemic Stroke. *Stroke, 46*(5), 1180-1186. doi:10.1161/STROKEAHA.114.008323

Zhao, Z., Nelson, A. R., Betsholtz, C., & Zlokovic, B. V. (2015). Establishment and Dysfunction of the Blood-Brain Barrier. *Cell, 163*(5), 1064-1078. doi:10.1016/j.cell.2015.10.067

Zuo, D. Y., Zhang, Y. H., Cao, Y., Wu, C. F., Tanaka, M., & Wu, Y. L. (2006). Effect of acute and chronic MK-801 administration on extracellular glutamate and

ascorbic acid release in the prefrontal cortex of freely moving mice on line with open-field behavior. *Life Sci, 78*(19), 2172-2178. doi:10.1016/j.lfs.2005.09.022

Chapter 6
Appendix

List of abbreviations

AIRE	Autoimmune regulator
ANAs	Antinuclear antibodies
APCs	Antigen presenting cells
ApoE	Apolipoprotein E
APS-1	Autoimmune polyendocrine syndrome type 1
BBB	Blood-brain barrier
CNS	Central nervous system
CSF	Cerebrospinal fluid
CTLA4	Cytotoxic T-lymphocyte-associated antigen 4
CypA	Cyclophilin A
ELISA	Enzyme-Linked Immunosorbent Assay
EPSP	Excitatory postsynaptic potential
FACS	Fluorescence-activated cell sorting
IA-2A	Insulinoma-associated antigen 2 autoantibodies
IAA	Insulin autoantibodies
IFN-γ	Interferon gamma
Ig	Immunoglobulin
iGluR	Ionotropic glutamate receptor
IL17	Interleukin 17
LTP	Long-term potentiation
mGluR	Metabotropic glutamate receptor
MK801	Dizocilpine
NMDA receptor	N-methyl-D-aspartate receptor
NMDAR1-AB	Antibodies against NMDA receptor subunit GluN1 (NR1)
SLE	Systemic lupus erythematosus
SNP	Single-nucleotide polymorphism
Th cells	T helper cells
TLR	Toll-like Receptor
TNF-α	Tumor necrosis factor alpha
Tregs	Regulatory T cells
WT	Wildtype

Co-autor publications

I

Castillo-Gómez E, Oliveira B, Tapken D, Bertrand S, Klein-Schmidt C, **Pan H**, Zafeiriou P, Steiner J, Jurek B, Trippe R, Prüss H, Zimmermann WH, Bertrand D, Ehrenreich H, Hollmann M. All naturally occurring autoantibodies against the NMDA receptor subunit NR1 have pathogenic potential irrespective of epitope and immunoglobulin class. Mol Psychiatry. 2017 Dec;22(12):1776-1784. doi: 10.1038/mp.2016.125. Epub 2016 Aug 9.

Contribution: Helped with experimental data acquision on NMDAR1-AB determination in human patients (Figure 3c).

II

Janova H, Arinrad S, Balmuth E, Mitjans M, Hertel J, Habes M, Bittner RA, **Pan H**, Goebbels S, Begemann M, Gerwig UC, Langner S, Werner HB, Kittel-Schneider S, Homuth G, Davatzikos C, Völzke H, West BL, Reif A, Grabe HJ, Boretius S, Ehrenreich H, Nave KA. Microglia ablation alleviates myelin-associated catatonic signs in mice. J Clin Invest. 2018 Feb 1;128(2):734-745. doi: 10.1172/JCI97032. Epub 2017 Dec 18.

Contribution: Helped with experimental data acquision (mouse perfusions, immnohistochemisty, and etc.)

Molecular Psychiatry (2017) 22, 1776–1784
www.nature.com/mp

OPEN

ORIGINAL ARTICLE

All naturally occurring autoantibodies against the NMDA receptor subunit NR1 have pathogenic potential irrespective of epitope and immunoglobulin class

E Castillo-Gómez[1,9], B Oliveira[1,9], D Tapken[2,9], S Bertrand[3], C Klein-Schmidt[2], H Pan[1], P Zafeiriou[4], J Steiner[5], B Jurek[6,7], R Trippe[2], H Prüss[6,7], W-H Zimmermann[4], D Bertrand[3], H Ehrenreich[1,8,10] and M Hollmann[2,10]

Autoantibodies of the IgG class against *N*-methyl-D-aspartate-receptor subunit NR1 (NMDAR1) were first described in anti-NMDAR encephalitis and seen as disease indicators. Recent work on together over 5000 individuals challenged this exclusive view by showing age-dependently up to >20% NMDAR1-autoantibody seroprevalence with comparable immunoglobulin class and titer distribution across health and disease. The key question therefore is to understand the properties of these autoantibodies, also in healthy carriers, in order to assess secondary complications and possible contributions to neuropsychiatric disease. Here, we believe we provide for human NMDAR1-autoantibodies the first comprehensive analysis of their target epitopes and functionality. We selected sera of representative carriers, healthy or diagnosed with very diverse conditions, that is, schizophrenia, age-related disorders like hypertension and diabetes, or anti-NMDAR encephalitis. We show that *all* positive sera investigated, regardless of source (ill or healthy donor) and immunoglobulin class, provoked NMDAR1 internalization in human-induced pluripotent stem cell-derived neurons and reduction of glutamate-evoked currents in NR1-1b/NR2A-expressing *Xenopus* oocytes. They displayed frequently polyclonal/polyspecific epitope recognition in the extracellular or intracellular NMDAR1 domains and some additionally in NR2A. We conclude that *all* circulating NMDAR1-autoantibodies have pathogenic potential regarding the whole spectrum of neuronal NMDAR-mediated effects upon access to the brain in situations of increased blood–brain–barrier permeability.

Molecular Psychiatry (2017) **22,** 1776–1784; doi:10.1038/mp.2016.125; published online 9 August 2016

INTRODUCTION

Circulating autoantibodies (AB) directed against brain epitopes have long been documented, mainly in connection with classical autoimmune diseases or paraneoplastic syndromes.[1–4] AB targeting the *N*-methyl-D-aspartate-receptor subunit NR1 (NMDAR1; *new nomenclature GluN1 disregarded here for consistency with the respective literature, except in the molecular biological section*) have attracted considerable attention lately. NMDAR1-AB of the IgG class were first described in connection with a condition named anti-NMDAR encephalitis[5] and induced a flood of publications, among them many case reports. In several of them, immunosuppressive treatment of seropositive subjects is recommended.[6–8] Anti-NMDAR encephalitis symptoms typically include psychosis, cognitive decline, seizures, dyskinesia, decreased consciousness and autonomic instability.[5] These symptoms are reminiscent of those found upon NMDAR antagonism by ketamine, MK801, or related drugs, and have been explained by reduced surface expression of NMDAR1 upon exposure to NMDAR1-AB.[5]

Rendering the situation more complex, a high age-dependent seroprevalence of NMDAR1-AB has been recognized recently.[9–14] According to these findings in meanwhile >5000 subjects, any 40-year-old person has an ~10%, any 80-year-old person an ~20% chance of displaying NMDAR1-AB seropositivity.[11] Disease groups, ranging from schizophrenia and major depression, over multiple sclerosis, Parkinson's and Alzheimer's disease, to hypertension, diabetes and stroke, as well as healthy individuals, share not only similar NMDAR1-AB seroprevalence but also immunoglobulin (Ig) class distribution (IgM, IgA and IgG) and titer range.[9–11,13] These unexpected results raised the question of functionality and relevance of the highly seroprevalent NMDAR1-AB. In translational mouse studies, similar effects of the different classes (IgG, IgM and IgA) of NMDAR1-AB on behavioral readouts were observed.[9] Likewise, in a human study, an equivalent impact of circulating NMDAR1-AB of all three isotypes on evolution of lesion size after ischemic stroke was noticed.[11] Detectable neuropsychiatric consequences of circulating NMDAR1-AB of all three classes were restricted to individuals with compromised blood–brain–barrier, for example, *ApoE*/*APOE* carrier status, both clinically and experimentally.[9,11,15] In studies using rodent hippocampal neurons, we found NMDAR1 internalization upon NMDAR1-AB (IgM, IgA, IgG) binding as explanation of its reduced surface expression.[9,15] A comparable finding had previously been described only for IgG.[5,16]

[1]Clinical Neuroscience, Max Planck Institute of Experimental Medicine, Göttingen, Germany; [2]Department of Biochemistry I – Receptor Biochemistry, Ruhr University, Bochum, Germany; [3]HiQscreen, Geneva, Switzerland; [4]Institute of Pharmacology and Toxicology, University Medical Center, Göttingen, Germany; [5]Department of Psychiatry, University of Magdeburg, Magdeburg, Germany; [6]Department of Neurology, Charité, University Medicine, Berlin, Germany; [7]German Center for Neurodegenerative Disorders (DZNE), Berlin, Germany and [8]DFG Research Center for Nanoscale Microscopy and Molecular Physiology of the Brain (CNMPB), Göttingen, Germany. Correspondence: Professor H Ehrenreich, Clinical Neuroscience, Max Planck Institute of Experimental Medicine, Hermann-Rein-Strasse 3, Göttingen 37075, Germany.
E-mail: ehrenreich@em.mpg.de
[9]These authors share first authorship.
[10]These authors share last authorship.
Received 18 March 2016; revised 3 May 2016; accepted 1 June 2016; published online 9 August 2016

Table 1. Overview of donors of NMDAR1-AB-positive and -negative serum samples

	Seropositive individuals (N = 14)	*Seronegative individuals (N = 15)*	*P-value*
Gender, No. (%), women[a]	10 (71.4)	7 (46.7)	0.176
Age at examination, mean ± s.d., years[b]	62.87 ± 24.44	65.24 ± 10.99	0.234
Diagnosis, No. (%)[a]			
Healthy	2 (14.3)	4 (26.7)	
NMDAR1-AB encephalitis	2 (14.3)	0 (0.0)	
Psychiatric conditions[c]	1 (7.1)	1 (6.3)	
Diabetes	0 (0.0)	2 (13.3)	0.418
Hypertension	7 (50.0)	6 (40.0)	
Diabetes and hypertension	2 (14.3)	1 (6.7)	
Other medical conditions[d]	0 (0.0)	1 (6.7)	
NMDAR1-AB seroprevalence, titers, No.[e]			
IgA (1:10; 1:32; 1:100; 1:320; 1:1000; 1:3200)	2; 0; 0; 0; 4; 0		
IgG (1:10; 1:32; 1:100; 1:320; 1:1000; 1:3200)	0; 0; 1; 1; 1; 1		n/a
IgM (1:10; 1:32; 1:100; 1:320; 1:1000; 1:3200)	0; 0; 1; 1; 5; 1		

Abbreviations: AB, autoantibodies; IG, immunoglobulin; n/a, not applicable; NMDAR1, *N*-methyl-D-aspartate-receptor subunit NR1. [a]Chi-square test. [b]Mann–Whitney *U*-test. [c]'Psychiatric conditions' include two schizophrenia patients. [d]'Other medical conditions' include hypercholesterolemia, asthma bronchiale and glaucoma. [e]Note that of the total sample *N* = 4 individuals were seropositive for both IgA and IgM.

Considering the high seroprevalence of NMDAR1-AB across health and disease, the key question is to understand the properties of these AB, also in healthy carriers, in order to assess secondary complications and possible contributions to neuropsychiatric disease, for example, cognitive decline, psychotic symptoms or epileptic seizures. Are they like a 'ticking time bomb' once the blood barrier opens?

Here, we believe we provide for human NMDAR1-AB the first comprehensive analysis of their target epitopes and of functionality. We investigated whether NMDAR1-AB of different Ig classes, derived from sera of subjects with very diverse conditions, would (i) reveal functionality in an internalization assay using human induced pluripotent stem cell (IPSC)-derived cortical neurons; (ii) lead to electrophysiological consequences in NR1-1b/NR2A-expressing *Xenopus* oocytes; and (iii) be directed against the same or against different epitopes of NMDAR1.

We report as most important take-home message that, independent of any medical condition or Ig class, NMDAR1-AB are functional, leading to decreased NMDAR surface expression and reduced glutamate-evoked currents. The AB recognize epitopes in the extracellular and/or intracellular NMDAR1 domains and, surprisingly, some positive sera also in the NR2A subunit of NMDAR. Thus, most intriguingly, they all have potentially (patho) physiological relevance regarding brain functions.

MATERIALS AND METHODS

All experiments were performed by researchers unaware of group assignment ('fully blinded').

Human samples

Serum specimens ($N = 29$) from our phenotyping/biomarker trials[8,10,11,17] were selected to (i) cover a spectrum of diseases and health, (ii) include all NMDAR1-AB Ig classes and (iii) build on enough material for extensive testing (Table 1). In addition, samples ($N = 7$; few µl available) for targeted epitope mapping were obtained from anti-NMDAR encephalitis patients (Charité, HP). Subject data/human materials (including IPSC) were collected according to ethical guidelines/Helsinki Declaration including subjects' informed consent.

NMDAR1-AB titer determination

Recombinant immunofluorescence tests (Euroimmun, Lübeck, Germany), clinical standard procedures, were used to detect NMDAR1-AB, based on HEK293T cells transfected with NMDAR1,[5,6] and secondary AB against human IgG, IgM or IgA. Results were independently assessed by three investigators.

Dialysis of serum samples

Functional studies were conducted with sera following ammonium sulfate precipitation of immunoglobulins[18] and dialysis (Slide-A-Lyzer Mini-Dialysis-Units, 10 000 MWCO Plus Float, Thermo Fisher Scientific, Rockford, IL, USA).

Reprogramming of human fibroblasts and differentiation into neurons

Human fibroblasts from gingiva biopsies were reprogrammed using STEMCCA system (Merck Millipore, Darmstadt, Germany) for introduction of OCT4, SOX2, KLF4 and c-MYC.[19] Clones were tested for pluripotency markers following standard procedures.[19] After reprogramming, IPSC was adapted to feeder-free culture system (Matrigel matrix, Corning, Wiesbaden, Germany) and TeSR™-E8™ medium (Stem Cell Technologies, Cologne, Germany). Neural induction was based on dual SMAD inhibition (Figure 1a).[20]

Endocytosis assay

Human IPSC-derived cortical neurons grown on coverslips, 70 days post neural induction, were pre-cooled on ice (10 min), and washed 3× with cold HBSS (Hank's balanced salt solution; Life Technologies, Darmstadt, Germany). Culture media were kept at 37 or 4 °C. Neurons were incubated (30 min) in cold HBSS with 1:100 diluted sera (14 seropositive; 6 seronegative), control NMDAR1-AB (M68, mouse IgG, SYSY, Göttingen, Germany) or HBSS alone (negative control). After three HBSS washes to remove unbound AB, neurons were returned to their media and incubated for 20 min at 37 °C (2 coverslips/sample, to allow endocytosis) or 4 °C (1 coverslip/sample, endocytosis control). After ice-cold HBSS wash, coverslips were kept on ice (5 min). Remaining surface NMDAR1 was exposed to a mouse NMDAR1-AB (N-terminal; Abcam, Cambridge, UK, 1:100), 10 min on ice, followed (after ice-cold HBSS wash) by secondary donkey anti-mouse IgG (Life Technologies, Alexa-Fluor546, 1:100) for 10 min on ice in dark, and finally three ice-cold HBSS washes to remove unbound AB. Neurons were fixed with ice-cold 4% paraformaldehyde (30 min) and washed 3× (5 min) with 0.1 M phosphate-buffered saline (PBS). Then, cells were blocked and permeabilized for 1 h at RT (5% normal goat, 5% normal horse, 5% fetal calf serum, 0.5% Triton X in PBS), double-stained at 4 °C overnight with chicken anti-NeuN-AB (SYSY, 1:500) and secondary donkey anti-chicken AB (Life Technologies, Alexa Fluor 488, 1:250) for 1 h at RT (all dark) (Figure 1b). Nuclei were visualized using DAPI (Sigma-Aldrich, Munich, Germany, 0.01 µg ml^{-1}). After PBS wash,

coverslips were mounted on Super-Frost slides with Mowiol-mounting-media (Sigma-Aldrich). Confocal laser-scanning microscopy was used to quantify cell-surface NMDAR1 density (×63 glycerol objective; TCS-SP5 Leica-Microsystems, Mannheim, Germany). From each coverslip, Z-series of optical sections (0.5 µm apart) covering the three-dimensional extension of neurons were acquired (sequential scanning mode, identical acquisition parameters). For analysis, 50 NeuN+ cells/coverslip were randomly selected using FIJI-ImageJ software.[21] Soma profile including NMDAR1 surface expression was drawn and fluorescence intensity/cell surface area (Alexa-Fluor546) automatically measured. Background was subtracted, mean intensity for each coverslip determined and fluorescence intensity ratio (37 °C/4 °C) calculated.

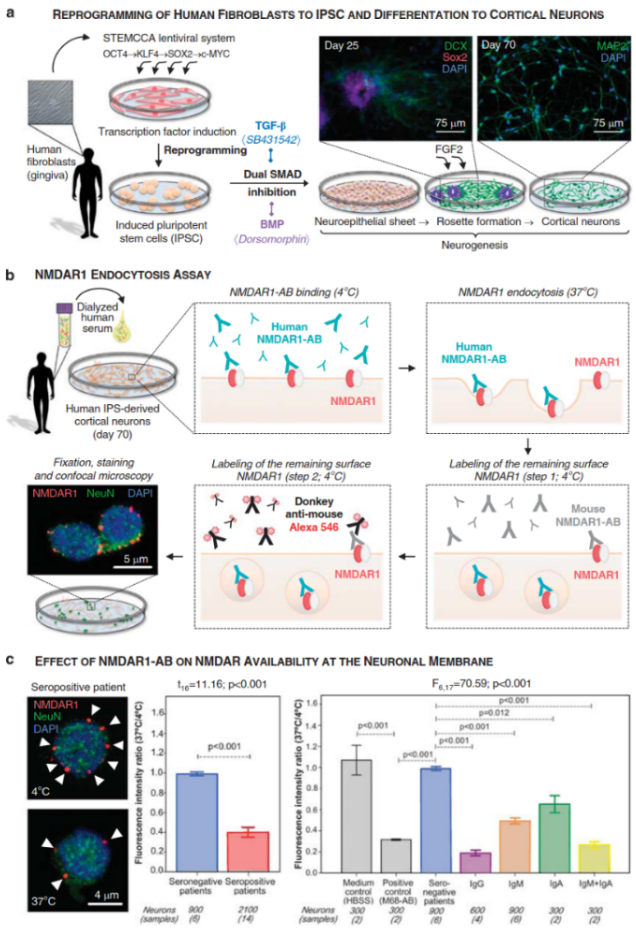

Oocyte preparation and injection

Xenopus laevis oocytes were prepared, injected and tested using standard procedures. Briefly, ovaries were harvested from *Xenopus* females in deep anesthesia by hypothermia (4 °C) and MS-222 (Sigma-Aldrich, 150 mg l^{-1}). Animals were decapitated and pithed obeying animal rights (Geneva, Switzerland). A small piece of ovary was isolated for immediate preparation while the remaining part was placed at 4 °C in sterile Barth-solution containing [mM]: NaCl 88, KCl 1, $NaHCO_3$ 2.4, HEPES 10, $MgSO_4.7H_2O$ 0.82, $Ca(NO_3)_2.4H_2O$ 0.33, $CaCl_2.6H_2O$ 0.41, at pH 7.4, supplemented with 100 U ml^{-1} penicillin/100 µg ml^{-1} streptomycin (Life Technologies). Automatic injection of mRNAs encoding for human NMDAR (NR1-1/NR2A) was performed in batches of 95 oocytes using Roboinject[22] (Multi Channel Systems, Reutlingen, Germany) (Figure 2a). Optimal expression of NMDAR was obtained with injection of 15 nl containing 0.2 µg $µl^{-1}$ of RNAs, ratio NR1-1b:NR2A = 1:1; mRNA was prepared using mMessage mMachine SP6 transcription kit for NR1-1b and T7 for NR2A (Thermo Fisher Scientific).

Electrophysiological recordings and experimental protocol

NMDAR activity was validated 60 h after mRNA injection by 2-electrode voltage clamp (Figure 2a). All electrophysiological recordings were performed using an automated HiClamp system (Multi Channel Systems) at 18 °C and with cells superfused with OR2 medium (mM: NaCl 88, KCl 2.5, HEPES 5, $CaCl_2.2H_2O$ 1.8, pH 7.85). To chelate zinc contaminant, 10 µM EDTA was added to all solutions. Unless otherwise indicated, cells were maintained at holding potential of −80 mV and compounds/AB incubations conducted in 96-well-microtiter plates (Thermo Fisher Scientific). Only cells displaying low leak current and responses >0.5 µA to a test pulse containing 0.3 µM glutamate/10 µM glycine (Sigma-Aldrich) were retained for successive testing (Figures 2a and b). Cells were then challenged with pre-incubation of 120 s in control medium (OR2 medium) followed by brief exposures to 0.3 µM glutamate/10 µM glycine (10 s) every 2 min for 10 min (Figure 2b, steps 1 and 2). The last 4 min was considered as control response-amplitude to glutamate (Figure 2c, right-side graphs, −4–0 min). Upon stabilization, cells were exposed for 16 min to dialyzed serum samples (titer dilution for seropositive and 1:1000 for seronegative samples) or to positive control (M68-AB, 1:1000). NMDAR activity was tested by brief exposure to 0.3 µM glutamate/10 µM glycine (10 s) every 2 min for 16 min in presence of the dialyzed serum (Figure 2b, steps 3 and 4). To evaluate the cellular response, area-under-the-curve (AUC) for each glutamate-evoked current was computed and normalized to AUC of control responses (−4–0 min). Data were analyzed using custom-made software (Matlab-Mathworks, Ismaning, Germany). For each sample, a mean of ⩾3 oocytes was calculated (Figure 2c, left-side graphs).

Epitope mapping using NMDAR1 constructs

NMDAR1 constructs were generated based on the longest splice variant, GluN1-1b (GenBank accession #U08263; Figures 3a and b). All cDNAs (including GluN2A: #AF001423; GluN2B: #U11419) were cloned into pcDNA4/TO/*myc*-HisA (Invitrogen, Carlsbad, CA, USA) such that the encoded receptor had a myc-His-tag connected to its *C*-terminus by a short peptide linker (SRGPF). Chimeras and mutants for epitope analysis were constructed by overlap-extension-PCR using chimeric or mutagenic primers.[23,24] To transiently express glutamate receptor subunits, HEK293T cells were cultured in high-glucose DMEM (Life Technologies). On a 35-mm dish, 50 000 cells were plated, grown for 3 days, transfected with receptor cDNA (3 µg) using Metafectene-Pro (Biontex, Munich, Germany) and, 24 h after transfection, seeded onto poly-D-lysine-coated coverslips (Sigma-Aldrich). At 2 days after transfection, cells were fixed with 5% paraformaldehyde (20 min), washed 5× with 0.1 M PBS, permeabilized with 0.1% Triton X-100 (5 min), again washed 5× with PBS, blocked for 1 h with 5% normal goat serum (Sigma-Aldrich). After 5× PBS washes, cells were incubated with serum (1:10–1:200) or monoclonal mouse anti-myc antibody (transfection efficiency control; self-made, purified from mouse-clone-9E10) for 1 h, washed 10× with PBS, incubated for 1 h with Alexa Fluor 488-labeled goat anti-human secondary AB (IgG: Southern Biotech, Birmingham, AL, USA; IgA: Jackson ImmunoResearch, West Grove, PA, USA; IgM: Thermo Fisher Scientific) or anti-mouse IgG (controls; Thermo Fisher Scientific), washed 5× with PBS, incubated with TO-PRO-3 iodide nuclear-stain (Molecular Probes, Eugene, OR, USA) (15 min), and washed 5× with PBS. Cells were mounted in Fluoromount-G (Southern Biotech) and analyzed by confocal microscopy (63× oil objective, TCS SP2 AOBS, Leica-Microsystems). All results are consensus judgements from at least four independent investigators of two different laboratories.

Statistics

All statistical analyses were performed using SPSS for Windows version 17.0 (IBM-Deutschland, Munich, Germany). Group differences in categorical and continuous variables were assessed using Chi-square and Mann–Whitney *U*-test. One-way or repeated-measures ANOVA, followed by multiple pair-wise comparisons with Bonferroni's post hoc correction, was employed to determine the significance of fluorescence intensity or AUC; *P*-values <0.05 were considered as significant; data in figures are mean ± s.e.m.

RESULTS

In human IPSC-derived cortical neurons, exposure to all NMDAR1-AB-positive sera tested, independent of Ig class and titer, led to receptor endocytosis, reflected by decreased cell-surface fluorescence intensity ratio 37 °C/4 °C (perikaryal labeling). Negative sera had no effect (*unpaired Student's t-test:* $t_{16} = 11.16$; $P < 0.001$; seronegative samples: $n = 6$, neurons $n = 900$; seropositive samples: $n = 14$, neurons $n = 2100$) (Figure 1c). Analyzing the impact of Ig classes separately, significant results remained for all (one-way ANOVA: $F_{6,17} = 70.59$; $P < 0.001$ with Bonferroni post hoc

Figure 1. NMDAR1 endocytosis in human induced pluripotent stem cell (IPSC)-derived cortical neurons after autoantibodies (AB) exposure. (**a**) Reprogramming strategy: Human fibroblasts obtained from gingiva biopsies were transduced using a lentiviral system to simultaneously integrate the transcription factors OCT4, KLF4, SOX2 and c-MYC. Transcription factor expression leads to cell reprogramming and colony formation of IPSC, which are differentiated into cortical neurons using a dual SMAD inhibition strategy (selective blocking of TGF-β and BMP pathways). Cells acquire neuronal identity forming a neural stem cell monolayer. Dissociation of the neuroepithelial sheath leads to rearrangement of neural stem cells (SOX2+) in a rosette-like structure, further expanded by application of the mitogen FGF2. Immature neurons (DCX+) emerge from these structures during the neurogenesis period to give rise mainly to MAP2+ cortical excitatory neurons. (**b**) At day 70 of maturation, neurons are exposed to human sera. NMDAR1-AB binding to NMDAR1 (at 4 °C) leads to rapid endocytosis of the receptor–antibody complex at 37 °C. The remaining cell-surface NMDAR1 is detected by combining mouse anti-NMDAR1-AB (step 1) and secondary donkey anti-mouse Alexa 546-AB (step 2). Neurons are defined as NeuN+ cells. (**c**) Representative confocal images of neurons exposed to an IgG seropositive sample are shown on the left. Both pictures are Z-projections of three consecutive focal planes 0.5 µm apart, taken at ×100 magnification under confocal laser-scanning microscope. The upper picture depicts a neuron (NeuN+, labeled in green), kept at 4 °C (no endocytosis allowed—control condition) and the lower picture a neuron at 37 °C (endocytosis). For each serum sample, cell membrane NMDAR1 (labeled in red; arrow heads) is quantified. Degree of internalization is expressed as ratio of fluorescence intensity measured at both temperatures. Seropositive samples show reduced fluorescence intensity ratio (37 °C/4 °C) compared with seronegative samples (graph on the left; *unpaired* Student's *t*-test: $t_{16} = 11.16$; $P < 0.001$), consistent with a decrease in surface NMDAR1 after exposure to NMDAR1-AB. Right graph: Fluorescence intensity ratio is lower for all seropositive samples (separate analyses shown for samples with only IgG, IgM, IgA or IgM+IgA, in purple, orange, green and yellow columns, respectively) and the positive control (IgG M68-AB). *One-way ANOVA*: $F_{6,17} = 70.59$; $P < 0.001$; multiple comparisons with *Bonferroni's post hoc correction*, *P*-value < 0.05; results given as mean ± s.e.m. BMP, bone morphogenic pathway; *c-MYC*, avian myelocytomatosis virus oncogene cellular homolog; DAPI, 4′,6-diamidino-2-phenylindole; DCX, doublecortin; FGF2, fibroblast growth factor 2; KLF4, Krüppel-like factor 4; MAP2, microtubule-associated protein 2; NMDAR1, *N*-methyl-D-aspartate-receptor subunit NR1; NeuN, neuronal nuclear antigen; OCT4, octamer-binding transcription factor 4; SOX2, sex determining region Y-homeobox 2; STEMCCA, stem cell cassette; TGF-β, transforming growth factor-β.

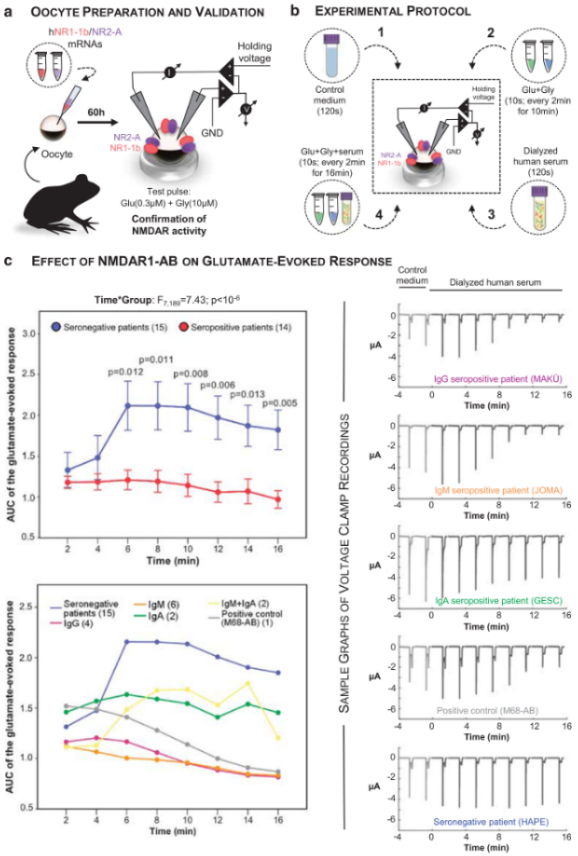

Figure 2. Decreased NMDAR activity after autoantibodies (AB) exposure. (**a**) NMDAR activity in *Xenopus laevis* oocytes expressing human NR1-1b/NR2A is confirmed using 2-electrode voltage clamp recordings. (**b**) Control glutamate response of each oocyte is tested after 120 s incubation in control medium followed by 10 s exposure to glutamate and glycine every 2 min for 10 min (steps 1 and 2). Cells are afterwards exposed for 120 s to dialyzed serum samples or to positive control (M68-AB), followed by 10 s exposures to glutamate and glycine every 2 min for 16 min (steps 3 and 4). (**c**) An increase in AUC of the glutamate-evoked response starting at 6 min and lasting for at least 16 min is observed in seronegative but not in seropositive samples (left upper graph; *one-way repeated-measures ANOVA*: time × group interaction: $F_{7,189} = 7.43$, $P < 10^{-6}$; *Bonferroni's* post hoc correction for multiple comparison: only *P*-values < 0.05 are shown). The left lower graph shows curves for Ig classes separately which all are below the seronegative curve (*one-way repeated-measures ANOVA*: time × group interaction: $F_{35,168} = 1.98$, $P = 0.002$). On the right side, five representative recordings of cells exposed to IgG, IgM and IgA seropositive samples, positive control sample (M68-AB) and a seronegative sample are shown. The first two curves of every graph show the last 4 min of the control response to glutamate (see Materials and methods for detailed information). AUC, area-under-the-curve; Glu, glutamate; Gly, glycine; GND, signal ground; I, intensity; Ig, immunoglobulin; NMDAR, *N*-methyl-D-aspartate receptor; V, voltage.

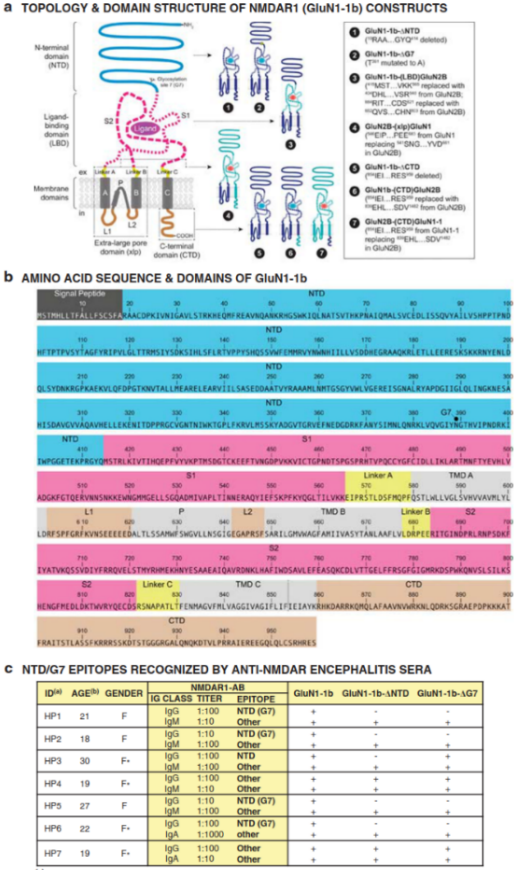

c NTD/G7 EPITOPES RECOGNIZED BY ANTI-NMDAR ENCEPHALITIS SERA

ID[a]	AGE[b]	GENDER	NMDAR1-AB IG CLASS	TITER	EPITOPE	GluN1-1b	GluN1-1b-ΔNTD	GluN1-1b-ΔG7
HP1	21	F	IgG	1:100	NTD (G7)	+	-	-
			IgM	1:10	Other	+	+	+
HP2	18	F	IgG	1:10	NTD (G7)	+	-	-
			IgM	1:100	Other	+	+	+
HP3	30	F•	IgG	1:100	NTD	+	-	+
			IgM	1:100	Other	+	+	+
HP4	19	F•	IgG	1:100	Other	+	+	+
			IgM	1:10	Other	+	+	+
HP5	27	F	IgG	1:10	NTD (G7)	+	-	-
			IgM	1:100	Other	+	+	+
HP6	22	F•	IgG	1:100	NTD (G7)	+	-	-
			IgA	1:1000	other	+	+	+
HP7	19	F•	IgG	1:100	Other	+	+	+
			IgA	1:10	Other	+	+	+

[a] Scrambled identification code; [b] Age at examination (years); *cases with ovarian teratoma.

Figure 3. GluN1-1b constructs for epitope mapping of NMDAR1-AB. (**a**) Topology and domain structure of the GluN1-1b constructs used. The scheme on the left side shows the membrane topology of the GluN1-1b subunit, with domains colored as in (**b**). Chimeras and mutagenic constructs targeting the different domains of GluN1 are explained on the right (all residue numbers include the signal peptide; GluN1 and GluN2B constructs were generated based on GenBank accession numbers U08263 and NM_012574, respectively). (**b**) Amino-acid sequence and domains of GluN1-1b. The position marked in the sequence as G7 (glycosylation site 7) is the residue to which the oligosaccharide is attached (N^{389}). The recognition site for this type of glycosylation is N-X-S/T; therefore, mutation of T^{391} to A in the construct number 2 (GluN1-1b-ΔG7) prevents glycosylation 2 residues upstream of it (N^{389}). (**c**) NTD/G7 epitopes recognized by serum NMDAR1-AB of different Ig classes from seven female patients with diagnosed anti-NMDAR encephalitis. AB, antibodies; CTD, C-terminal domain; L1, intracellular loop 1; L2, intracellular loop 2; LBD, ligand-binding domain; NMDAR1, *N*-methyl-D-aspartate-receptor subunit NR1; NTD, N-terminal domain; P, ion channel pore; TMD, transmembrane domains; xlp, extra-large pore domain.

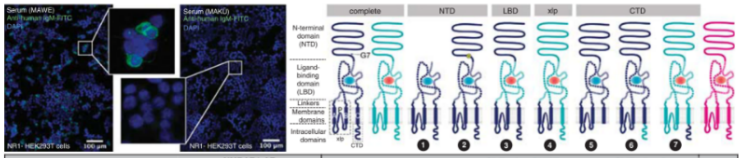

ID[a]	AGE[b]	GENDER	DIAGNOSIS	NMDAR1-AB IG CLASS	TITER	EPITOPE	GluN1-1b	GluN2B	GluN1-1b-ΔNTD	GluN1-1b-ΔG7	GluN1-1b-(LBD)GluN2B	GluN2B-(xlp)GluN1-1b	GluN1-1b-ΔCTD	GluN1-1b-(CTD)GluN2B	GluN2B-(CTD)GluN1-1b	GluN2A
MAKÜ	81	M	Hypertension	IgG	1:3200	LBD	+	-	+	+	-	-	+	+	-	IgM
SANI	29	F	Schizophrenia	IgG	1:320	NTD	+	-	-	+	+	-	+	+	-	IgM/A
BLKA	18	F	Encephalitis	IgG	1:1000	NTD (G7)	+	-	-	-	+	-	+	+	-	IgM
GEJE	27	F	Encephalitis	IgG	1:100	NTD (G7)	+	-	-	-	+	-	+	+	-	-
MAWE	85	F	Hypertension	IgM	1:3200	NTD+CTD/LBD+CTD	+	-	+	+	+	-	+	+	+	-
JOMA	72	M	Hypertension	IgM	1:1000	NTD+CTD/LBD+CTD	+	-	+	+	+	-	+	+	+	-
ANFR	83	F	Healthy	IgM	1:1000	NTD+LBD	+	-	+	+	+	-	+	+	-	-
CHSC	77	F	Hypertension	IgM	1:1000	NTD+CTD/LBD+CTD	+	-	+	+	+	-	+	+	+	-
ALMA	37	F	Healthy	IgM	1:320	NTD+CTD/LBD+CTD	+	-	+	+	+	-	+	+	+	IgM
RELÜ	67	F	Hypertension	IgM	1:1000	CTD	+	-	+	+	+	-	-	-	+	IgM
GESC	84	M	Hypertension	IgA	1:1000	CTD	+	-	+	+	+	-	-	+	-	IgG/M/A
ANKL	75	F	Hypertension	IgA	1:1000	CTD	+	-	+	+	+	-	-	-	+	IgG/M
GEPA	81	F	Diabetes and hypertension	IgA IgM	1:1000 1:1000	CTD NTD+LBD	+ +	- -	+ +	+ +	+ +	- -	- +	- +	+ -	IgA
MAZA	78	M	Diabetes and hypertension	IgA IgM	1:1000 1:100	NTD+LBD CTD+xlp	+ +	- -	+ +	+ +	+ +	- +	+ +	+ +	- +	IgM
M68-AB	-	-	Positive control	IgG (mouse)	1:1000	LBD	+	-	+	+	-	-	+	+	-	-

[a]Scrambled identification code; [b]Age at examination (years).

Figure 4. NMDAR1-AB recognize several GluN1-1b epitopes. The figure-table, summarizing the results of NMDAR1-AB epitope mapping, includes only seropositive individuals. *Upper left:* Representative tilescan confocal images of HEK293T cells transfected with NMDAR1 as used for serum testing are shown. NMDAR1-AB seropositivity (left) and seronegativity (right) is illustrated for IgM as example (anti-human IgM FITC-labeled as secondary antibody). Insets are ×4 magnifications of the squared areas in their respective images. All images are Z-projections of 10 consecutive focal planes located 0.5 µm apart and were taken under a confocal laser-scanning microscope using ×100 oil objective (Leica TSC-SP5). *Upper right:* Schematic drawings of the different constructs used to transfect HEK293T cells (compare Figure 3). The first two constructs represent the complete version of the GluN1-1b and GluN2B subunits of NMDAR. The next seven constructs present deletions, mutations or replacements of defined regions, allowing identification of the epitopes recognized by NMDAR1-AB from healthy and ill individuals. Positivity (+) or negativity (−) for every construct in every sample is listed underneath. On the very right side, anti-GluN2A seropositivity/Ig class is listed (anti-GluN2A titers range from 1:10 up to 1:200). AB, autoantibodies; CTD, C-terminal domain; Ig, immunoglobulin; NMDAR1, *N*-methyl-D-aspartate-receptor subunit NR1; NTD, N-terminal domain.

test *P*-values: IgG: $P < 0.001$; IgM: $P < 0.001$; IgA: $P = 0.012$ and IgM +IgA: $P < 0.001$).

To investigate the impact of NMDAR1-AB on activity, glutamate-evoked responses were evaluated in *Xenopus laevis* oocytes co-expressing human NR1-1/NR2A subunits. Only 6 min after exposure of oocytes to human sera, the AUC of the glutamate-evoked response was significantly lower in seropositive compared with seronegative samples. This effect was sustained for at least 16 min (Figure 2c; one-way repeated-measures ANOVA: time × group interaction: $F_{7,189} = 7.431$, $P < 10^{-6}$; Bonferroni *post hoc* correction for multiple comparison: only *P*-values < 0.05 are shown). Evaluating Ig classes separately, the significant global effect remained (one-way repeated-measures ANOVA: time × group interaction: $F_{35,168} = 1.98$; $P = 0.002$; Figure 2c, left lower graph).

Epitope mapping using seven different NMDAR1 constructs (Figures 3a and b) revealed recognition by the NMDAR1-AB-positive sera of different epitopes, located in the extracellular ligand-binding domain and N-terminal domain (NTD) as well as the intracellular C-terminal domain (CTD) and extra-large pore domain (xlp). NMDAR1-AB seropositivity was polyclonal/polyspecific in 7/14 sera and likely mono- or oligoclonal/oligospecific (mainly IgG) in 7/14. Whereas no GluN2B-AB (0/14) was found, GluN2A-AB (9/14) was frequently detected in the NMDAR1-AB-positive sera (Figure 4). Separate exploratory analyses of GluN2A-AB carrier versus non-carrier sera regarding internalization assay and electrophysiology results did not reveal differences. Overall, no particular disease-related pattern appeared.

The G7 site of the NTD, an epitope believed to be crucial for NMDAR1-AB found in encephalitis,[25] was recognized in 2/10 sera binding to NTD (Figure 4, negativity for construct 2). Since these sera were from two anti-NMDAR encephalitis cases reported previously (without epitope mapping),[8] we tested another seven sera from anti-NMDAR encephalitis patients specifically for this epitope. All seven sera had NMDAR1-AB of two Ig classes. Epitope location in NTD was seen in 5/7 sera for IgG, with 4/7 recognizing G7. IgM and IgA recognized other epitopes, as did IgG in 2/7 sera (not further determined due to lack of material) (Figure 3c).

DISCUSSION

The present paper systematically analyzed for the first time NMDAR1-AB of three Ig classes (IgM, IgG and IgA), derived from randomly selected individuals of different age, gender and medical condition, regarding *in vitro* functionality and epitope location. All NMDAR1-AB-positive sera tested led to NMDAR1 internalization in IPSC-derived human cortical neurons and to reduced glutamate-evoked response in NR1-1b/NR2A-expressing oocytes. Several different epitopes were identified, located in the extracellular part of NMDAR1 (NTD, ligand-binding domain) or intracellular, CTD and in the xlp, which were recognized by NMDAR1-AB of the IgG, IgA and IgM class. Importantly, there was no consistent functional or epitope pattern detectable regarding Ig class or health/disease state.

In light of the comparable functionality of all NMDAR1-AB tested here, the high seroprevalence (up to > 20%) of NMDAR1-AB is even more puzzling and may indicate a previously unknown dimension of 'physiological autoimmunity' that increases with age.[9–13] But what are the inducers of such abundant formation of NMDAR1-AB that potentially influence brain function? So far, associations were found with certain forms of cancer, mainly ovarian teratoma,[5] influenza A and B,[9–13] as well as with a genome-wide significant marker on chromosome 1, rs524991,[9] close to *NFIA*, a transcription factor mediating neuroprotective effects of NMDAR.[26] There are certainly more hitherto unknown predisposing factors for carrying these AB. Broader significance of NMDAR1-AB is underscored by their presence in mammalians other than humans.[27] This is less surprising in view of the substantial seroprevalence also of other brain-directed AB in species like rabbits, pigs and cows.[28]

While irrespective of the epitope, all 14 NMDAR1-AB-positive sera investigated here (IgM, IgG, IgA) revealed similar AB functionality (internalization, electrophysiology), the AB-inducing factors may have determined the epitopes via mechanisms like molecular mimicry.[29,30] Published work on NMDAR1-AB epitopes is scarce[25,31,32] and focused on IgG recognizing NTD and the NTD-G7 domain (N^{368}/G^{369}), probably because this region and Ig class was first deemed pathognomonic for anti-NMDAR-encephalitis.[5,25] Indeed, the sera investigated here of two young females with diagnosed anti-NMDAR-encephalitis, originally reported within a series of schizophrenia cases,[8] also recognized this epitope, however, without sticking out functionally (that is, regarding internalization or electrophysiology). Therefore, we analyzed sera of seven additional young female patients, diagnosed with anti-NMDAR encephalitis (4/7 with ovarian teratoma), in an NTD-G7-targeted epitope screen. Interestingly, all 7 subjects carried NMDAR1-AB of 2 Ig classes, but only IgG recognized NTD or NTD-G7 in 5/7 sera. Similarly, in a recent study on young females with neuropsychiatric manifestation of systemic lupus erythematosus, two epitopes in the NTD (outside G7) were recognized by NMDAR1-AB (only IgG tested). Regrettably, NTD was the only mapped region, functionality was not evaluated, and instead of a cell-based assay, the accepted gold standard, an ELISA was used.[32] Together, these data suggest that factors predisposing young women to neuropsychiatric manifestations of NMDAR-associated autoimmunity are connected with NTD or NTD-G7 epitopes. The accentuated role of IgG in this context is still a matter of speculation but may be related to inflammation-induced class-switch in the brain.[33] Regarding NMDAR1-AB of the IgA class, a single study, mapping epitopes of two female patients, found in one of them evidence of NTD/G7 as a target epitope (likely among other epitopes).[31] Interestingly, the significance of AB for brain manifestation of lupus erythematosus seems still debatable. In a recent study, lack of B cells and autoantibodies in a murine model of systemic lupus did not prevent the development of key features of neuropsychiatric lupus.[34]

To conclude, all naturally occurring serum NMDAR1-AB obviously have pathogenic potential. For still unexplored reasons, they are highly frequent and their prevalence increases with age. NMDAR-AB seropositivity alone definitely does not justify immunosuppressive treatment. Syndromal relevance of serum NMDAR1-AB depends on accessibility to the brain, that is, blood–brain–barrier permeability.[9,11,13,15] This permeability might differ regionally, thereby explaining individually variable symptomatic consequences.[2] Moreover, inflammation in the brain likely has a crucial role in determining syndrome acuteness and severity as contributed by circulating NMDAR1-AB and respective plasma cells, including boost in AB titers (upon epitope recognition) and class-switch to IgG.[33] Especially in individuals where an overt encephalitis diagnosis is unlikely, determination of blood–brain–barrier disruption, for example, by a novel magnetic resonance imaging method,[35] may prove helpful for estimating necessity and benefit of immunosuppressive therapeutic interventions.

CONFLICT OF INTEREST

The authors declare no conflict of interest.

ACKNOWLEDGMENTS

This work was supported by the Max Planck Society, the Deutsche Forschungsgemeinschaft (Center for Nanoscale Microscopy & Molecular Physiology of the Brain), EXTRABRAIN EU-FP7 and the Niedersachsen-Research Network on Neuroinfectiology (N-RENNT). The assistance by the UMG-Stem Cell Unit (S. Chen and L. Cyganek) is greatly appreciated.

AUTHOR CONTRIBUTIONS

HE, MH and DB contributed to concept and design of the study. ECG, BO, DT, SB, RT, PZ, JS, CK, HoP, BJ, HP, WHZ, DB, MH and HE contributed to data acquisition/analysis/interpretation. HE, ECG, BO, DT and MH contributed to drafting manuscript and figures. All authors read and approved the final version of the manuscript.

REFERENCES

1 Sutton I, Winer JB. The immunopathogenesis of paraneoplastic neurological syndromes. *Clin Sci* 2002; **102**: 475–486.
2 Diamond B, Huerta P, Mina-Osorio P, Kowal C, Volpe B. Losing your nerves? Maybe it's the antibodies. *Nat Rev Immunol* 2009; **9**: 449–456.
3 Coutinho E, Harrison P, Vincent A. Do neuronal autoantibodies cause psychosis? A neuroimmunological perspective. *Biol Psychiatry* 2014; **75**: 269–275.
4 Crisp SJ, Kullmann DM, Vincent A. Autoimmune synaptopathies. *Nat Rev Neurosci* 2016; **17**: 103–117.
5 Dalmau J, Gleichman AJ, Hughes EG, Rossi JE, Peng X, Lai M *et al.* Anti-NMDA-receptor encephalitis: case series and analysis of the effects of antibodies. *Lancet Neurol* 2008; **7**: 1091–1098.
6 Wandinger KP, Saschenbrecker S, Stoecker W, Dalmau J. Anti-NMDA-receptor encephalitis: a severe, multistage, treatable disorder presenting with psychosis. *J Neuroimmunol* 2011; **231**: 86–91.
7 Zandi MS, Irani SR, Lang B, Waters P, Jones PB, McKenna P *et al.* Disease-relevant autoantibodies in first episode schizophrenia. *J Neurol* 2011; **258**: 686–688.
8 Steiner J, Walter M, Glanz W, Sarnyai Z, Bernstein HG, Vielhaber S *et al.* Increased prevalence of diverse N-methyl-D-aspartate glutamate receptor antibodies in patients with an initial diagnosis of schizophrenia: specific relevance of IgG NR1a antibodies for distinction from N-methyl-D-aspartate glutamate receptor encephalitis. *JAMA Psychiatry* 2013; **70**: 271–278.
9 Hammer C, Stepniak B, Schneider A, Papiol S, Tantra M, Begemann M *et al.* Neuropsychiatric disease relevance of circulating anti-NMDA receptor autoantibodies depends on blood–brain–barrier integrity. *Mol Psychiatry* 2013; **19**: 1143–1149.
10 Dahm L, Ott C, Steiner J, Stepniak B, Teegen B, Saschenbrecker S *et al.* Seroprevalence of autoantibodies against brain antigens in health and disease. *Ann Neurol* 2014; **76**: 82–94.
11 Zerche M, Weissenborn K, Ott C, Dere E, Asif AR, Worthmann H *et al.* Preexisting serum autoantibodies against the NMDAR subunit NR1 modulate evolution of lesion size in acute ischemic stroke. *Stroke* 2015; **46**: 1180–1186.
12 Steiner J, Teegen B, Schiltz K, Bernstein H-G, Stoecker W, Bogerts B. Prevalence of N-methyl-D-aspartate receptor autoantibodies in the peripheral blood: healthy control samples revisited. *JAMA Psychiatry* 2014; **71**: 839.
13 Castillo-Gomez E, Kastner A, Steiner J, Schneider A, Hettling B, Poggi G *et al.* The brain as 'immunoprecipitator' of serum autoantibodies against NMDAR1. *Ann Neurol* 2015; **79**: 144–151.
14 Busse S, Busse M, Brix B, Probst C, Genz A, Bogerts B *et al.* Seroprevalence of N-methyl-D-aspartate glutamate receptor (NMDA-R) autoantibodies in aging

subjects without neuropsychiatric disorders and in dementia patients. *Eur Arch Psychiatry Clin Neurosci* 2014; **264**: 545–550.
15 Hammer C, Zerche M, Schneider A, Begemann M, Nave KA, Ehrenreich H. Apolipoprotein E4 carrier status plus circulating anti-NMDAR1 autoantibodies: association with schizoaffective disorder. *Mol Psychiatry* 2014; **19**: 1054–1056.
16 Moscato EH, Peng X, Jain A, Parsons TD, Dalmau J, Balice-Gordon RJ. Acute mechanisms underlying antibody effects in anti–N-methyl-D-aspartate receptor encephalitis. *Ann Neurol* 2014; **76**: 108–119.
17 Begemann M, Grube S, Papiol S, Malzahn D, Krampe H, Ribbe K *et al*. Modification of cognitive performance in schizophrenia by complexin 2 gene polymorphisms. *Arch Gen Psychiatry* 2010; **67**: 879–888.
18 Toyka K, Brachman D, Pestronk A, Kao I. Myasthenia gravis: passive transfer from man to mouse. *Science* 1975; **190**: 397–399.
19 Streckfuss-Bomeke K, Wolf F, Azizian A, Stauske M, Tiburcy M, Wagner S *et al*. Comparative study of human-induced pluripotent stem cells derived from bone marrow cells, hair keratinocytes, and skin fibroblasts. *Eur Heart J* 2013; **34**: 2618–2629.
20 Shi Y, Kirwan P, Livesey FJ. Directed differentiation of human pluripotent stem cells to cerebral cortex neurons and neural networks. *Nat Protoc* 2012; **7**: 1836–1846.
21 Schindelin J, Arganda-Carreras I, Frise E, Kaynig V, Longair M, Pietzsch T *et al*. Fiji: an open-source platform for biological-image analysis. *Nat Methods* 2012; **9**: 676–682.
22 Hogg RC, Bandelier F, Benoit A, Dosch R, Bertrand D. An automated system for intracellular and intranuclear injection. *J Neurosci Methods* 2008; **169**: 65–75.
23 Ho S, Hunt H, Horton R, Pullen J, Pease L. Site-directed mutagenesis by overlap extension using the polymerase chain reaction. *Gene* 1989; **77**: 51–59.
24 Wurch T, Lestienne F, Pauwels P. A modified overlap extension PCR method to create chimeric genes in the absence of restriction enzymes. *Biotechnol Tech* 1998; **12**: 653–657.
25 Gleichman AJ, Spruce LA, Dalmau J, Seeholzer SH, Lynch DR. Anti-NMDA receptor encephalitis antibody binding is dependent on amino acid identity of a small region within the GluN1 amino terminal domain. *J Neurosci* 2012; **32**: 11082–11094.
26 Zheng S, Eacker SM, Hong SJ, Gronostajski RM, Dawson TM, Dawson VL. NMDA-induced neuronal survival is mediated through nuclear factor I-A in mice. *J Clin Invest* 2010; **120**: 2446–2456.
27 Pruss H, Leubner J, Wenke NK, Czirjak GA, Szentiks CA, Greenwood AD. Anti-NMDA receptor encephalitis in the polar bear (Ursus maritimus) Knut. *Sci Rep* 2015; **5**: 12805.
28 DeMarshall C, Sarkar A, Nagele EP, Goldwaser E, Godsey G, Acharya NK *et al*. Utility of autoantibodies as biomarkers for diagnosis and staging of neurodegenerative diseases. *Int Rev Neurobiol* 2015; **122**: 1–51.
29 Diamond B, Honig G, Mader S, Brimberg L, Volpe BT. Brain-reactive antibodies and disease. *Annu Rev of Immunol* 2013; **31**: 345–385.
30 Bhat R, Steinman L. Innate and adaptive autoimmunity directed to the central nervous system. *Neuron* 2009; **1**: 123–132.
31 Doss S, Wandinger KP, Hyman BT, Panzer JA, Synofzik M, Dickerson B *et al*. High prevalence of NMDA receptor IgA/IgM antibodies in different dementia types. *Ann Clin Transl Neurol* 2014; **1**: 822–832.
32 Ogawa E, Nagai T, Sakuma Y, Arinuma Y, Hirohata S. Association of antibodies to the NR1 subunit of N-methyl-D-aspartate receptors with neuropsychiatric systemic lupus erythematosus. *Mod Rheumatol* 2015; **1**: 1–7.
33 Zhang J, Jacobi AM, Wang T, Berlin R, Volpe BT, Diamond B. Polyreactive autoantibodies in systemic lupus erythematosus have pathogenic potential. *J Autoimmun* 2009; **33**: 270–274.
34 Wen J, Doerner J, Chalmers S, Stock A, Wang H, Gullinello M *et al*. B cell and/or autoantibody deficiency do not prevent neuropsychiatric disease in murine systemic lupus erythematosus. *J Neuroinflammation* 2016; **13**: 73.
35 Montagne A, Barnes SR, Sweeney MD, Halliday MR, Sagare AP, Zhao Z *et al*. Blood-brain barrier breakdown in the aging human hippocampus. *Neuron* 2015; **85**: 296–302.

Microglia ablation alleviates myelin-associated catatonic signs in mice

Hana Janova,[1,2] Sahab Arinrad,[1] Evan Balmuth,[1] Marina Mitjans,[1,2] Johannes Hertel,[3] Mohamad Habes,[3,4] Robert A. Bittner,[5] Hong Pan,[1] Sandra Goebbels,[2,6] Martin Begemann,[1,2,7] Ulrike C. Gerwig,[6] Sönke Langner,[8] Hauke B. Werner,[6] Sarah Kittel-Schneider,[5] Georg Homuth,[9] Christos Davatzikos,[4] Henry Völzke,[10] Brian L. West,[11] Andreas Reif,[5] Hans Jörgen Grabe,[3] Susann Boretius,[2,12] Hannelore Ehrenreich,[1,2] and Klaus-Armin Nave[2,6]

[1]Clinical Neuroscience, Max Planck Institute of Experimental Medicine, Göttingen, Germany. [2]DFG Research Center for Nanoscale Microscopy and Molecular Physiology of the Brain (CNMPB), Göttingen, Germany. [3]Department of Psychiatry and Psychotherapy, University Medicine, and German Center for Neurodegenerative Diseases (DZNE), Greifswald, Germany. [4]Center for Biomedical Image Computing and Analytics, University of Pennsylvania, Philadelphia, Pennsylvania, USA. [5]Department of Psychiatry, Psychosomatic Medicine and Psychotherapy, University Hospital, Goethe University, Frankfurt, Germany. [6]Department of Neurogenetics, Max Planck Institute of Experimental Medicine, Göttingen, Germany. [7]Department of Psychiatry and Psychotherapy, University Medical Center Göttingen (UMG), Georg-August-University, Göttingen, Germany. [8]Institute of Diagnostic Radiology and Neuroradiology, [9]Interfaculty Institute for Genetics and Functional Genomics, and [10]Institute for Community Medicine, University Medicine Greifswald, Greifswald, Germany. [11]Translational Pharmacology, Plexxikon Inc., Berkeley, California, USA. [12]Functional Imaging Laboratory, Leibniz Institute for Primate Research, Göttingen, Germany.

The underlying cellular mechanisms of catatonia, an executive "psychomotor" syndrome that is observed across neuropsychiatric diseases, have remained obscure. In humans and mice, reduced expression of the structural myelin protein CNP is associated with catatonic signs in an age-dependent manner, pointing to the involvement of myelin-producing oligodendrocytes. Here, we showed that the underlying cause of catatonic signs is the low-grade inflammation of white matter tracts, which marks a final common pathway in *Cnp*-deficient and other mutant mice with minor myelin abnormalities. The inhibitor of CSF1 receptor kinase signaling PLX5622 depleted microglia and alleviated the catatonic symptoms of *Cnp* mutants. Thus, microglia and low-grade inflammation of myelinated tracts emerged as the trigger of a previously unexplained mental condition. We observed a very high (25%) prevalence of individuals with catatonic signs in a deeply phenotyped schizophrenia sample (n = 1095). Additionally, we found the loss-of-function allele of a myelin-specific gene (*CNP* rs2070106-AA) associated with catatonia in 2 independent schizophrenia cohorts and also associated with white matter hyperintensities in a general population sample. Since the catatonic syndrome is likely a surrogate marker for other executive function defects, we suggest that microglia-directed therapies may be considered in psychiatric disorders associated with myelin abnormalities.

Introduction

White matter tracts in the CNS largely comprise long axons, associated glial cells, and the ensheathment of axons with myelin. While the role of myelin for axonal conduction and normal motor-sensory function is well known (1), the contribution of white matter integrity to cortical networks and higher cognition is just emerging. Moreover, myelin defects are increasingly linked to mental disease, but mechanistic insight is still lacking and the relationship between cause and consequence difficult to establish in humans (2, 3).

Catatonia is among the most mysterious and as yet poorly understood neuropsychiatric phenotypes. Appearing as a "psychomotor syndrome," it reflects temporary disruption of executive control in the absence of any "classical" motor dysfunction. Catatonia is typically characterized by a fluctuating course with episodic exacerbations and has historically been associated with schizophrenia, for which it is classified as a positive symptom. Catatonia is, however, also observed in mood- and substance-induced psychotic disorders, malignant neuroleptic syndrome, most encephalitides, and even general medical conditions (4, 5). Reports on brain areas involved in catatonia are scarce. Available data point to frontal lobe regions, such as the pronounced catatonia in a case of butterfly glioma of the frontal corpus callosum (6) or frontal activation in akinetic catatonic patients detected by functional MRI (7).

▶ Related Commentary: p. 564

Authorship note: H. Janova, S. Arinrad, and E. Balmuth contributed equally to this work. H. Ehrenreich and K.A. Nave contributed equally to this work.
Conflict of Interest: Brian West is an employee of Plexxikon Inc.
Submitted: August 22, 2017; **Accepted:** November 7, 2017.
Reference information: *J Clin Invest*. 2018;128(2):734–745.
https://doi.org/10.1172/JCI97032.

The full-blown clinical picture of catatonia is dominated by immobility, catalepsy, or stupor, sometimes suddenly switching from "frozen posturing" to excessive motor activity ("movement storm"). Milder forms are more common, even though frequently missed in the diagnostic process, and addressed as catatonic signs (8). In schizophrenia, prevalence is estimated at 0.2%–3.0% (5). Treatment with benzodiazepines or electroconvulsive therapy is nonspecific and not always effective (4, 5).

Similarly to what occurs in humans, catatonia appears in mice as a state of transient immobility in which mice persist in an externally imposed abnormal posture. However, in animals, catatonia has previously been reported only upon induction by body pinch or drug exposure (9, 10). More recently, we detected catatonia in aging mice heterozygous for either *Cnp* or *Mbp* (also known as shiverer), both encoding structural proteins of the myelin sheath, 2′-3′-cyclic nucleotide 3′-phosphodiesterase (Cnp) and myelin basic protein (Mbp). Interestingly, in aging *Mbp* heterozygotes, Cnp expression in the forebrain is also reduced by 50% (11, 12). Correspondingly, individuals homozygous for the A allele of the SNP rs2070106 in human *CNP* show reduced mRNA expression (13) and association with catatonia (11). Therefore, mutant oligodendrocytes yield a predisposition to catatonia, which is not explained by any paucity of myelin; however, the responsible mechanisms have remained obscure.

The neuropathology of *Cnp* and *Mbp* heterozygous mice starts late in life and is surprisingly mild, but in either mutant accompanied by an increased number of microglial cells (11, 12, 14). We therefore hypothesized that neuroinflammation of subcortical white matter, possibly spreading into the prefrontal cortex, could be the cause of catatonic signs. Such a mechanism would be in line with the emerging role of microglia for behavioral phenotypes (15–18).

Here, we demonstrate an unexpectedly high, age-associated prevalence of catatonic signs in more than 25% of deeply phenotyped schizophrenic subjects. In 2 independent schizophrenia cohorts, we found severe catatonic signs associated with the *CNP* partial loss-of-function genotype rs2070106-AA. Moreover, we show by MRI that *CNP* rs2070106-AA carriers in the general population are more likely than G carriers (GG or AG) to display frontotemporal white matter hyperintensities (WMH) on T2-weighted images as proposed subclinical signs of vascular changes, neuroinflammation, and demyelination (19–21).

To provide proof-of-principle for microgliosis as the key disease mechanism, we studied *Cnp*$^{-/-}$ (null) mutant mice. Surprisingly, they developed neuroinflammation with catatonic signs by the early age of 8 weeks. Indeed, we show causality by depletion of microglia with the colony-stimulating factor 1 receptor (CSF1R)

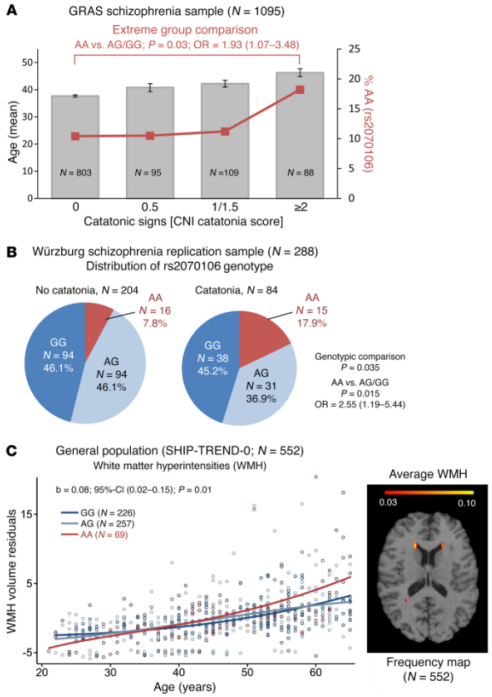

Figure 1. Age-dependent association of the loss-of-function genotype *CNP* rs2070106-AA with catatonia in 2 independent schizophrenia cohorts and with WMH in a general population sample. (**A**) Bars show mean age of schizophrenic subjects (GRAS), sorted by severity of catatonic signs. Red line denotes percentage of risk for genotype carriers (rs2070106-AA) within each severity group. Note that severity of catatonic signs increases with age. Two-sided values for Kruskal-Wallis (P = 7.6×10^{-5}) and Jonckheere-Terpstra (P = 1.3×10^{-5}). Mean ± SEM. Also note that *CNP* rs2070106-AA carriers are most frequent (18.2%) among individuals with highest expression of catatonic signs compared with noncatatonic subjects (10.4%). Two-sided P value for Mann-Whitney U test for extreme-group comparison given in the figure. (**B**) Distribution of *CNP* rs2070106 genotype in the Würzburg replication sample of schizophrenia patients based on dichotomous catatonia classification. The AA genotype is significantly more prevalent in patients with (17.9%) than without catatonia (7.8%). Two-sided P values from χ^2 test given. (**C**) Left panel: interaction effect between age and genotype in SHIP-TREND-0 sample on overall WMH volume (minimum 10 mm^3 per single WMH cluster). Shown are WMH volume residuals after correcting for intracranial volume, age (nonlinear), and gender. Genotype and age-genotype interaction term contributed 1.1% of variance to overall WMH volumes. Right panel: frequency map averaging all subjects of the general population (SHIP-TREND-0; n = 552), analyzed here. Data highlight WMH appearance predominantly in frontal regions.

Table 1. ROI analyses of WMH in analogous regressions showing that frontotemporal regions including deep structures contribute most to the overall increase of WMH in AA carriers versus subjects with AG/GG genotype

Brain region	Age-genotype interaction[A] (95% CI)	*P* value	Variance contribution (Δ adj. R^2)
Frontal	0.06 (0.01;0.10)	**0.013**	0.68%
Deep structures[B]	0.02 (0.00;0.03)	**0.048**	0.36%
Parietal	0.05 (−0.00;0.09)	0.054	0.71%
Temporal	0.05 (0.00;0.10)	**0.032**	1.17%
Occipital	0.02 (−0.02;0.05)	0.333	0.13%

[A]Regression weight. [B]Deep structures include anterior limb of internal capsule, fornix, and posterior limb of internal capsule including cerebral peduncle. Δ adj. R^2 calculated by comparing the whole model with the model devoid of the genotype and the age-genotype interaction term. Analyses are adjusted for intracranial volume, age (nonlinear), and gender. All *P* values are 2 sided. Bold numbers indicate $P < 0.05$.

inhibitor PLX5622 (22, 23), which blocks a critical microglial survival pathway. The so-caused ablation of microglia prevents catatonia onset in young mutants and ameliorates existing catatonia in adult *Cnp*$^{-/-}$ mice. These findings shed light on the nature of catatonia and suggest that this striking neuropsychiatric syndrome — and possibly related executive function deficits — may be preventable as well as treatable.

Results

Catatonic signs are highly prevalent in schizophrenia and associated with the CNP partial loss-of-function genotype rs2070106-AA in independent samples. Within the Göttingen Research Association for Schizophrenia (GRAS) population of deeply phenotyped schizophrenic subjects, 26.7% exhibited signs of catatonia. The severity of catatonic signs clearly increases with age (Figure 1A). The percentage of *CNP* loss-of-function SNP rs2070106-AA carriers among individuals with the highest expression (≥2) of catatonic signs is greater compared with that in noncatatonic subjects (18.2% versus 10.4%; $P = 0.03$; OR = 1.93; Figure 1A). This association between catatonia and rs2070106-AA is replicable in an independent sample of schizophrenic individuals (17.9% versus 7.8%; $P = 0.015$; OR = 2.55; Figure 1B), categorically classified for catatonia according to Leonhard (24).

CNP rs2070106-AA carriers in the general population display increased age-dependent WMH in frontal and temporal brain areas. We wondered whether the *CNP* loss-of-function rs2070106-AA would reveal any measurable effects on suggested MRI indicators of neuroinflammation and white matter alterations. Employing a subsample of the baseline cohort of Study of Health in Pomerania (SHIP-TREND-0), namely general population subjects with MRI scans available, we quantified WMH. AA carriers showed age-dependent higher WMH volume residuals as compared with GG and AG carriers, most prominently in frontotemporal brain regions and deep brain structures, with all analyses adjusted for total intracranial volume, age (nonlinear), and gender (Figure 1C and Table 1). Control covariance analyses, stepwise including further (potentially interfering) covariates alone or together, namely education, waist circumference, serum triglycerides, and smoking, did not appreciably alter the results. Importantly, peripheral inflammation markers, namely C-reactive protein serum levels (natural logarithm) and white blood cell count were tested as covariates, but also did not substantially change the significance level ($P = 0.013$ and $P = 0.014$, respectively).

Catatonic signs in Cnp-null mutant mice start at around 8 weeks of age and are prevented by the CSF1R inhibitor PLX5622. To show proof-of-principle for the causal relationship of inflammation and catatonic signs in a construct-valid experimental model, we turned to *Cnp*$^{-/-}$ mutant mice. As early as the age of 8 weeks, *Cnp*$^{-/-}$ mice developed catatonic signs (Figure 2, A and B). For illustration, Supplemental Video 1 (supplemental material available online with this article; https://doi.org/10.1172/JCI97032DS1) demonstrates a striking example of catatonia in a young *Cnp*$^{-/-}$ mutant, tested on the bar, followed by normal-appearing motor performance. This exemplifies the transiently obvious executive dysfunction in the absence of an underlying motor disturbance. Supplemental Video 2 shows excerpts of undisturbed home-cage observation in an enriched environment of another *Cnp*$^{-/-}$ mutant with normal motor performance and phases of spontaneous catatonia-like posturing (note the "manneristic" stretching of hind limbs when on the bar).

Catatonic signs were prevented by a 5-week oral application of the CSF1R inhibitor PLX5622 via food pellets, starting at 3 weeks of age, immediately after weaning (Figure 2, C and D), consistent with a nearly complete depletion of microglia as reported earlier (22, 23) and reproduced by pilot experiments in preparation of the present study (8-week-old WT mice, treated for 5 or 8 weeks with PLX5622 versus untreated: 1–2 versus ~260 ionized calcium binding adaptor molecule-1 positive [Iba1$^+$] cells/mm^2 corpus callosum area, as delineated in Figure 2E). Intriguingly, immunohistochemical (IHC) analysis of the corpus callosum of these mice after 4 weeks of drug recovery showed still lower numbers of Iba1$^+$ cells and amyloid precursor protein–positive (APP$^+$) swellings compared with nontreated *Cnp*$^{-/-}$ mice, suggesting that PLX5622 treatment has a persistent antiinflammatory benefit, since it is known that microglia recover from inhibition within only 1 week (22, 23). The slightly enhanced glial fibrillary acidic protein–positive (GFAP$^+$) area (Figure 2, E and F) as well as the mildly extended CD68$^+$ (macrosialin) area (0.8% ± 0.04% in WT versus 6.8% ± 0.7% in *Cnp*$^{-/-}$; $P < 0.014$) in young mutants is not reduced after PLX5622 treatment.

Magnetic resonance spectroscopy signs of white and gray matter inflammation in Cnp$^{-/-}$ *mice and their prevention by CSF1R inhibition.* An independent cohort of WT and *Cnp*$^{-/-}$ mice underwent a follow-up magnetic resonance spectroscopy (MRS) study at 8 and 13 weeks of age (design shown in Figure 2C), focusing on regions of interest (ROI) in corpus callosum (white matter) and cortex (gray matter) (Figure 3A). The first MRS in 8-week-old mice was performed after 5 weeks of control versus PLX5622 diet (starting at age 3 weeks, as in the prevention study above), and the second MRS was performed in the same mice at the age of 13 weeks, i.e., after 5 weeks of PLX5622 food cessation/microglia repopulation. Brain myoinositol is seen as a global marker of glial activation including microglia that strongly correlates with neuroinflam-

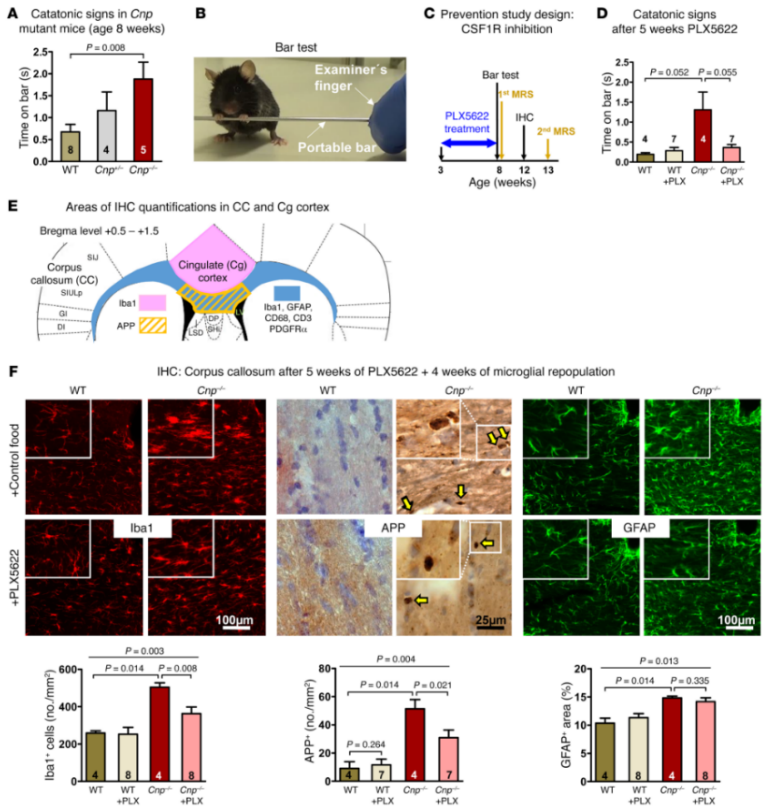

Figure 2. Early catatonia and white matter inflammation in *Cnp* mutant mice and their prevention by CSF1R inhibition. (**A**) Catatonic signs measured by the bar test in WT, *Cnp*$^{+/-}$, and *Cnp*$^{-/-}$ mice at the age of 8 weeks (Kruskal-Wallis, $P = 0.034$). (**B**) Image illustrating a mouse with typical catatonic posture during the bar test. (**C**) Schematic overview of the prevention study design, including PLX5622 (versus regular food) feeding phase (blue arrow) and time points of testing/analyses. Black arrows: bar test (results in Figure 2D) and IHC (results in Figure 2F); yellow arrows: MRS measurements (results in Figure 3). (**D**) Catatonic signs in WT and *Cnp*$^{-/-}$ mice (age 8 weeks) after 5-week PLX5622 or control food diet (Kruskal-Wallis, $P = 0.165$). (**E**) Schematic overview illustrating corpus callosum and neighboring cingulate cortex areas for IHC quantifications: defined ROI for quantifying APP$^+$ swellings, Iba1$^+$ and CD3$^+$ cells as well as GFAP$^+$ and CD68$^+$ areas (densitometric analysis) shown by the yellow striped field and the blue area, respectively; cingulate area (Cg1/Cg2) for Iba1$^+$ cell quantification displayed in rose. (**F**) IHC quantification within the corpus callosum of WT or *Cnp*$^{-/-}$ mice (age 12 weeks) at 4 weeks of microglia repopulation after 5 weeks of PLX5622 or control diet, as shown in **C** and **E**. Upper panels show representative images, including higher-magnification inserts, of the quantifications shown underneath: Iba1$^+$ cells (no./mm^2; 1 section/brain), APP$^+$ swellings (yellow arrows indicating APP$^+$ spheroids; no./mm^2; 3 sections/brain), and densitometric analysis of GFAP$^+$ area (%; 1 section/brain). Original magnification (insets), ×2 (Iba1, GFAP); ×4 (APP). All data in **A**, **D**, and **F** were individually tested for Gaussian distribution using the Kolmogorov-Smirnov test. Nonparametric Kruskal-Wallis test was performed for **A**, **D** and **F** for multiple group comparisons, followed by post hoc 1-tailed Mann-Whitney *U* test. All data are shown as mean ± SEM; *n* indicated within bars.

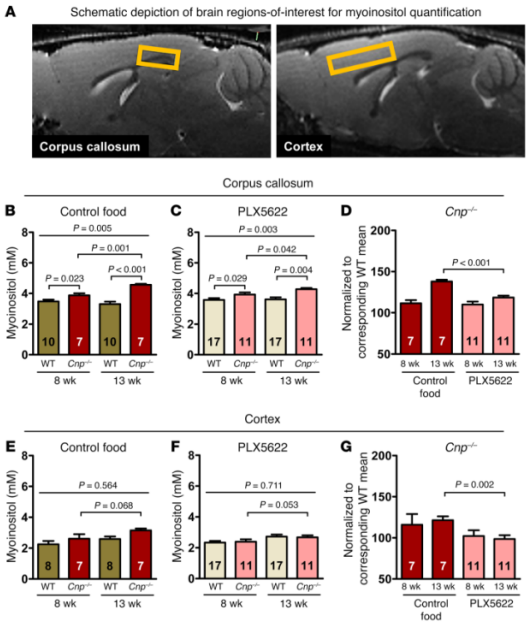

Figure 3. MRS signs of white matter (corpus callosum) and gray matter (cortex) inflammation (myoinositol) in *Cnp*$^{-/-}$ mice and prevention by CSF1R inhibition. (**A**) Representative sagittal MR images illustrating corpus callosum and cortex ROI for analysis of myoinositol levels (yellow squares). (**B**–**D**) Corpus callosum: follow-up MRS for quantification of myoinositol in WT and *Cnp*$^{-/-}$ mice at 8 and 13 weeks of age (experimental design shown in Figure 2C). Statistical comparison of the first MRS in 8-week-old mice, after 5 weeks of control (**B**) versus PLX5622 (**C**) diet (starting at age 3 weeks) and the second MRS in these same mice at the age of 13 weeks, after 5 weeks of regular food (repopulation after PLX5622). (**D**) Note the return to nearly WT level in PLX5622-treated *Cnp*$^{-/-}$ mice. (**E**–**G**) Cortex: same design as for corpus callosum. (**E**) Inflammatory phenotype of *Cnp*$^{-/-}$ mice less pronounced. (**F** and **G**) Effect of PLX5622 less prominent. All data in **B**–**G** were individually tested for Gaussian distribution using the Kolmogorov-Smirnov test. Two-way ANOVA was performed for **B**, **E**, and **F**, followed by post hoc 1-tailed *t* tests. Nonparametric Kruskal-Wallis test was used for multiple group comparisons in **C**, followed by post hoc 1-tailed Mann-Whitney *U* test. Two-way ANOVA for treatment × time interaction performed in **D** and **G**, followed by post hoc unpaired *t* test. $P = 0.008$ (**D**); $P = 0.52$ (**G**). All data shown as mean ± SEM; *n* indicated within bars.

mation (12, 25–27). Quantification of myoinositol in the corpus callosum showed a distinct genotype difference and progression of inflammation over time in *Cnp*$^{-/-}$ mice (Figure 3B). Upon PLX5622, the progressive inflammatory phenotype of *Cnp*$^{-/-}$ mice was reduced to nearly the level seen in WT (Figure 3, C and D). A similar but less prominent effect of PLX5622 was observed in the cortex, where the MRS-detectable neuroinflammation in *Cnp*$^{-/-}$ mice was also less pronounced in treated mice (Figure 3, E–G).

Catatonia and IHC markers of brain inflammation and neurodegeneration in 6-month-old Cnp$^{-/-}$ *mice are reduced by PLX5622 treatment*. The encouraging results of the prevention study made us wonder whether similar effects of microglia depletion by CSF1R inhibition could be observed at a more progressed disease state with advanced neurodegeneration (14) (Figures 4, A–F, and Figure 5, A–G). As expected, *Cnp*$^{-/-}$ mice at the age of 27 weeks were catatonic (Figure 5G). After 5 and 8 weeks of PLX5622, catatonic signs were reduced (Figure 4B). In agreement with the literature, PLX5622-treated WT mice were almost completely depleted of Iba1$^+$ cells (22, 23), even though — compared with young mice — around 10 times more microglial cells/mm^2 corpus callosum area were retained. In contrast, *Cnp*$^{-/-}$ mice showed substantially reduced microglia numbers upon PLX5622 administration to one-third of untreated *Cnp*$^{-/-}$ mice, but just reached untreated WT levels (Figure 4C). This finding may imply that upon aging and/or in situations of strong inflammatory stimulation, a considerable number of microglia lose their responsiveness to CSF1R inhibition. CD68 immunostaining, localized to the lysosomal membrane and used as an additional readout of microglia activation that is upregulated in actively phagocytic cells (28), displayed a pattern very similar to that of Iba1 (Figure 4, D–F). Interestingly, quantification of microglia in the neighboring cingulate cortex as a crucial part of the prefrontal cortex also revealed a distinct increase in Iba1$^+$ cells in *Cnp*$^{-/-}$ mice (Figure 2E and Figure 4E). This demonstrates that white matter inflammation in mutants spreads onto gray matter areas where PLX5622 again leads to a considerable reduction in Iba1$^+$ cells.

Both the remarkably increased axonal swellings (APP$^+$) and the strongly enhanced GFAP$^+$ area seen in untreated *Cnp*$^{-/-}$ mice were diminished under PLX5622, but remained greater than that seen in WT (Figure 5, A and B). The same holds true for CD3$^+$ T lymphocytes, which are attracted by chemokines and cytokines into the inflammatory brain and were also considerably reduced upon

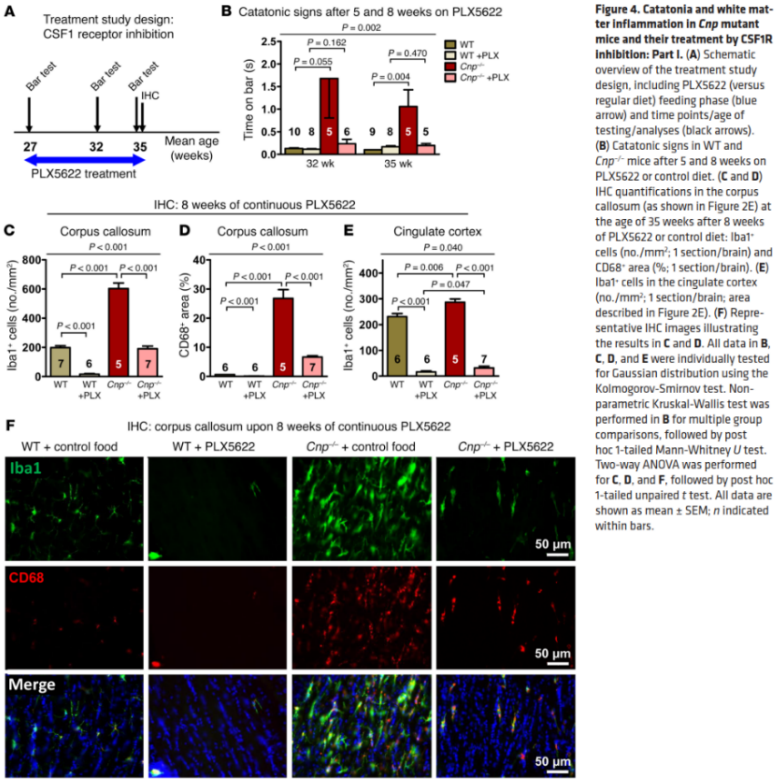

Figure 4. Catatonia and white matter inflammation in *Cnp* mutant mice and their treatment by CSF1R inhibition: Part I. (**A**) Schematic overview of the treatment study design, including PLX5622 (versus regular diet) feeding phase (blue arrow) and time points/age of testing/analyses (black arrows). (**B**) Catatonic signs in WT and *Cnp*$^{-/-}$ mice after 5 and 8 weeks on PLX5622 or control diet. (**C** and **D**) IHC quantifications in the corpus callosum (as shown in Figure 2E) at the age of 35 weeks after 8 weeks of PLX5622 or control diet: Iba1$^+$ cells (no./mm^2; 1 section/brain) and CD68$^+$ area (%; 1 section/brain). (**E**) Iba1$^+$ cells in the cingulate cortex (no./mm^2; 1 section/brain; area described in Figure 2E). (**F**) Representative IHC images illustrating the results in **C** and **D**. All data in **B**, **C**, **D**, and **E** were individually tested for Gaussian distribution using the Kolmogorov-Smirnov test. Nonparametric Kruskal-Wallis test was performed in **B** for multiple group comparisons, followed by post hoc 1-tailed Mann-Whitney *U* test. Two-way ANOVA was performed for **C**, **D**, and **F**, followed by post hoc 1-tailed unpaired *t* test. All data are shown as mean ± SEM; *n* indicated within bars.

PLX5622 treatment (Figure 5, C and D). Since the abundance of oligodendrocyte precursor cells is known to be influenced by microglia and CSF1R inhibition during postnatal development was shown to decrease their numbers (29), PDGFRα staining was also performed. Indeed, *Cnp*$^{-/-}$ mice, with their elevated numbers of PDGFRα$^+$ oligodendrocyte precursors, as well as WT mice respond to PLX5622 with a reduction of PDGFRα$^+$ cells to nearly 50% (Figure 5, E and F).

Other myelin mutants with neuroinflammation also develop catatonia. Finally, we asked whether and when other mouse mutants exhibiting subtle myelin abnormalities and mild neuroinflammation later in life would likewise display a catatonic phenotype. This included mice heterozygous for *Mbp* (12) and *Plp*-null mutant mice (30). Behavioral testing began at 8 weeks of age and was repeated every 4 to 6 weeks. Indeed, we detected signs of catatonia in heterozygous *Mbp*$^{+/-}$ mice at ages 60 to 72 weeks, similar to those seen in the aging phenotype of *Cnp*$^{+/-}$ mice (11). Hemizygous *Plp*$^{-/y}$ mice displayed catatonic signs already at 25 weeks of age (Figure 5G). We note, however, that in all of these mouse lines, including *Cnp* mutants, and similarly across the different age groups, catatonic signs show some variability regarding time on the bar. While as a group, catatonic mice clearly differ from WT mice, the severity range is sometimes considerable.

To test for specificity of catatonic signs as a white matter problem, the bar test was performed at various ages in a wide range

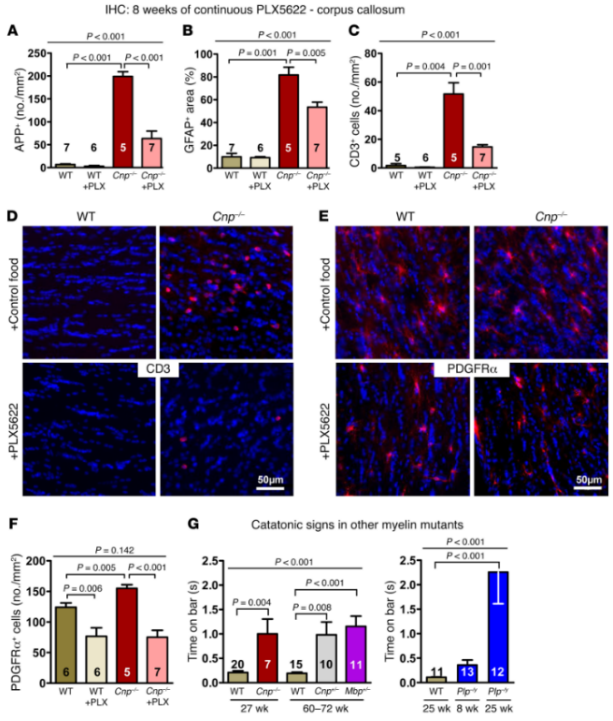

Figure 5. Catatonia and white matter inflammation in *Cnp* mutant mice and their treatment by CSF1R inhibition: Part II. (**A**) APP$^+$ swellings (indicating APP$^+$ spheroids; no./mm^2; 3 sections/brain) and (**B**) densitometric analysis of GFAP$^+$ area (%; indicating astrogliosis; 1 section/brain). (**C**) CD3$^+$ cells (no./mm^2; indicating T lymphocyte invasion; 1 section/brain). (**D** and **E**) Representative IHC images illustrating CD3 and PDGFRα staining. (**F**) PDGFRα$^+$ cells (no./mm^2; indicating oligodendrocyte precursors; 1 section/brain). (**G**) Catatonic signs in WT, *Cnp*$^{-/-}$ (age of onset at 8 weeks of age, shown in Figure 2A), and *Cnp*$^{-/-}$ mice compared with mice with mutations in other myelin-related genes (*Mbp*$^{-/-}$, *Plp*$^{-/y}$). Age of onset of catatonia in heterozygous mice (*Cnp*$^{+/-}$, *Mbp*$^{+/-}$) seen at around 60–72 weeks and in *Plp*$^{+/y}$ mice at 25 weeks. All data in **A**, **B**, **C**, **F**, and **G** were individually tested for Gaussian distribution using the Kolmogorov-Smirnov test. Nonparametric Kruskal-Wallis test was performed for **B**, **C**, and **G** for multiple group comparisons, followed by post hoc 1-tailed Mann-Whitney *U* test. Two-way ANOVA was performed for **A** and **F**, followed by post hoc 1-tailed unpaired *t* test. All data are shown as mean ± SEM; *n* indicated within bars.

of CNS mutants with reported behavioral phenotypes relevant for other facets of neuropsychiatric disease, e.g., autistic, cognitive, or metabolic syndromes. This included mutations of synaptic genes *Nlgn4*$^{-/-}$ (31), *Caps1*$^{-/-}$ (32), *Psd93*$^{-/-}$, and *Psd95*$^{-/-}$ (33), autophagy dysfunction in *Ambra1*$^{+/-}$ mutants (34), and *ApoE*$^{-/-}$ mice with a disturbed blood-brain barrier (35), yet none of these control mice revealed catatonic signs (all $P \geq 0.2$ compared with respective WT). In addition, normal WT (C57BL/6N) mice were tested at 1, 6, 10, or 14 weeks after a single injection of high-dose LPS (5 mg/kg i.p. given at the age of 4 months), known to induce persistent microgliosis (36). Also here, no catatonic signs were observed (all $P \geq 0.2$ compared with respective untreated controls). Interestingly, even catatonic *Plp*$^{-/y}$ mice did not reveal any further increase in their catatonic signs upon LPS (5 mg/kg i.p.) when tested at 1, 4, 8, or 12 weeks after a single injection (all $P \geq 0.8$ compared with PBS-injected controls), suggesting that just the myelin-associated inflammation is critical for catatonic signs.

Discussion

We have identified altered myelin gene expression and minor structural abnormalities of CNS myelin as the trigger of an inflammatory response predominantly in white matter tracts and an underlying cause of catatonic signs in the behavior of mice and humans. This provides a mechanistic insight into a previously enigmatic neuropsychiatric phenotype and expands our view on the role of white matter integrity in cognitive and executive functions in general. Importantly, we have discovered a potential therapy by targeting microglial cells, which emerge as mediators of this neuropsychiatric syndrome.

Our study was based on the previously reported "catatonia-depression" phenotype of aged mice heterozygous for *Cnp* (11), which led us to a translational approach from mice to humans and back. Studying the deeply phenotyped GRAS sample of schizophrenic patients (37, 38), we first demonstrated an age-dependent, unexpectedly high prevalence of more than 25% of catatonic signs, exceeding by far the current estimates of approximately 0.2%–3.0% catatonia in schizophrenic subjects (5). This major discrepancy is likely explained by the often-missed clinical diagnosis, in particular of the milder forms that are much more common and classified as neurological soft signs (8).

Importantly, we noticed that the more severe catatonic signs of GRAS patients are associated with rs2070106-AA, a *CNP* partial loss-of-function genotype (13, 39, 40), a finding that we replicated in an independent schizophrenia cohort. We could further show by MRI in a general population sample that *CNP* rs2070106-AA subjects were more likely than G carriers (GG or AG) to display WMH in frontal and temporal brain areas as well as in deep brain structures. These subclinical findings are not unusual in healthy individuals, where they have been associated with vascular changes, demyelination, and activated microglia (19–21). Even though this literature is suggestive, we have of course no direct proof (e.g., brain biopsies) that inflammation is increased in white matter tracts of live human AA carriers. We note, however, that diffusion tensor imaging identified higher axial diffusivity and a higher apparent diffusion coefficient in the frontal part of the corpus callosum of AA as compared with GG subjects, consistent with a more progressed axonal loss/degeneration (11). This finding further supports the presence of at least low-grade inflammation in AA individuals.

While WMH in humans may be an indirect indicator of white matter inflammation, presence of the latter in *Cnp*$^{-/-}$ mice and its reduction upon microglia depletion were directly shown in the present study. In fact, since microgliosis is a feature of *Cnp* mutant mice (14) and aged *Cnp* heterozygotes exhibit a catatonia-depression phenotype together with late-onset brain inflammation (11), we tested our hypothesis that neuroinflammation itself is causal for the catatonic signs of myelin mutant mice. We chose to treat Cnp-null mutant mice at an age at which they were still free of motor impairments, and indeed, we could completely prevent catatonia onset in these young animals by depleting microglia via administration of the CSF1R inhibitor PLX5622 (22, 23, 41) immediately after weaning. The CSF1R inhibitor also proved effective for treatment of existing catatonia in older *Cnp*$^{-/-}$ mutants, in which it caused a reduction (but not prevention) of axonal degeneration. This is in line with CNP deficiency as a "driver" of neurodegeneration following traumatic brain injury (42). However, the complete prevention of catatonic signs in the young *Cnp*-null mutants strongly suggests that catatonia is not caused by axonal degeneration but is primarily a "microglial disease" induced by mild myelin perturbations. This conclusion is also supported by the catatonic phenotype in aged heterozygous *Mbp* mice that exhibit microglial activation (12), but will not develop the axonal degeneration phenotype of *Plp*- and *Cnp*-null mutant mice with motor impairments (14, 43).

We note that catatonic signs in mice are presently measured by the bar test only, which requires an experienced examiner to yield reproducible results. Having to build on a single readout may explain the cohort-to-cohort variation in the expression severity of this phenotype, which does not show consistent worsening over time (compared with WT controls). Thus, catatonic signs constitute a dichotomous variable in mice (yes/no) rather than a continuous one, as in humans. In fact, several readouts underlie the severity rating used here for humans (9 subtests of Cambridge Neurological Inventory [CNI], including gait mannerisms, gegenhalten, mitgehen, imposed posture, abrupt, or exaggerated spontaneous movements, iterative movements, automatic obedience, and echopraxia; ref. 8). To obtain a similarly robust continuous measure for mice, more catatonia tests are presently being developed in our laboratory, but these tests still require replications in independent mouse cohorts and extensive crossvalidation with bar test results. We hope to ultimately provide a catatonia severity composite score for mice — as we previously established for autistic phenotypes (44) — which will then help diminish sample heterogeneity as typically obtained for single tests.

Interestingly, treating older *Cnp* mutants with PLX5622 was less effective in eliminating microglial cells. Thus, at least a subpopulation of microglia seems to become unresponsive to CSF1R inhibition in the course of neurodegeneration. This represents a therapeutically relevant observation that may reflect the activation status of these cells and deserves further investigation. Based on our data, we cannot exclude that some of these resilient cells are invading peripheral macrophages, known to be Iba1$^+$ and perhaps resistant to PLX5622, or that a higher dose of PLX5622 would have eliminated even those seemingly less responsive cells. The fact, however, that in our pilot experiments with older WT mice, a higher cumulative dose (8-week treatment versus 5-week treatment) had not resulted in any stronger depletion may point against this interpretation.

We point out that CSF1R inhibition also affects cells other than microglia, which may have contributed to the catatonic phenotype (45). Upon CSF1R inhibition, we saw not only a decline in CD3$^+$ T cells that are attracted to the brain by the inflammatory milieu and may influence microglial behavior, but also a decrease in the GFAP$^+$ area as a measure of robust astrogliosis. In addition, we noted a diminished number of PDGFRα$^+$ oligodendrocyte precursors following CSF1R inhibition, similar to what was shown earlier during brain development (29). We thus have to assume that indirect effects could add to the therapeutic benefit of PLX5622.

A large number of studies in mouse models of neuropsychiatric disease have analyzed the contributions of single genes and developmental defects on cognitive dysfunction, autistic traits, signs of depression, and other mental disease–relevant phenotypes (46–49). However, this research has mainly focused on negative and cognitive symptoms, which are easier to model in mice than any of the positive symptoms (delusions, hallucinations), most of which are considered human specific. Catatonia, defined in DSM-5 as a disease specifier for schizophrenia and major mood disorders (5), emerges as an intriguing exception, a positive symptom, and quantifiable readout that can be studied across species.

Our study is, to our knowledge, the first molecular-genetic approach to catatonia and catatonic signs. However, we have to assume that the etiology of these conditions might be heterogeneous. Myelin perturbations may be just one of several possible causes. Further studies are needed to determine whether secondary neuroinflammation is always essential in the "final common pathway" to catatonia. The inefficiency, however, of LPS-mediated brain inflammation to induce catatonic signs in WT mice or to further enhance them in catatonic *Plp*$^{-/y}$ mutants supports the concept of primary myelin alterations (or other underlying causes) being of critical importance for the development of a catatonic phenotype. In fact, peripheral LPS injection most likely acts by causing the liver to produce high levels of circulating TNF-α, which enters the brain at specific sites to incite the abnormal stimulation of endogenous microglia and trigger a vicious and long-lasting circle of events that may even lead to neurodegeneration (50, 51). Here, gray matter areas, such as dopaminergic nuclei, seem to be at higher risk than white matter, whereas myelin-associated inflammation is a unique feature of *Cnp*$^{-/-}$ and other myelin mutant mice.

The sudden loss of motor control in catatonia, followed by an equally sudden regaining of control — often within seconds — ultimately suggests a dysfunction of synaptic circuitry. Importantly, we could show that chronic neuroinflammation in the subcortical white matter progresses into the cingulate cortex, where activated microglia are known to perturb normal synaptic function (16). The production of nitric oxide and axonal conduction blocks, for instance, constitute well-established links between activated microglia and neurodegeneration (52). Within the cortex, the inflammation associated with myelinated fibers may also affect nonmyelinated axons and dendrites (as bystanders), but is probably rather transient or fluctuating because neuronal somata (unlike axons) and the synaptic circuitry are more likely to recover from acute mitochondrial perturbations caused by reactive oxygen species such as NO, as seen in chronic progressive multiple sclerosis (53).

Inflammation, identified in the present study as a major mechanism of catatonic signs, might also affect other phenotypes of mental disease, which could explain the frequently observed fluctuations in their clinical presentation ("episodes"). Alteration of the body's inflammatory state, as encountered in infectious diseases or even during the normal estrous cycle (luteolysis), may have an additional amplifying impact on inflammation within the CNS and thus contribute to the still poorly explained episodic course of many neuropsychiatric diseases. Also, the most severe acute form of catatonia, the life-threatening febrile pernicious catatonia (4), may represent a fulminant inflammation of white matter tracts.

Catatonia in *Cnp* mutant mice was prevented by depletion of microglia at a young age and was even treatable in older animals. While this is important as a proof-of-principle, more research will be needed to define effects of repeated treatment cycles with CSF1R inhibitors as well as to delineate more specific pharmacological targets in activated microglia. In fact, repeated treatment cycles with treatment-free intervals may still be effective, but reduce the risk of side effects, potentially resembling hereditary diffuse leukoencephalopathy with spheroids (HDLS), a CNS white matter disease described in individuals with loss-of-function mutations of the *CSF1R* gene (54). Catatonic signs in patients with schizophrenia are generally mild and per se may not even require specific treatments. However, they likely constitute a surrogate marker for disturbance of broader executive functions and for cognitive deficits, which are severely disabling and currently untreatable, but may also be responsive to specific microglia-targeting antiinflammatory therapies.

Methods

Human studies

GRAS sample of schizophrenic subjects. The GRAS data collection (37, 38) involved deeply phenotyped patients (n = 1095, age 39.1 ± 12.7 years; 66.8% men) diagnosed with schizophrenia or schizoaffective disorder according to DSM-IV-TR (55). Catatonic signs as the present study's target phenotype are from the CNI (8). Genotyping of *CNP* SNP rs2070106 was performed using a semi-custom Axiom MyDesign Genotyping Array (Affymetrix) as reported previously (35, 56).

Würzburg replication sample. Schizophrenic subjects (n = 288, age 41.4 ± 13.5 years; 54.5% men) were assessed categorically into catatonia versus no catatonia according to Leonhard's classification (24), as described earlier (57). Genotyping of *CNP* SNP rs2070106 was performed by means of a quantitative reverse-transcriptase PCR–based (qRT-PCR-based) system using a custom-made primer (KASP assay, LGC Genomics).

SHIP general population sample. A subsample (n = 552, age 46.2 ± 11.4 years; 42.6% men) of the baseline cohort of SHIP-TREND-0 (accessible via application at www.community-medicine.com) was analyzed (58). Only individuals with available SNP information, valid brain MRI scans, complete covariate data, and no neurological conditions were included. Genotyping was performed using the Illumina HumanOmni2.5-Quad and imputation of genotypes via IMPUTE v.2.1.2.3 against the HapMap II (CUv22, Build36) reference panel. The call rate was very high for the CNP SNP rs2070106 (1.00).

MRI acquisition. T1- and T2-weighted MRI were used to measure regional patterns of WMH. All images were obtained using a 1.5T Siemens MRI scanner (Magnetom Avanto, Siemens Medical Systems) with an axial T1-weighted MPRAGE sequence and the following parameters: 1 mm isotropic voxels (flip-angle 15°); 3.37 ms echo time; 1900 ms repetition time, and 1100 ms inversion time. Axial T2-FLAIR sequence had the following parameters: 0.9 × 0.9 mm in-plane spatial resolution; 3.0 mm slice thickness (flip-angle 15°); 325 ms echo time; 5,000 ms repetition time. An automated multimodal segmentation algorithm for WMH determination produced a probabilistic map, thresholded to generate a binary image. Thresholding was based on the default threshold value obtained from algorithm training data. To calculate WMH volume within specific ROI, we applied a multiatlas segmentation method. This included nonlinear registration of multiple atlases with ground-truth labels for every individual scan. Finally, WMH was determined for every region of the brain by masking WMH from all other regions (20).

Mouse studies

In all experiments, the experimenter was unaware of mouse genotypes and treatments (fully blinded).

Mouse maintenance and genotyping. Male and female mice were group-housed separately in ventilated cabinets (Scantainers; Scanbur Karlslunde) unless otherwise indicated for experiments requiring single housing. Mice were maintained on a 12-hour light/12-hour dark cycle (lights off at 7 pm) at 20–22°C, with access to food and water ad libitum, woodchip bedding, and paper tissue as nesting material. Mutant mice (all C56BL/6J background) were genotyped as previously described for *Cnp* (11, 14), *Mbp* (12), and *Plp* (30). Only males were used for experiments with *Mbp* and *Plp* mutants, while both females and males were used for experiments with *Cnp* mutants (housing and testing were always separated). We did not observe any gender differences in catatonic signs. The following neuropsychiatric phenotype-relevant mouse lines, with mutations affecting synapses, blood-brain barrier function or autophagy, were used as controls: *Psd93*$^{-/-}$ (*Dlg2*$^{-/-}$), *Psd95*$^{-/-}$ (*Dlg4*$^{-/-}$) (33), *Nlgn4*$^{-/-}$ (31), *Cadps1*$^{-/-}$ (32), *ApoE*$^{-/-}$ (35), and *Ambra1*$^{+/-}$ (34).

Treatments. PLX5622 (formulated in AIN-76A standard chow by Research Diets; 1,200 ppm) and control food (AIN-76A) were provided by Plexxikon Inc. (22, 23). For tracking of potential batch-to-batch variations in future studies, PLX5622 lot numbers are given: 17032710A5TT1.0i; 16010809A9TT1.0i; 17010309A7TT1.0i; and 16092608A1TT1.0i. LPS was injected intraperitoneally (5 mg/kg LPS; O111:B4; Sigma-Aldrich).

Bar test for catatonia. All mice were transferred to the experimental room 30 minutes prior to testing for habituation. The bar test was performed as previously described (11, 59). Briefly, the mouse was gently carried by the tail to a horizontal bar made of stainless steel (12 cm length, 2.5 mm diameter). Upon grasping the bar with both forepaws, the mouse was moved downwards so that its hind paws had contact with the floor before its tail was released. All experiments were recorded using a high-resolution camcorder (Sony HDR-CX405, Sony Europe Limited). Catatonic signs were scored manually from video recordings as the duration of uninterrupted time a mouse stood nonmoving with at least 1 forepaw on the bar and both hind paws on the ground. Scoring was performed by trained observers blinded to treatments and genotypes (for illustration, see Supplemental Video 1).

Immunohistochemistry. Anesthetized mice were perfused with Ringer's solution (Braun) followed by 4% formaldehyde. Brains were collected, postfixed overnight in 4% formaldehyde, cryoprotected in 30% sucrose, and stored at –80°C. Whole mouse brains were cut into 30-μm–thick coronal sections on a cryostat (Leica, CM1950) and kept in storage solution (25% ethylene glycol/25% glycerol in PBS) at –20°C. For APP and CD3 staining, sections were microwaved in citrate buffer (1 mM, pH 6.0) and for APP detection further pretreated in 3% H_2O_2. All sections were permeabilized and blocked with 5% normal horse serum (NHS)/0.5% Triton X-100 in PBS for 1 hour at room temperature. Sections at a bregma level between +1.15 and +0.5 mm were immunostained for Iba1 (rabbit, 1:1,000, catalog 019-19741, Wako), GFAP (mouse, 1:500, catalog NCL-GFAP-GA5, Novocastra-Leica), CD3 (rat, clone CD3-12, 1:100, catalog MCA1477, Bio-Rad), CD68 (rat, 1:400, catalog MCA1957GA, Bio-Rad), PDGFRα (rabbit, 1:300, catalog 3174, Cell Signaling), or APP (mouse, 1:850, catalog MAB348, Chemicon-Millipore) in 3% NHS/0.5% Triton X-100 in PBS over 2 nights at 4°C. For fluorescent microscopy, 1 hour incubation at room temperature with donkey anti-rabbit Alexa Fluor 647 (catalog A-31573), donkey anti-mouse Alexa Fluor 488 (catalog A-21202), goat anti-rat Alexa Fluor 647 (catalog A-21247), or goat anti-rabbit Alexa Fluor 555 (catalog A-21428) antibodies (1:1,000; Thermo Fisher Scientific-Life Technologies) in 3% NHS/0.5% Triton X-100 in PBS was used. For DAB-based immunostaining, biotinylated horse anti-mouse antibody (1:200; Vector Laboratories) in 3% NHS/0.5% Triton X-100 in PBS and subsequent Vectastain Elite ABC Kit (Vector Laboratories) were used according to the manufacturer's instructions. Cell nuclei were counterstained with DAPI (1:5,000, Sigma-Aldrich) or Mayer's hemalum solution (Merck).

Morphometry. For the analysis of Iba1, GFAP, CD3, CD68, and PDGFRα fluorescent staining, brain slices were scanned using an inverted epifluorescent microscope with a 20×/NA0.4 or 40×/NA0.6 objective lens (Leica, DMI6000B) and quantified using Fiji software (http://fiji.sc/Fiji). Corpus callosum or cingulate cortex (Cg1 and Cg2) of each brain was defined on a DAPI channel as ROI. Iba1$^+$DAPI$^+$, CD3$^+$DAPI$^+$, and PDGFRα$^+$DAPI$^+$ cells were manually counted and density calculated with normalization to ROI. GFAP$^+$ and CD68$^+$ regions were quantified upon uniform thresholding with the respective area expressed as percentage of corpus callosum. APP$^+$ swellings were manually counted using a light microscope (Olympus BX-50) connected to a computer-driven motorized stage, z-axis position encoder (microcator), and a microfire video camera interfaced to a PC using Stereo Investigator 6.55 software (MicroBrightfield Inc.). Representative images of APP$^+$ swellings were taken with a light microscope with a 100×/NA 1.30 oil objective lens (Zeiss Imager Z1).

MRI and ^{1}H-MRS. Mice were anesthetized with 5% isoflurane, intubated, and kept at 1.75% isoflurane by active ventilation with a constant respiratory frequency of 85 breaths/min (Animal Respirator Advanced, TSE Systems). MRI and localized ^{1}H-MRS were performed at a magnetic field strength of 9.4T (Bruker BioSpin). MRI consisted of T2-weighted images (2D-FSE, TR/TE = 2800/11 ms, 100 × 100 × 300 μm^3) based on which respective volumes of interest for localized proton-MR spectra were positioned. MR spectra (STEAM, TR/TE/TM = 6,000/10/10 ms) were obtained from a volume of interest in the cortex (3.9 × 0.7 × 3.2 mm^3) and corpus callosum (3.9 × 0.7 × 1.7 mm^3). Metabolite quantification was completed with spectral evaluation by LCModel (Version 6.3-1L). Results with Cramer-Rao lower bounds greater than 20% were excluded from further analysis.

Statistics

Group differences for continuous variables in human samples were assessed using the Kruskal-Wallis and Jonckheere-Terpstra trend tests. Genotype comparisons used the χ^2 test. Multivariate linear regression models were run with WMH volume as a dependent variable and rs2070106 genotype-age interaction term as a predictor of interest. WMH volumes were transformed via cubic root due to their highly skewed distributions (20). For whole brain, total WMH volume was calculated summing all clusters greater than 10 mm^3 to

reduce noise, followed by hypothesis-driven (11) post hoc testing of WMH from 5 predefined ROI (frontal, temporal, parietal and, as control, occipital lobes, as well as deep structures). For sensitivity analyses, all models described above were rerun using bootstrap methodology (2,000 replications) to derive SEM and CI independently of parametric assumptions such as Gaussian distribution or homoscedasticity. No major differences in standard ordinary least squares results were found. For mouse statistics, data distribution and variance homogeneity were determined by Kolmogorov-Smirnov test and outliers via the Grubbs test (https://graphpad.com/quickcalcs/Grubbs1.cfm). Two-way ANOVA with/without repeated measures was used for normally distributed data. Kruskal-Wallis test was used for data without normal distribution. Between-group comparisons were performed by Student's *t* test for dependent/independent samples or Mann-Whitney *U* test. $P \leq 0.05$ was considered significant. All statistical analyses were performed using SPSS (v 17.0; IBM-Deutschland GmbH), STATA14/MP (Stata Inc.), or Prism 5 software (GraphPad Software).

Study approval

The GRAS study was approved by the ethics committees of Georg-August-University and participating centers across Germany, complying with the Helsinki Declaration. The Würzburg replication sample was approved by the Würzburg University Ethics Committee. The baseline cohort of SHIP-TREND-0, conducted in Northeast Germany, was approved by the Greifswald University Ethics Committee. All subjects (and/or legal representatives) gave written, informed consent. All animal tests were approved by the local Animal Care and Use Committee (LAVES, Niedersächsisches Landesamt für Verbraucherschutz und Lebensmittelsicherheit, Oldenburg, Germany) in accordance with the German Animal Protection Law.

Author contributions

HE and KAN created the concept and designed and supervised the study. MM, JH, MH, RAB, MB, SL, SKS, GH, CD, HV, AR, HJG, and HE acquired, analyzed, and interpreted data for human studies. HJ, SA, EB, HP, BLW, KAN, SB, and HE acquired, analyzed, and interpreted data for mouse phenotyping. HJ, SA, EB, SG, UCG, HBW, KAN, and HE acquired, analyzed, and interpreted data for mouse genetics. HE and KAN drafted the manuscript. HE, KAN, MM, HJ, SA, and EB drafted display items. All authors read and approved the final version of the manuscript.

Acknowledgments

This work was supported by the Max Planck Society, the Max Planck Förderstiftung, the Deutsche Forschungsgemeinschaft (DFG) (CNMPB and SPP1757), EXTRABRAIN EU-FP7, and the Niedersachsen-Research Network on Neuroinfectiology (N-RENNT). SHIP is part of the Community Medicine Research Net of the University Medicine Greifswald, which is funded by the Federal State of Mecklenburg-West Pomerania. Genome-wide data in SHIP have been supported by a joint grant from Siemens Healthineers, Erlangen, and the Federal State of Mecklenburg-West Pomerania. KAN holds a European Research Council Advanced Investigator grant. The authors thank all subjects for participating in the study, and all colleagues who have contributed over the past decade to GRAS data collection.

Address correspondence to: Klaus-Armin Nave or Hannelore Ehrenreich, Max Planck Institute of Experimental Medicine, Hermann-Rein-Strasse 3, 37075 Göttingen, Germany. Phone: 49.551.3899 ext 754; Email: nave@em.mpg.de (K.A. Nave). Phone: 49.551.3899 ext 628; Email: ehrenreich@em.mpg.de.

1. Nave KA, Werner HB. Myelination of the nervous system: mechanisms and functions. *Annu Rev Cell Dev Biol*. 2014;30:503–533.
2. Filley CM, Fields RD. White matter and cognition: making the connection. *J Neurophysiol*. 2016;116(5):2093–2104.
3. Nave KA, Ehrenreich H. Myelination and oligodendrocyte functions in psychiatric diseases. *JAMA Psychiatry*. 2014;71(5):582–584.
4. Fink M, Taylor MA. *Catatonia: a clinician's guide to diagnosis and treatment*. Cambridge, UK: Cambridge University Press; 2003.
5. Tandon R, et al. Catatonia in DSM-5. *Schizophr Res*. 2013;150(1):26–30.
6. Arora M, Praharaj SK. Butterfly glioma of corpus callosum presenting as catatonia. *World J Biol Psychiatry*. 2007;8(1):54–55.
7. Northoff G, et al. Orbitofrontal cortical dysfunction in akinetic catatonia: a functional magnetic resonance imaging study during negative emotional stimulation. *Schizophr Bull*. 2004;30(2):405–427.
8. Chen EY, et al. The Cambridge Neurological Inventory: a clinical instrument for assessment of soft neurological signs in psychiatric patients. *Psychiatry Res*. 1995;56(2):183–204.
9. Amir S. Catalepsy induced by body pinch: relation to stress-induced analgesia. *Ann N Y Acad Sci*. 1986;467:226–237.
10. Chaperon F, Thiébot MH. Behavioral effects of cannabinoid agents in animals. *Crit Rev Neurobiol*. 1999;13(3):243–281.
11. Hagemeyer N, et al. A myelin gene causative of a catatonia-depression syndrome upon aging. *EMBO Mol Med*. 2012;4(6):528–539.
12. Poggi G, et al. Cortical network dysfunction caused by a subtle defect of myelination. *Glia*. 2016;64(11):2025–2040.
13. Peirce TR, et al. Convergent evidence for 2',3'-cyclic nucleotide 3'-phosphodiesterase as a possible susceptibility gene for schizophrenia. *Arch Gen Psychiatry*. 2006;63(1):18–24.
14. Lappe-Siefke C, et al. Disruption of Cnp1 uncouples oligodendroglial functions in axonal support and myelination. *Nat Genet*. 2003;33(3):366–374.
15. Chen SK, et al. Hematopoietic origin of pathological grooming in Hoxb8 mutant mice. *Cell*. 2010;141(5):775–785.
16. Hong S, Dissing-Olesen L, Stevens B. New insights on the role of microglia in synaptic pruning in health and disease. *Curr Opin Neurobiol*. 2016;36:128–134.
17. Parkhurst CN, et al. Microglia promote learning-dependent synapse formation through brain-derived neurotrophic factor. *Cell*. 2013;155(7):1596–1609.
18. Prinz M, Priller J. Microglia and brain macrophages in the molecular age: from origin to neuropsychiatric disease. *Nat Rev Neurosci*. 2014;15(5):300–312.
19. Fazekas F, et al. The morphologic correlate of incidental punctate white matter hyperintensities on MR images. *AJNR Am J Neuroradiol*. 1991;12(5):915–921.
20. Habes M, et al. White matter hyperintensities and imaging patterns of brain ageing in the general population. *Brain*. 2016;139(Pt 4):1164–1179.
21. Simpson JE, et al. Microglial activation in white matter lesions and nonlesional white matter of ageing brains. *Neuropathol Appl Neurobiol*. 2007;33(6):670–683.
22. Dagher NN, et al. Colony-stimulating factor 1 receptor inhibition prevents microglial plaque association and improves cognition in 3xTg-AD mice. *J Neuroinflammation*. 2015;12:139.
23. Elmore MR, et al. Colony-stimulating factor 1 receptor signaling is necessary for microglia viability, unmasking a microglia progenitor cell in the adult brain. *Neuron*. 2014;82(2):380–397.
24. Leonhard K. *Classification of Endogenous Psychoses and Their Differentiated Etiology*. Wien, Austria: Springer-Verlag Wien; 1999.
25. Badar-Goffer RS, Ben-Yoseph O, Bachelard HS, Morris PG. Neuronal-glial metabolism under depolarizing conditions. A 13C-n.m.r. study. *Biochem J*. 1992;282(Pt 1):225–230.
26. Chang L, Munsaka SM, Kraft-Terry S, Ernst T. Magnetic resonance spectroscopy to assess neuroinflammation and neuropathic pain. *J Neuroimmune Pharmacol*. 2013;8(3):576–593.
27. Ross BD, Bluml S, Cowan R, Danielsen E, Farrow N, Gruetter R. In vivo magnetic resonance spectroscopy of human brain: the biophysical basis of dementia. *Biophys Chem*. 1997;68(1–3):161–172.
28. Zotova E, et al. Inflammatory components in human Alzheimer's disease and after active amyloid-β42 immunization. *Brain*. 2013;136(Pt 9):2677–2696.
29. Hagemeyer N, et al. Microglia contribute to normal myelinogenesis to oligodendrocyte progenitor maintenance during adulthood. *Acta Neuropathol*. 2017;134(3):441–458.
30. Klugmann M, et al. Assembly of CNS myelin in the absence of proteolipid protein. *Neuron*. 1997;18(1):59–70.
31. Jamain S, et al. Reduced social interaction and ultrasonic communication in a mouse model of monogenic heritable autism. *Proc Natl Acad Sci U S A*. 2008;105(5):1710–1715.
32. Jockusch WJ, et al. CAPS-1 and CAPS-2 are essential synaptic vesicle priming proteins. *Cell*. 2007;131(4):796–808.
33. Winkler D, et al. Hypersocial behavior biological redundancy in mice with reduced expression of PSD95 or PSD93 [published online ahead of print February 9, 2017]. *Behav Brain Res*. https://doi.org/10.1016/j.bbr.2017.02.011.
34. Dere E, et al. Heterozygous ambra1 deficiency in mice: a genetic trait with autism-like behavior restricted to the female gender. *Front Behav Neurosci*. 2014;8:181.
35. Hammer C, et al. Neuropsychiatric disease relevance of circulating anti-NMDA receptor autoantibodies depends on blood-brain barrier integrity. *Mol Psychiatry*. 2014;19(10):1143–1149.
36. Qin L, Liu Y, Hong JS, Crews FT. NADPH oxidase and aging drive microglial activation, oxidative stress, and dopaminergic neurodegeneration following systemic LPS administration. *Glia*. 2013;61(6):855–868.
37. Begemann M, et al. Modification of cognitive performance in schizophrenia by complexin 2 gene polymorphisms. *Arch Gen Psychiatry*. 2010;67(9):879–888.
38. Ribbe K, et al. The cross-sectional GRAS sample: a comprehensive phenotypical data collection of schizophrenic patients. *BMC Psychiatry*. 2010;10:91.
39. Iwamoto K, Ueda J, Bundo M, Nakano Y, Kato T. Effect of a functional single nucleotide polymorphism in the 2',3'-cyclic nucleotide 3'-phosphodiesterase gene on the expression of oligodendrocyte-related genes in schizophrenia. *Psychiatry Clin Neurosci*. 2008;62(1):103–108.
40. Mitkus SN, et al. Expression of oligodendrocyte-associated genes in dorsolateral prefrontal cortex of patients with schizophrenia. *Schizophr Res*. 2008;98(1–3):129–138.
41. Waisman A, Ginhoux F, Greter M, Bruttger J. Homeostasis of microglia in the adult brain: review of novel microglia depletion systems. *Trends Immunol*. 2015;36 (10):625–636.
42. Wieser GL, et al. Neuroinflammation in white matter tracts of Cnp1 mutant mice amplified by a minor brain injury. *Glia*. 2013;61 (6):869–880.
43. Griffiths I, et al. Axonal swellings and degeneration in mice lacking the major proteolipid of myelin. *Science*. 1998;280(5369):1610–1613.
44. El-Kordi A, et al. Development of an autism severity score for mice using Nlgn4 null mutants as a construct-valid model of heritable monogenic autism. *Behav Brain Res*. 2013;251:41–49.
45. Chitu V, Gokhan Ş, Nandi S, Mehler MF, Stanley ER. Emerging roles for CSF-1 receptor and its ligands in the nervous system. *Trends Neurosci*. 2016;39(6):378–393.
46. Lee YS, Silva AJ. The molecular and cellular biology of enhanced cognition. *Nat Rev Neurosci*. 2009;10(2):126–140.
47. Nestler EJ, Hyman SE. Animal models of neuropsychiatric disorders. *Nat Neurosci*. 2010;13(10):1161–1169.
48. Schroeder JC, Reim D, Boeckers TM, Schmeisser MJ. Genetic animal models for autism spectrum disorder. *Curr Top Behav Neurosci*. 2017;30:311–324.
49. Silverman JL, Yang M, Lord C, Crawley JN. Behavioural phenotyping assays for mouse models of autism. *Nat Rev Neurosci*. 2010;11(7):490–502.
50. Jeong HK, Jou I, Joe EH. Systemic LPS administration induces brain inflammation but not dopaminergic neuronal death in the substantia nigra. *Exp Mol Med*. 2010;42(12):823–832.
51. Qin L, et al. Systemic LPS causes chronic neuroinflammation and progressive neurodegeneration. *Glia*. 2007;55(5):453–462.
52. Block ML, Zecca L, Hong JS. Microglia-mediated neurotoxicity: uncovering the molecular mechanisms. *Nat Rev Neurosci*. 2007;8(1):57–69.
53. Lassmann H, van Horssen J, Mahad D. Progressive multiple sclerosis: pathology and pathogenesis. *Nat Rev Neurol*. 2012;8(11):647–656.
54. Rademakers R, et al. Mutations in the colony stimulating factor 1 receptor (CSF1R) gene cause hereditary diffuse leukoencephalopathy with spheroids. *Nat Genet*. 2011;44(2):200–205.
55. American Psychiatric Association. *Diagnostic statistical manual of mental disorders: DSM-IV-TR*. Washington, DC: American Psychiatric Association; 2000.
56. Stepniak B, et al. Accumulated environmental risk determining age at schizophrenia onset: a deep phenotyping-based study. *Lancet Psychiatry*. 2014;1(6):444–453.
57. Reif A, et al. A neuronal nitric oxide synthase (NOS-I) haplotype associated with schizophrenia modifies prefrontal cortex function. *Mol Psychiatry*. 2006;11(3):286–300.
58. Völzke H, et al. Cohort profile: the study of health in Pomerania. *Int J Epidemiol*. 2011;40(2):294–307.
59. Kuschinsky K, Hornykiewicz O. Morphine catalepsy in the rat: relation to striatal dopamine metabolism. *Eur J Pharmacol*. 1972;19(1):119–122.